SMITHSONIAN CONTRIBUTIONS TO THE EARTH SCIENCES • NUMBER 24

Catalog of Meteorites from Victoria Land, Antarctica, 1978–1980

Ursula B. Marvin
and Brian Mason

EDITORS

SMITHSONIAN INSTITUTION PRESS
City of Washington
1982

ABSTRACT

Marvin, Ursula B., and Brian Mason, editors. Catalog of Meteorites from Victoria Land, Antarctica, 1978–1980. *Smithsonian Contributions to the Earth Sciences*, number 24, 97 pages, frontispiece, 41 figures, 13 tables, 1982.—This is the second catalog of meteorite specimens collected on expeditions to Victoria Land led by William A. Cassidy of the University of Pittsburgh. The first (*Catalog of Antarctic Meteorites, 1977–1978*, U. B. Marvin and B. Mason, editors, 1980) presented the results of the 1976–1977 and 1977–1978 field seasons and described the collection and curation procedures that were adopted under a three-agency agreement between the National Science Foundation, the National Aeronautics and Space Administration, and the Smithsonian Institution for the purpose of protecting the meteorites from terrestrial contamination and allocating them for research. This catalog reports the results of the subsequent two seasons: 309 specimens were collected in 1978–1979, and 73 in 1979–1980. Classifications are given for all specimens weighing more than about 100 grams and also for some smaller pieces from each of the four field seasons. The catalog describes the field camps, the geodetic measurements of ice motion and ablation at the Allan Hills site, and the search for new concentrations. Current information about the character of the collections and new types of meteorites represented in them is outlined in brief articles describing Antarctic achondrites, carbonaceous chondrites and irons, and meteorite weathering and terrestrial residence times on the polar icecap. There is a bibliography of major articles on Antarctic meteorites. An Appendix lists all of the Victoria Land specimens classified as of December 1980, by numerical order for each locality and by meteorite class.

OFFICIAL PUBLICATION DATE is handstamped in a limited number of initial copies and is recorded in the Institution's annual report, *Smithsonian Year.* SERIES COVER DESIGN: Aerial view of Ulawan Volcano, New Britain.

Library of Congress Cataloging in Publication Data
Main entry under title:
Catalog of meteorites from Victoria Land, Antarctica, 1978–1980.
(Smithsonian contributions to the earth sciences ; no. 24)
Bibliography: p.
Includes bibliographies.
Contents: The field season in Victoria Land, 1978–1979 / by Ursula B. Marvin — The traverse to Reckling Peak, 1979–1980 / by William A. Cassidy and L. A. Rancitelli — The Allan Hills Icefield and its relationship to meteorite concentration / by John O. Annexstad — [etc.]
Supt. of Docs. no.: SI 1.26:24
1. Meteorites—Antarctic regions—Catalogs. 2. Meteorites—Antarctic regions—Addresses, essays, lectures. I. Marvin, Ursula B. II. Mason, Brian Harold, 1917– . III. Series.
QE1.S227 no. 24. [QB755] 550s [523.5'1'09989] 81-607125 AACR2

Contents

Frontispiece.—The midnight sun of 6 January 1979 illuminates the Allan Hills campsite, with snow crystals streaming northward before the polar wind.

Catalog of Meteorites from Victoria Land, Antarctica 1978–1980

Editors' Introduction

Ursula B. Marvin and Brian Mason

The United States has sent yearly meteorite collecting expeditions, under the leadership of William A. Cassidy of the University of Pittsburgh, to Victoria Land, Antarctica, since the austral summer of 1976. This catalog describes those specimens weighing more than 100 grams that were collected during the expeditions of 1978–1979 and 1979–1980. In addition, it describes some of the cherry-sized meteorites collected in these and other years. Descriptions of the larger specimens from the 1976–1977 and 1977–1978 expeditions are presented in the Catalog of Antarctic Meteorites, 1977–1978 (Marvin and Mason, 1980). That earlier catalog also provides descriptions of field areas, collecting procedures, and curation procedures.

Current research results show that the Antarctic specimens include mineralogical and textural varieties of meteorites that are new to the world collections. In order to make this catalog more informative we include brief reviews of the range of compositions observed among the achondrites, carbonaceous chondrites, and irons, and progress reports on topics such as geodetic measurements of ice motion and ablation at the Allan Hills site, meteorite weathering under polar conditions, and aluminum-26 determinations of terrestrial residence times.

The field parties collected 11 meteorite specimens the first year (1976–1977), 300 specimens in 1977–1978, 309 specimens in 1978–1979, and 73 in 1979–1980 — a season when most of the effort was devoted to measuring ice motion and searching for new meteorite concentrations. Table 1 shows the distribution of meteorite types found in the latter two seasons. All of the Victoria Land specimens that were classified as of December 1980 are listed in the three-part appendix. Appendix Table A lists specimens for each locality by consecutive numbers; Appendix Table B lists specimens consecutively by meteorite class; and Appendix Table C lists the paired meteorites that have been identified according to our current, but far from complete, knowledge of them.

The final entry in the catalog is a bibliography of the literature on Antarctic meteorites. Articles containing substantive data (analytical information, petrographic descriptions, comparisons with other meteorites, etc.) for Antarctic meteorites have been included. In general, brief abstracts of

Ursula B. Marvin, Smithsonian Astrophysical Observatory, 60 Garden Street, Cambridge, Massachusetts 02138. Brian Mason, Department of Mineral Sciences, National Museum of Natural History, Smithsonian Institution, Washington, D.C. 20560.

TABLE 1.—Meteorite specimens collected in 1978–1979 and 1979–1980

Type	*Allan Hills*	*Darwin Glacier*	*Elephant Moraine*	*Reckling Peak*	*Totals*
			1978–1979		
Irons	2	9			11
Achondrites	6				6
Carbonaceous chondrites	1				1
Chondrites	253	34		4	291
Totals	262	43		4	309
			1979–1980		
Irons				1	1
Achondrites	1		6		7
Chondrites	52		4	9	65
Totals	53		10	10	73

information published elsewhere in more complete form have been excluded. No attempt has been made to survey the literature in Japanese, although some frequently referenced papers are listed. We hope these additions will increase the usefulness of the catalog.

During the past three years research on Antarctic specimens has burgeoned in laboratories around the world. The procedures for collecting the specimens and maintaining them at below-freezing temperatures until they can be processed at the curatorial facility at the Johnson Space Center in Houston are governed by an interagency agreement between the National Science Foundation, the Smithsonian Institution, and the National Aeronautics and Space Administration and are outlined in the previous catalog (Marvin and Mason, 1980). Newly examined and classified specimens are described in the *Antarctic Meteorite Newsletter*, published periodically by the Meteorite Working Group, a committee with a rotating membership responsible for monitoring the program and allocating samples. Requests for the *Antarctic Meteorite Newsletter* or for specimens or thin sections for research should be addressed to the Secretary, Antarctic Meteorite Working Group, Lunar and Planetary Institute, 3303 NASA Road 1, Houston, Texas 77058. Sample requests should detail sample numbers, desired weights, and the type of studies planned.

The Antarctic Meteorite Working Group meets twice yearly, usually in April and September. Dates of meetings and deadlines for sample requests are published in the newsletter. Sample requests are welcome from all qualified scientists. Requests are considered on the basis of their merit, without regard to whether a scientist is currently funded for meteorite research. The allocation of Antarctic meteorite samples in no way commits any funding agency to support the proposed research.

Libraries of polished thin sections have been established in Washington, Houston, and Tokyo for the use of visitors who wish to make optical examinations. (Library thin sections are not available for loan.) To obtain meteorite samples from the Japanese collections or to use the thin section library in Tokyo, contact T. Nagata, Director, or K. Yanai, Curator, at the National Institute of Polar Research, 9–10, Kaga 1-chome, Itabushi-ku, Tokyo 173, Japan. Arrangements for using the thin-section library at the Johnson Space Center in Houston may be made by contacting the Secretary of the Antarctic Meteorite Working Group. To use the library at the National Museum of Natural History, Smithsonian Institution, Washington, DC 20560, contact Brian Mason, Curator.

The Field Season in Victoria Land, 1978–1979

Ursula B. Marvin

The 1978–1979 field season had three main objectives: to search new areas near the head of the Darwin Glacier for meteorite concentrations, to lay out a geodetic network to measure ice motion and ablation at the Allan Hills, and to continue systematic collection of specimens in the Allan Hills icefield.

This was the third and final year of the cooperative agreement by which scientists from the United States and Japan, working out of McMurdo Station, collected meteorites together and shared specimens equally. Led by William A. Cassidy, of the University of Pittsburgh, the participants included John O. Annexstad, NASA Johnson Space Center, Ursula B. Marvin, Smithsonian Astrophysical Observatory, Dean Clauter, University of Pittsburgh, and Fumihiko Nishio, Kazuyuki Shiraishi, and Minoru Funaki of the National Institute for Polar Research in Tokyo.

Annexstad and Nishio set up camp at Allan Hills on December 7 and remained there for 26 days (through more than one 4-day storm that kept them tentbound) installing a 15-km triangulation chain across the meteorite concentration field (see Annexstad, this issue). Without making any special effort to search for them, Annexstad and Nishio picked up nearly 100 meteorites along the snowmobile paths from their camp to the network stations.

Cassidy and Shiraishi began a careful search by helicopter of the region around the head of the Darwin Glacier (79°50′S, 158°00′E), where the National Science Foundation set up a camp to support a number of field parties during that season (Figure 1). A short time later Cassidy transferred to the Allan Hills camp and Marvin and Clauter joined Shiraishi at the Darwin Camp. The sites examined in that area included the Warren and Boomerang Ranges, Butcher, Finger, and Turnstile Ridges, Haven Mountain, and Westhaven, Bates, and Lonewolf Nunataks. Most of these sites proved barren, but six meteorites, all moderately weathered and looking suspiciously like fragments from a single fall, were collected near Bates Nunatak. The three largest, BTNA78001, 78002, and 78004, were later classified as L6, L6, and LL6 chondrites, respectively (see Appendix Table A).

Five specimens were found in the upland between the head of the Darwin Glacier and that of the Hatherton Glacier. Twenty-three specimens, most of them small and weathered to a chestnut brown, were collected from ripple identations on a rather steeply sloping, bare ice-surface near the west end of the Darwin Mountains. Their similar appearance and their distribution over an open slope suggested that they represented a relatively recent strewnfield from atmospheric break-up of a single meteorite.

In mid-December a group of geologists from the University of Waikato, New Zealand, led by Michael Selby, discovered six iron meteorites on the rocky slopes of Derrick Peak, a conical mountain visible on the northern skyline from Darwin Camp (Figure 2). They radioed the news to Cassidy at Darwin Camp and he and Shiraishi spent two days searching the slopes with the New Zea-

Ursula B. Marvin, Smithsonian Astrophysical Observatory, 60 Garden Street, Cambridge, Massachusetts 02138.

a

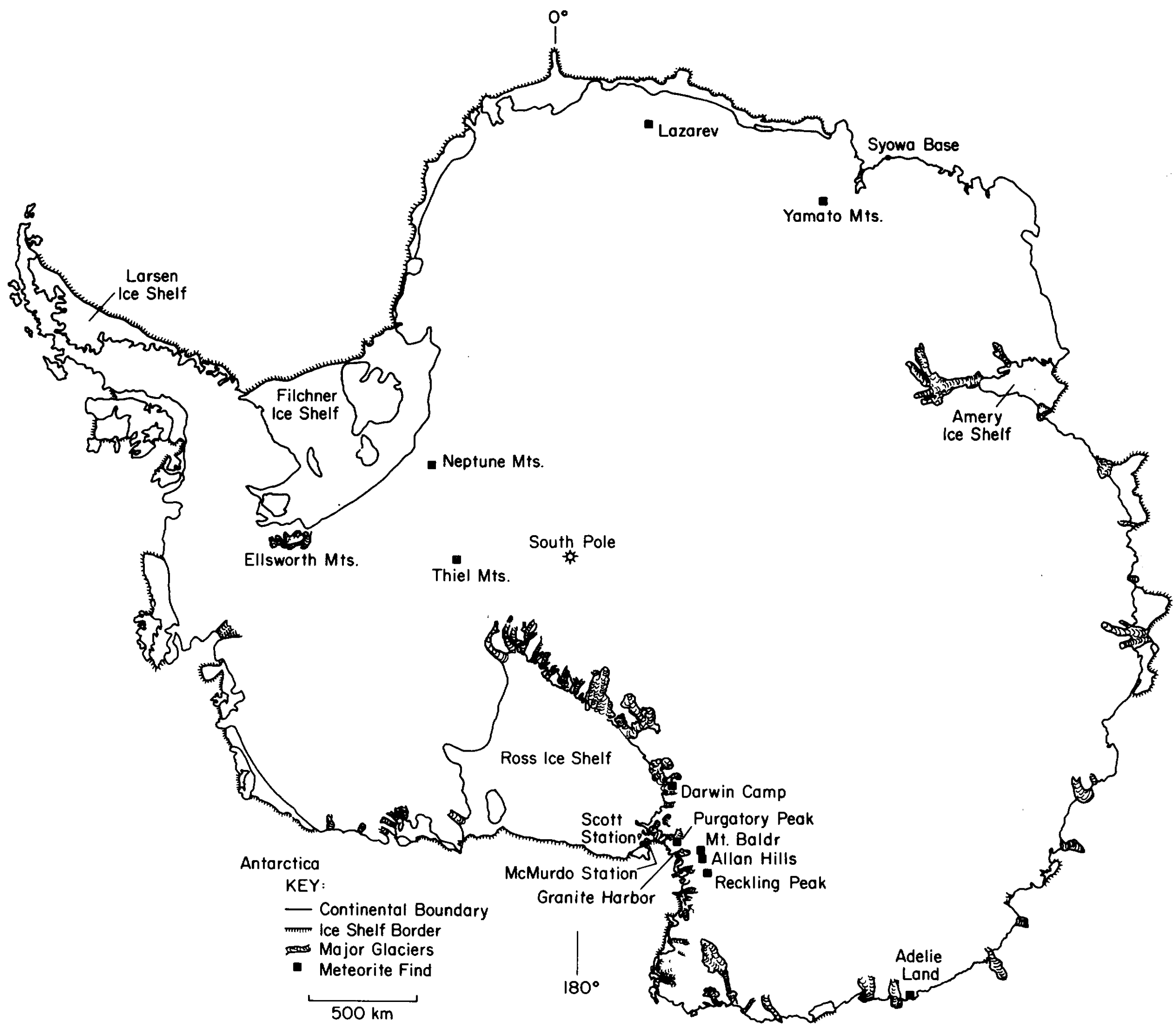

FIGURE 1.—Location maps of Antarctic meteorite finds: *a*, outline map of continent; *b*, areas searched and location of finds in Victoria Land.

land team. A short time later, Shiraishi, Marvin, and Clauter spent another day there. In all, nine more specimens were collected, and, later, another specimen was donated by Peter King, a New Zealand climber associated with the Darwin Base support group.

The Derrick Peak irons range in weight from about 130 grams to 138 kilograms (see Clarke, herein: 54–55). The two largest ones were strikingly handsome specimens, very difficult to carry from the steep mountainside to a waiting helicopter. All of these irons have a distinctive appearance, with large, elongate inclusions standing up in relief on surfaces hollowed by deep regmaglypts or corrosion pits. This unusual textural feature indicates that they belong to a single shower, and the distribution of the specimens high on an ice-free mountain side suggests they fell at that site rather than having been transported. Preliminary metallurgical observations b

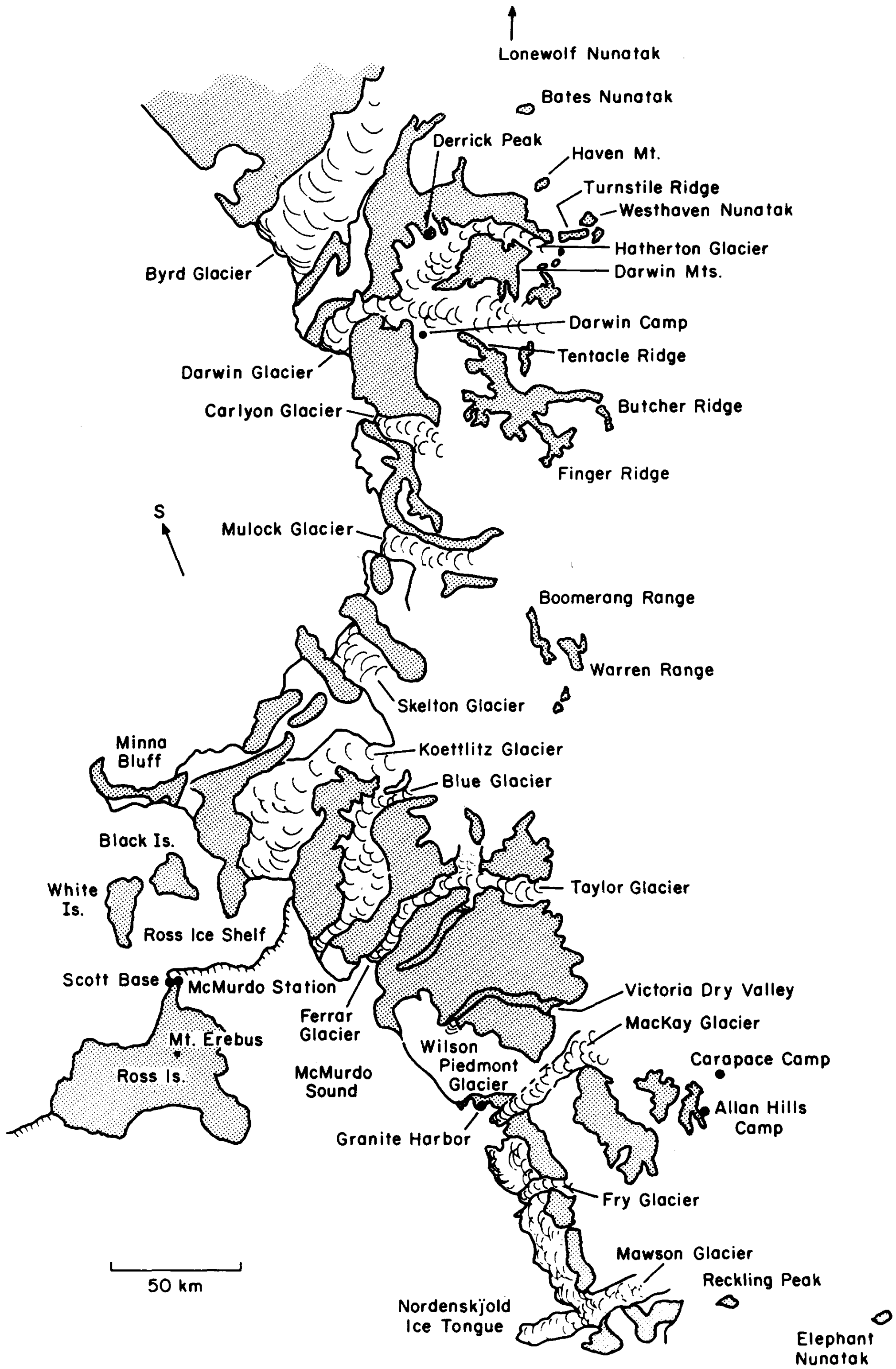

Lonewolf Nunatak
Bates Nunatak
Derrick Peak
Haven Mt.
Turnstile Ridge
Westhaven Nunatak
Hatherton Glacier
Darwin Mts.
Byrd Glacier
Darwin Camp
Tentacle Ridge
Darwin Glacier
Carlyon Glacier
Butcher Ridge
Finger Ridge
S
Mulock Glacier
Boomerang Range
Warren Range
Skelton Glacier
Minna Bluff
Koettlitz Glacier
Blue Glacier
Black Is.
White Is.
Taylor Glacier
Ross Ice Shelf
Scott Base
McMurdo Station
Victoria Dry Valley
Ferrar Glacier
MacKay Glacier
Mt. Erebus
Wilson Piedmont Glacier
Carapace Camp
Ross Is.
McMurdo Sound
Allan Hills Camp
Granite Harbor
Fry Glacier
Mawson Glacier
Reckling Peak
50 km
Nordenskjöld Ice Tongue
Elephant Nunatak

FIGURE 2.—Meteorite hunter on boulder-strewn slope of Derrick Peak.

have confirmed the common parentage of the individual specimens. The raised inclusions are crystals of schreibersite.

The Darwin Camp was located on the upper glacier amid superb mountain scenery. All facilities—bunkhouse, workroom, gallery, radio shack, repair shop—were housed in demountable Jamesway huts. A cook served three meals each day and, whenever the generators worked, there were a shower, flush toilets, a washer and dryer for laundry. Field parties came and went all season, but there were always enough people in camp for a volley-ball game at 5 o'clock in the afternoon.

The Darwin Camp lay about 320 km from McMurdo Station. Personnel and equipment were carried there by ski-equipped Hercules LC-130 cargo planes. Three helicopters were kept at Darwin to ferry parties in and out of the field. One fully operational helicopter was always on the ground for possible use in rescue missions.

All field parties gathered at Darwin Camp for a festive Christmas dinner featuring roast turkey and cranberry sauce, with a generous array of other dishes. The celebration helped alleviate the sense shared by many polar researchers of being too far from home at holiday time.

Shortly before New Year's Day, Shiriashi, Marvin, and Clauter left Darwin Camp for McMurdo, and on 2 January they joined Cassidy at Allan Hills. After a long and eventful season, Annexstad and Nishio left Allan Hills on the same helicopter that carried in the newcomers. In contrast to Darwin, the Allan Hills Camp was a traditional Antarctic do-it-yourself operation in which the campers pitched their own Scott tents and were expected to take turns cooking for the party over a Coleman stove. Happily for everyone, after sampling the efforts of others, Shiraishi, who was well supplied with frozen Japanese delicacies, voluntarily did more than his share of the cooking.

Daily trips were made by snowmobile to search for meteorites on the nearby expanse of blue ice, in a moraine at the foot of the Allan Hills ice monocline, or on the polar plateau above it. On the bare ice a fairly high percentage of the rocks present were meteorites. On the plateau, few rocks were sighted but all were meteorites. One iron

FIGURE 3.—Communications hut and tent city at Darwin Glacier Camp, with Roadend Nunatak in background.

meteorite was found part way up the slope to the plateau. In the moraine, meteorites occurred among cobbles and boulders of local ("trash") rocks. The moraines of this area are not similar to the lobate heaps of rubble and clay associated with mountain glaciers; they are collections of rocks, probably derived from a shallow subsurface ridge, scattered over the ice and snow. Keen observation is necessary to detect meteorites and to distinguish some of them from wind-polished dolerites, especially since our sterile collection procedures forbid picking up specimens for close examination. The wind scoops (Figure 4) that form around the base of large boulders proved to be good hunting ground for cherry-sized meteorites, which are small enough to skitter along the ice until they fall into the hollows. Laboratory studies of cherry-sized stones are revealing a high proportion of unequilibrated chondrites containing newly discovered assemblages of graphite and magnetite (Taylor et al., 1981).

Although some meteorites may be covered by snow, only one has been discovered frozen beneath the surface of the bare ice. That one was small, nearly flat, and had a bronzy luster suggestive of either an iron meteorite or a weathered piece of dolerite. Still frozen in a block of ice, the specimen was shipped to Houston where it proved to be a hexahedrite, ALHA78100.

The total number of specimens collected at Allan Hills in 1978–1979 was 262. The average size was smaller than that of previous seasons. It appears that, at any one site, the largest and most conspicuous specimens will be collected the first year. Thin drifts of snow may alternately conceal and expose smaller ones. An example of this occurred during an afternoon's search when one member of the party discovered a small ureilite within the moraine and marked the spot by building a cairn topped with a red flag. A short time later, when the whole party came to view the meteorite, no meteorite was seen. Presently the specimen was found under a fresh mound of wind-blown snow; the presence of the cairn had

FIGURE 4.—Wind scoop around boulder in a moraine, ideal trap for cherry-sized meteorites that skitter downwind along ice surface.

changed wind patterns enough to cover the meteorite within minutes.

Helicopter reconnaissance yielded five specimens from a patch of ice about 20 km west, and upstream in the sense of ice motion, from the Allan Hills concentration (Cassidy, 1979). The previous year, 25 specimens, all apparently from a single fall, had been found about midway between the two sites. The ice flowing toward Allan Hills from the west may be carrying many meteorites, most of them covered with snow.

Early in the season, Cassidy flew to the Ellsworth Mountains to check that area. He concluded that the ice was moving too rapidly to form any significant meteorite concentrations there. He also made reconnaissance flights over the Thiel Mountains, where one meteorite was discovered in 1969 and patches of blue ice are visible on satellite photographs. Cassidy feels that area holds sufficient promise to justify future field exploration.

During a geological traverse, Philip Kyle of Ohio State University, found five meteorites on a patch of ice a short distance west of Reckling Peak. His discovery led to a snowmobile traverse there in the 1979–1980 season (Cassidy and Rancitelli, this issue).

The meteorite types collected in the 1978–1979 and 1979–1980 field seasons are listed in Table 1. Much more laboratory work will be necessary before it will be possible to estimate the number of falls that are represented among the Victoria Land specimens.

The Traverse to Reckling Peak, 1979–1980

W.A. Cassidy and L.A. Rancitelli

Reckling Peak is located at 159°15′E, 76°16′S. A blue ice patch extends west from Reckling Peak for about 100 km. The effective limit for routine travel by helicopter from McMurdo Station is reached at Allan Hills, therefore to investigate the Reckling Peak ice patch we travelled north by snowmobile from our Allan Hills put-in site, towing our supplies on Nansen sledges (Figure 5). Other members of the group were J. O. Annexstad, NASA Johnson Space Center, and Lee Benda, University of Washington.

We left Allan Hills on 5 January and made 24 km before camping about 4 km west of Battlements Nunatak (Figure 6). On this traverse we skirted families of crevasses resulting from changes in ice flow velocity about the Battlements Nunatak barrier. The next two days were spent at this site due to high winds and consequent low visibility that made travel inadvisable. On 8 January the wind died, we broke camp, and made 32 km to a point where increasing size and frequency of crevassing made further progress difficult. We were approaching a change in elevation where the ice surface descends fairly steeply to become part of a well-defined convergence area leading to the David Glacier. Crevassing here results from the fact that at the crest of the slope each unit of ice volume at the upper surface is forced to travel a greater distance in the same time than any similar unit below it, i.e., acceleration by change of direction.

Kyle's party had descended somewhere near our location, and Annexstad and Benda soon found several of his trail markers from the previous year. We camped, and the next day descended the slope with some care—we had to make a detour at one point when the lead sledge made a hole at the edge of a snow bridge. The lower part of the slope was bare ice, and we used snowmobiles in tandem, one in front pulling and the other behind braking, to transfer each sledge to the bottom. At the bottom, we were on the ice patch within the area where Kyle's party had picked up five meteorites. In a rising wind, we proceeded to a clear, snow-covered spot in an adjacent moraine and set up our camp. We were located about 12 km west of Reckling Peak. During a day and a half spent searching, we recovered 13 meteorites (Figure 7*a*).

Travelling west along the northern edge of the ice patch on January 12, we were off the bare ice surface so we have no knowledge of whether or not meteorites can be found along its entire length. At a point about 65 km west of Reckling Peak we reached a second large moraine which, by a strange configuration of rock debris and ice sculpting, appears on the aerial photos to have the outline of an elephant. We refer to it as Elephant Moraine. One day's searching around Elephant Moraine netted 12 meteorite specimens (Figure 7*b*). On 14 January we recrossed the ice field there, ascended the monocline, and headed south again for a helicopter pickup near Allan Hills.

In assessing the results of this part of the 1979–1980 field effort, several interesting points emerged. The Reckling Peak ice field, 100 km

W.A. Cassidy, Department of Geology and Planetary Science, University of Pittsburgh, Pittsburgh, Pennsylvania 15260. L.A. Rancitelli, Battelle Memorial Institute, Columbus, Ohio 43201.

FIGURE 5.—Snowmobiles pulling sledges across Reckling Peak icefield during traverse from Allan Hills to Reckling Peak.

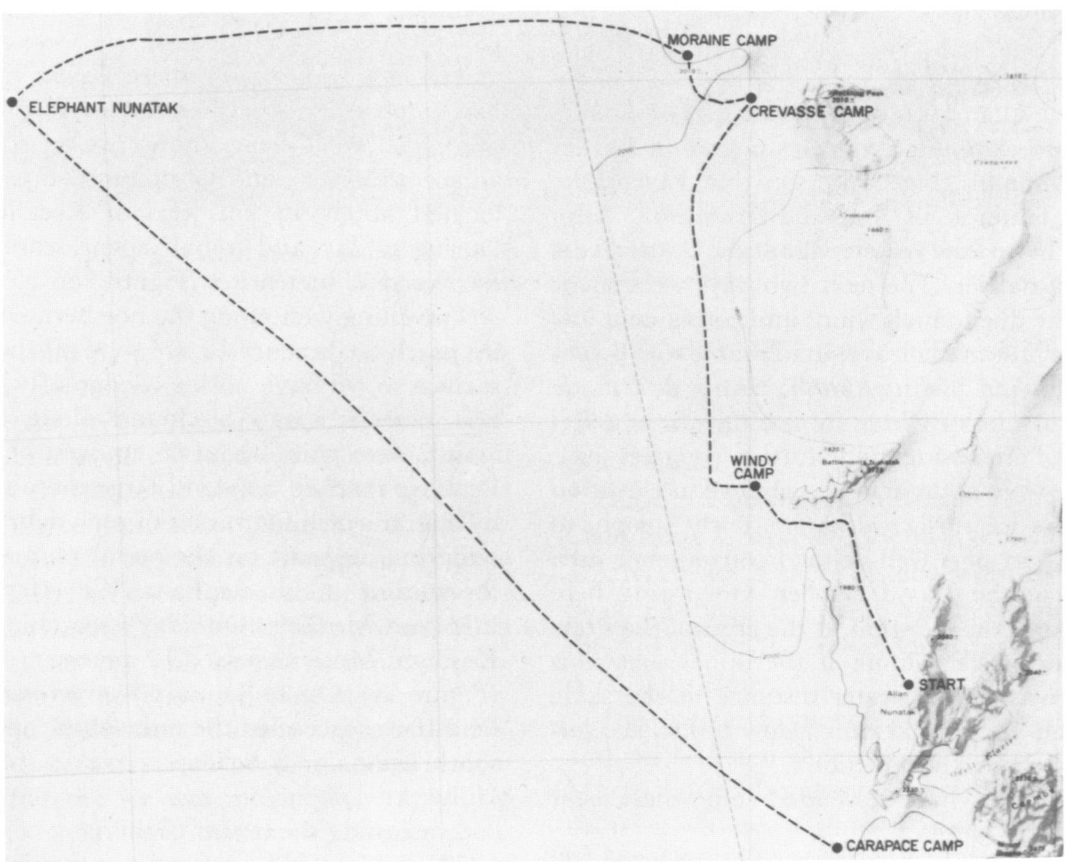

FIGURE 6.—Route of snowmobile traverse from Allan Hills to Reckling Peak and return via Elephant Moraine.

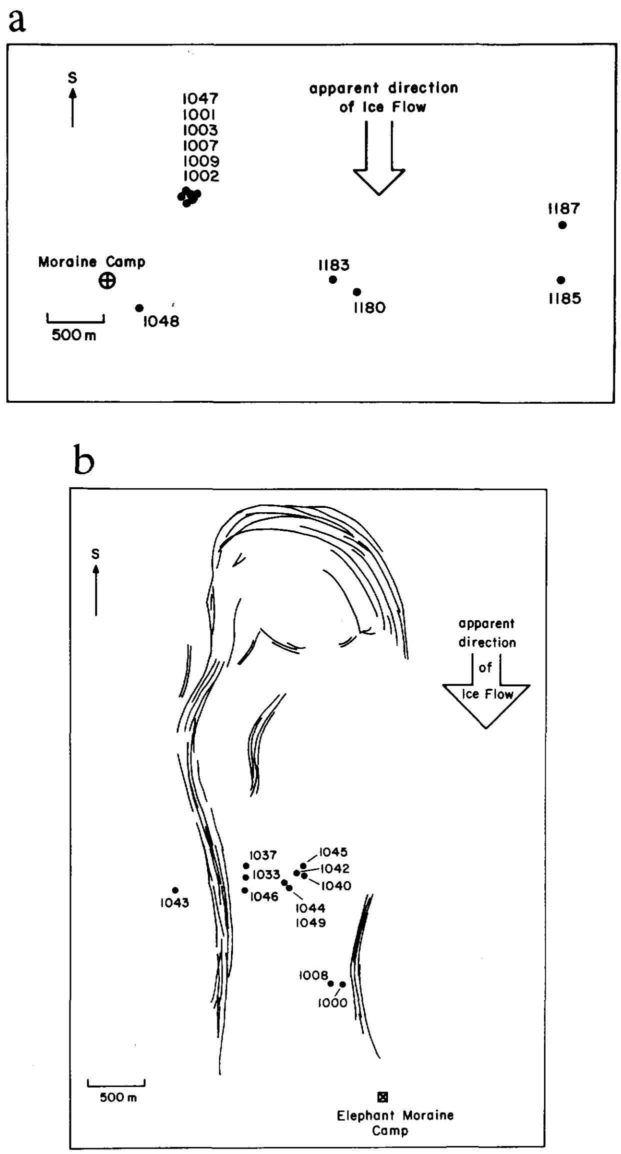

FIGURE 7.—Positions of majority of specimens at two sites relative to apparent direction of ice flow: *a*, Moraine Camp; *b*, Elephant Moraine Camp.

long by several km wide, seems to be associated with a bedrock barrier parallel to its long dimension over which ice spills in the same manner as at the Allan Hills and parts of the Yamato Mountains. This produces a step-like ice surface configuration. Aside from Reckling Peak, no rocks crop out along its entire length although morainal deposits, suggesting the presence of bedrock near the surface, are found at two points.

Meteorites have been concentrated in at least two locations along this linear ice field. They are associated with moraine deposits on the lower level of the ice step, but apparently are not found in such great numbers at Reckling Peak as at the Allan Hills site. The Allan Hills outcrop penetrates the ice and forms an absolute barrier to further ice flow downstream from the monocline. There is no such barrier at the Reckling Peak ice field. This may help explain the lower abundances of meteorites exposed at the latter site. We may find also that meteorite concentrations have a higher surface density when associated with moraines than they do elsewhere along the length of an ice field, because the bedrock barrier is closer to the surface at those locations and the ice may be flowing more slowly there. Further field reconnaissance is necessary before commenting further on this.

Our total recovery on the traverse was 26 specimens. An estimate of possible pairings suggests that at most we recovered only 15 individual falls at the two sites we examined. Of these 15, however, at least four (>25%) were relatively rare types (i.e., one iron and three achondrites; one of the achondrites is a shergottite). Inasmuch as the majority of meteorites in any random collection should be ordinary chondrites, one might project higher total numbers in this area than we report here. Alternatively, these two sites could be presenting samples that fell during some time frame when the meteorite flux at the earth had a different average composition. In either case, the Reckling Peak icefield appears to be a promising site for further work.

ACKNOWLEDGMENTS.—This field work was supported by grant NSF DPP 78100. Louis Rancitelli's efforts were supported in part under NASA contract NAS-9-11712. John Annexstad's expenses were supported in part by his organization, NASA Johnson Space Center.

The Allan Hills Icefield and Its Relationship to Meteorite Concentration

John O. Annexstad

The United States Antarctic Search for Meteorites (ANSMET) has centered on the Allan Hills icefield (76°45′S, 159°40′E) from 1976 through 1979. This area has yielded nearly 700 specimens of varying sizes and types. The main advantage of this icefield for meteorite search is its close proximity to McMurdo Station (230 kilometers) which makes it easily accessible by helicopter.

Figure 8 shows the Allan Hills in relation to McMurdo Station on Ross Island. The icefield extends from the west side of the Allan Hills on to the polar plateau.

The Allan Hills icefield has been described by Nishio and Annexstad (1979) as a limited icefield that has large concentrations of meteorites. The meteorites appear to be concentrated on the lower limb of an ice monocline (Cassidy, 1978) with other finds scattered throughout the field.

In an attempt to understand the mechanisms of meteorite concentration, a triangulation chain was established across the icefield during the 1978–1979 austral summer. This chain is composed of 20 stations, two of which are on bedrock, and extends westward from the Allan Hills a distance of 15 kilometers. Figure 9 shows the triangulation chain and its relationship to the meteorite concentrations.

Each station is marked by a bamboo or aluminum pole set into a 50–100 centimeter hole drilled into the ice or firn (Figure 10). Wild T-2 theodolites were used to establish the positions of each station and to measure their evaluations relative to the datum points (Stations 1 and 2). The datum points are located on bedrock at an adopted elevation of 2054 meters (barometric-altimetry) with a base line length of 1546.26 meters.

A small strain net of four stations, about 650 meters per side, was installed 1 kilometer north of station 11 during late December 1978. Weather problems precluded an accurate survey of this net at that time, but basic data were obtained for ablation measurements.

The triangulation net was resurveyed and the strain net was precisely located during December 1979. Values were measured for the rates of ablation, horizontal movement, and vertical emergence or submergence of the icefield. It should be noted that the first resurvey was accomplished after only one year because of the availability of personnel. Since the accumulated data are only one year old, they must of necessity be considered preliminary. A final resurvey of the triangulation net is planned for the 1984–1985 austral summer season.

John O. Annexstad, Curator's Office, Johnson Space Center, Houston, Texas 77058.

FIGURE 8.—Allan Hills in relation to McMurdo Station on Ross Island; icefield with meteorite concentrations extends from the Allan Hills westward onto polar plateau.

FIGURE 9.—Triangulation chain extending from Allan Hills, where datum points at Stations 1 and 2 are located on bedrock, westward across exposures of blue ice (dots = meteorite finds).

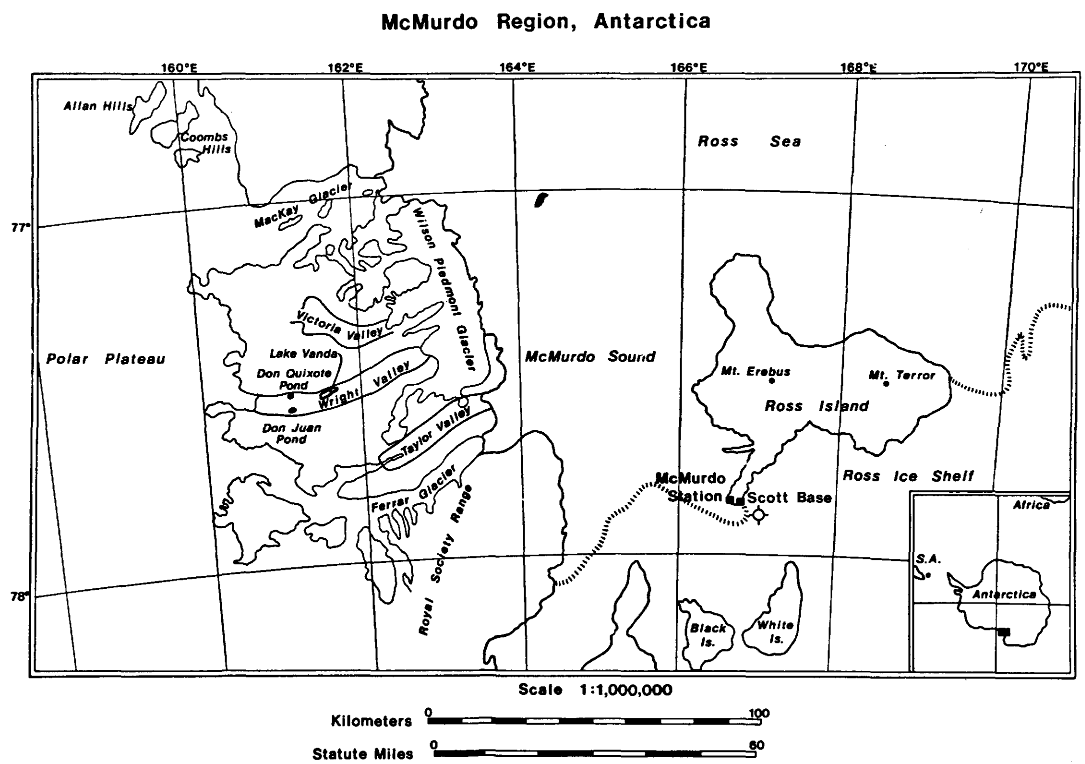
McMurdo Region, Antarctica
160°E
162°E
164°E
166°E
168°E
170°E
77°
78°
Allan Hills
Coombs Hills
Ross Sea
MacKay Glacier
Wilson Piedmont Glacier
Victoria Valley
Polar Plateau
Lake Vanda
Don Quixote Pond
Wright Valley
Don Juan Pond
Taylor Valley
Ferrar Glacier
Royal Society Range
McMurdo Sound
Mt. Erebus
Mt. Terror
Ross Island
Ross Ice Shelf
McMurdo Station
Scott Base
Black Is.
White Is.
Africa
S.A.
Antarctica
Scale 1:1,000,000
Kilometers
0
100
Statute Miles
0
60

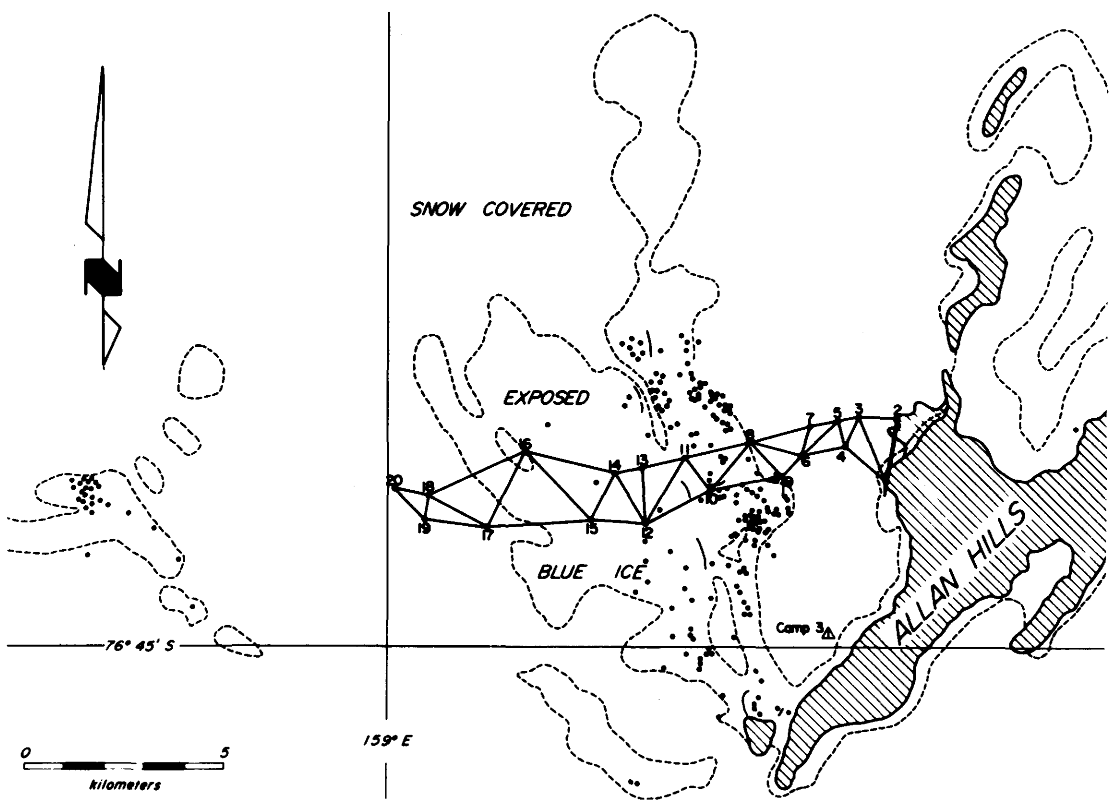
SNOW COVERED
EXPOSED
BLUE ICE
ALLAN HILLS
Camp 3
76° 45' S
159° E
0
5
kilometers

FIGURE 10.—Setting up triangulation network station: *a*, drilling ice with SIPRE auger; *b*, implanting bamboo flagpole to measured depth; *c*, locating survey point by theodolite.

TABLE 2.—Allan Hills triangulation network, preliminary survey data

Station number	*Elevation*	*Ablation (cm/yr)*	*Emergence (+) or submergence (−) velocity (cm/yr)*	*Horizontal velocity (cm/yr)*	*Type surface*
1	2054.00	0	0	0	Rock
2	1909.86	0	0	0	Rock
3	1945.69	−2.3	−0.6	7	Firn
4	1955.71	−2.3	−0.6	6	Firn
5	1952.81	−1.1	−0.8	10	Firn
6	1954.14	−1.6	+1.9	20	Firn
7	1951.79	−2.5	−1.2	17	Firn
8	1946.67	−3.7	+1.4	50	Firn
9	1949.42	−4.2	+4.6	30	Ice
10	1945.19	−6.5	+6.7	80	Ice
11	1944.51	−5.6	+7.1	100	Ice
12	2030.50	−4.5	−1.7	123	Ice
13	2008.37	−5.6	+6.5	129	Ice
14	2014.37	−7.0	+0.8	121	Ice
15	2046.54	−5.7	−2.7	140	Ice
16	2022.05	−4.2	−1.2	182	Ice
17	2075.30	−5.1	−1.0	202	Ice
18	2067.58	−4.5	−1.0	237	Ice
19	2075.06	−3.1	−3.5	234	Firn
20	2070.81	−1.8	−2.5	251	Firn
A	NA	−6.4	NA	NA	Ice
B	NA	−6.2	NA	NA	Ice
C	NA	−6.0	NA	NA	Ice
D	NA	−5.0	NA	NA	Ice

Table 2 (Annexstad and Nishio, 1980) shows a listing of each station along with its elevation, ablation rate, vertical velocity, horizontal velocity, and type of surface. Because the small 4-station strain net (Stations A,B,C,D) was not precisely located until December 1979, only the rate of ablation for the first year could be included.

The icefield gradually increases in altitude from those stations located near the Allan Hills to the westernmost region at Station 20. Stations 1 and 2 are located on bedrock with Station 1 on a promontory overlooking the icefield. The field exhibits a steplike topography between Stations 11 and 12 where the altitude increases 85 meters in less than a kilometer. The main area of meteorite concentration appears to be in the region of those stations (10 and 11) located on the lower part of the step.

Using Stations 10 and 11 as a guide in respect to the meteorite concentration mechanism, it can be seen that the rate of ablation is fairly constant at −6.5 and −5.6 cm per year respectively. This value compares closely with the rate of ablation measured by Naruse (1978) in the productive meteorite icefield near the Yamato Mountains. If all the stations are considered, (see Figure 11), the rate of ablation ranges from a low of 1.1 cm per year at Station 5 to a high of 7.0 cm per year at Station 14. The average rate of ablation on the ice surface alone is 5.7 cm per year (Figure 12) while that of the firn surface is less: 2.7 cm per year. The higher rate of ablation must be due to the more rapid sublimation of the ice surface once it is exposed. It is interesting to note, however, that the ice or firn is wearing away gradually at all 22 stations.

The velocity of emergence (+) or submergence

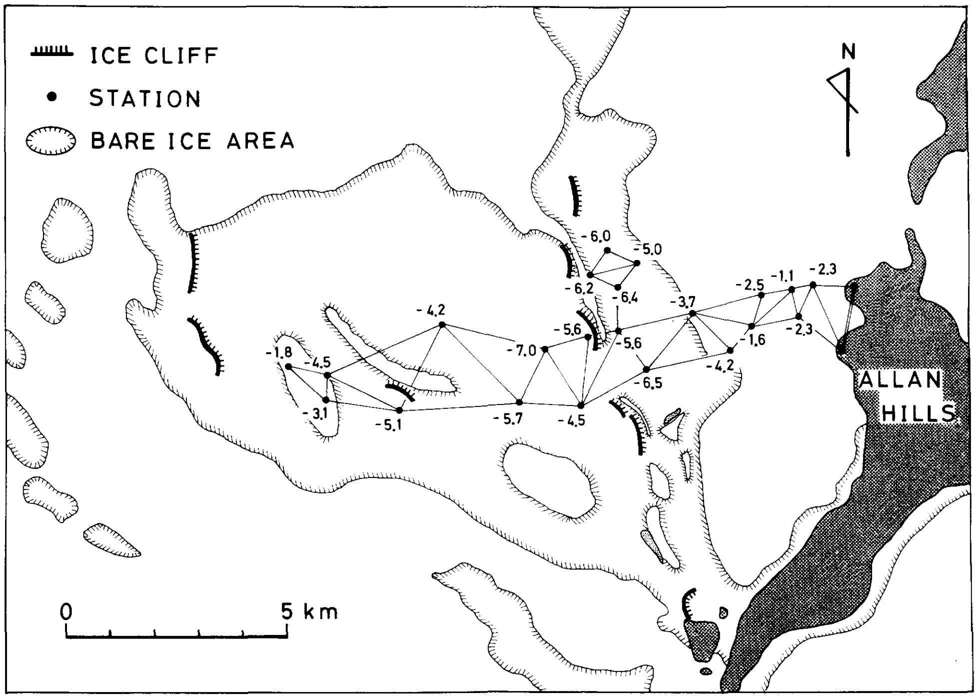

FIGURE 11.—Rates of ablation measured (cm) after one year at Allan Hills icefield (after Nishio and Annexstad, 1980).

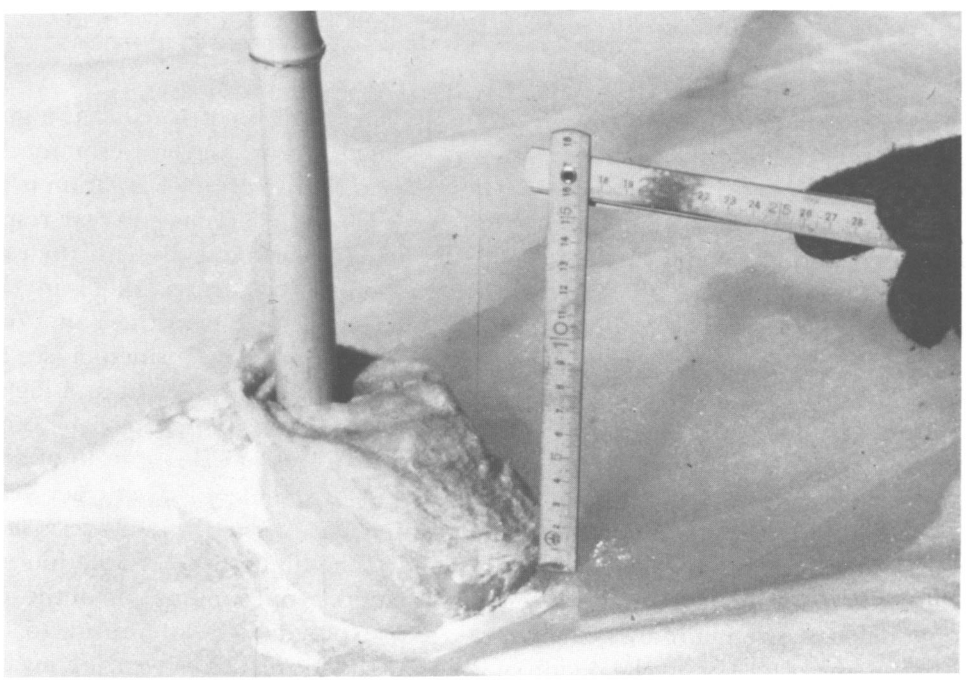

FIGURE 12.—Ablation lowered surface at Station 14 about 7 cm between 1978 and 1979 field seasons.

(−) is not so clear as the value of ablation. Nishio and Annexstad (1980) report that the relative error in these measurements can be as high as 100% at some stations. The authors note that these errors are the result of small velocity values after only one year that cannot be measured accurately within the tolerances of the instruments. It is instructional, however, to look at the values in the vicinity of Stations 10 and 11. In this region of the highest meteorite concentration it appears that the emergent velocity and the ablation rates nearly balance. It is possible that a steady state condition does exist in this part of the Allan Hills icefield.

The horizontal velocity gradually increases from a low of 6 cm per year at Station 4 to 251 cm per year at Station 21. Figure 13 shows a schematic representation of the horizontal ice flow by both vector direction and magnitude. The vector direction gradually shifts from NE at the westernmost station to nearly E as the Allan Hills are approached. The change in magnitude as the ice nears the hills indicates that the icefield is slowing down toward stagnation.

Although the Allan Hills icefield has yielded over 700 meteorite fragments, it still is a limited area of concentration. The direction of the horizontal movement vectors at the westernmost sta-

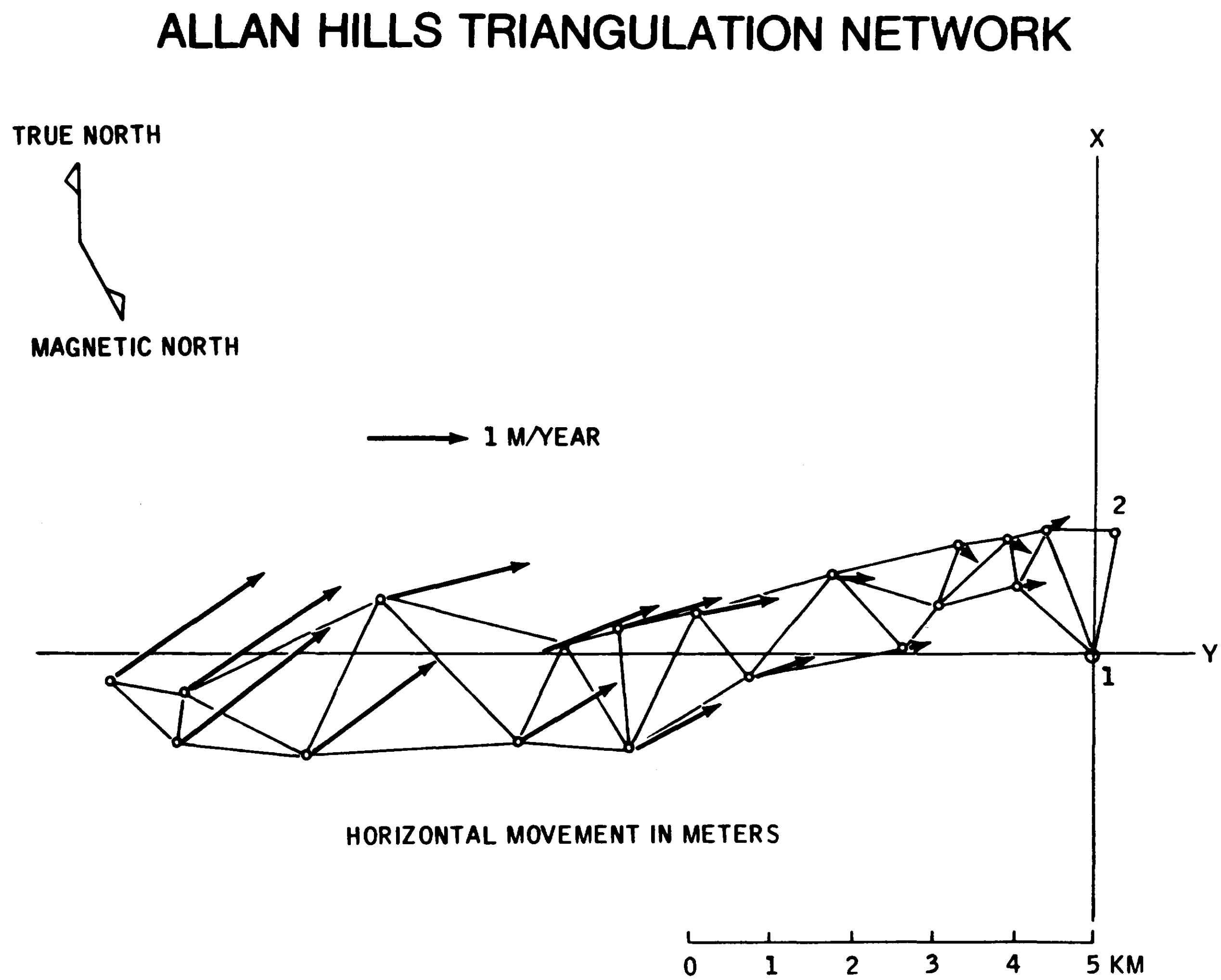

FIGURE 13.—Vector directions and magnitudes of ice flow across triangulation chain.

tions indicate that the flow of the icecap is generally NE in that vicinity. This implies that most of the ice flows into the large David Glacier (Drewy, 1980) that is north of the Allan Hills. Therefore, the majority of meteorites collected by the icecap are probably deposited by the large outlet glaciers that drain extensive sections of the eastern Antarctic icesheet. This might help to explain why the region around the dry valleys, where the glaciers are small and have correspondly small catchment areas, produce few meteorites. The Allan Hills area appears to be on the fringe of the major flow into the David Glacier with its correspondingly large catchment area. It is predicted that other blue ice fields that intercept large flow areas have the potential for producing many meteorites.

Descriptions of Stony Meteorites

Roberta Score, Trude V. V. King, Carol M. Schwarz, Arch M. Reid, and Brian Mason

This section provides descriptions of the individual specimens, arranged by class. Within the chondrites, the specimens are grouped according to the Van Schmus-Wood (1967) classification, and the descriptions follow the order of increasing petrographic type. The descriptions are based largely on those published in the Antarctic Meteorite Newsletter, with additional information as available. The letter-number designation for each meteorite concurs with guidelines recommended by the Committee on Nomenclature of the Meteoritical Society; it carries the following information: ALH (Allan Hills); A78 (Expedition A, 1978); XXX (digits indicating the number of the specimen). The original weight of the specimen is given to the nearest gram (nearest 0.1 gram for specimens weighing less than 100 grams).

This section comprises material on all characterized meteorites collected during the 1978–1979 and 1979–1980 field seasons, together with descriptions of some meteorites collected during the 1977–1978 field season and not included in the previous catalog (King et al., 1980). Specimens weighing less than 100 grams are listed without descriptions, unless they show distinctive features.

Roberta Score, Trude V. V. King, and Carol M. Schwarz, Northrop-Houston, Johnson Space Center, Houston, Texas 77058. Arch M. Reid, Geology Department, University of Cape Town, Rondebosch, South Africa. Brian Mason, Department of Mineral Sciences, National Museum of Natural History, Smithsonian Institution, Washington, D.C. 20560.

Chondrites

Class C2

Figure 14

ALHA78261 (5.1 g).—This triangular stone (2.5 × 1.5 × 1.0 cm) is totally covered with thin, dull black, polygonally fractured fusion crust, except along the edges where the fusion crust has abraded away. The matrix revealed in these areas is greenish black and has small (<1 mm), rounded, and irregular white clasts throughout. Small voids, as much as 1 mm in diameter, are present on two surfaces. Chipping the specimen during processing revealed abundant rounded and irregular inclusions in the meteorite.

The section shows numerous tiny grains (up to 0.1 mm) and irregular aggregates (up to 0.3 mm) of olivine and polysynthetically twinned clinopyroxene, and a few small chondrules, in a translucent isotropic olive-brown matrix. The section contains very little troilite as minute scattered grains, and a little nickel-iron as inclusions in the chondrules. Porous fusion crust, up to 2.5 mm thick, rims part of the section. Microprobe analyses show that both olivine and pyroxene have variable composition. Olivine ranges from Fa_0 to Fa_{50}, with an average of Fa_6; it has a notable chromium content, Cr_2O_3 ranging from 0.3–0.6 weight percent. Pyroxene is generally close to clinoenstatite in composition, ranging from Fs_1 to Fs_8, with an average of Fs_7. This meteorite shows

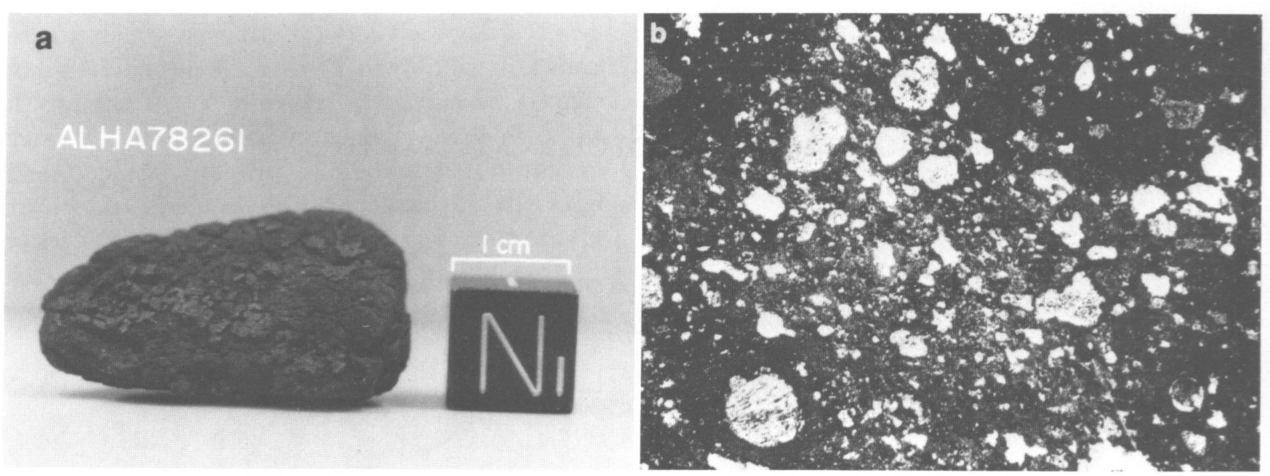

FIGURE 14.—ALHA78261, C2 chondrite: *a*, Remnants of fusion crust (lighter gray) present; *b*, photomicrograph of thin section (area of field is 3 × 2 mm); irregular grains and rare chondrules, mainly of olivine (white to light gray) in translucent to opaque matrix (dark gray to black).

a close similarity to ALHA77306, and is tentatively paired with it.

CLASS H3

FIGURE 15

ALHA78084 (14280 g).—This is a complete stone, covered with splotchy brown and black fusion crust. Several large fractures penetrate the interior. A thin white deposit was evident along some of these cracks after the meteorite was dried. Many light-colored, rounded, and irregular inclusions are apparent on the cut faces, some as large as 4 mm in diameter. Metal is visible, though most of the metal grains have oxidation halos around them, giving the cut faces a marbled look of small fresh areas and large oxidized areas.

The section shows a close-packed aggregate of chondrules, 0.3–1.2 mm in diameter, and a few angular enclaves (some are chondrule fragments) in a minor amount of fine-grained matrix. A wide variety of chondrules is present, the commonest being porphyritic olivine and olivine-pyroxene with interstitial glass; some of the glass is brown and transparent, but much of it is turbid and partly devitrified. The pyroxene is polysynthetically twinned clinobronzite. The matrix contains a considerable amount of fine-grained nickel-iron and a lesser amount of troilite. Weathering is extensive, with veins and patches of brown limonite throughout the section. Microprobe analyses show olivine of rather uniform composition, averaging Fa_{18}, and pyroxene of variable composition, Fs_{8-24}, average Fs_{13}. The mean composition of the olivine and the amount of nickel-iron indicate H group and the meteorite is tentatively classified as an H3 chondrite.

CLASS L3

FIGURES 16, 17

ALHA78038 (363 g).—This angular specimen is approximately 12 × 5 × 5 cm and appears shiny and reddish brown due to weathering and staining by iron oxidation. Several fractures penetrate deeply into the sample. One small remnant patch of shiny black fusion crust remains on the B surface. During processing the sample fell apart and revealed no unoxidized material.

The section shows a close-packed aggregate of chondrules, 0.3–2.7 mm in diameter, and a few angular enclaves (some are chondrule fragments) in a minor amount of dark fine-grained matrix. A wide variety of chondrule types are present, the

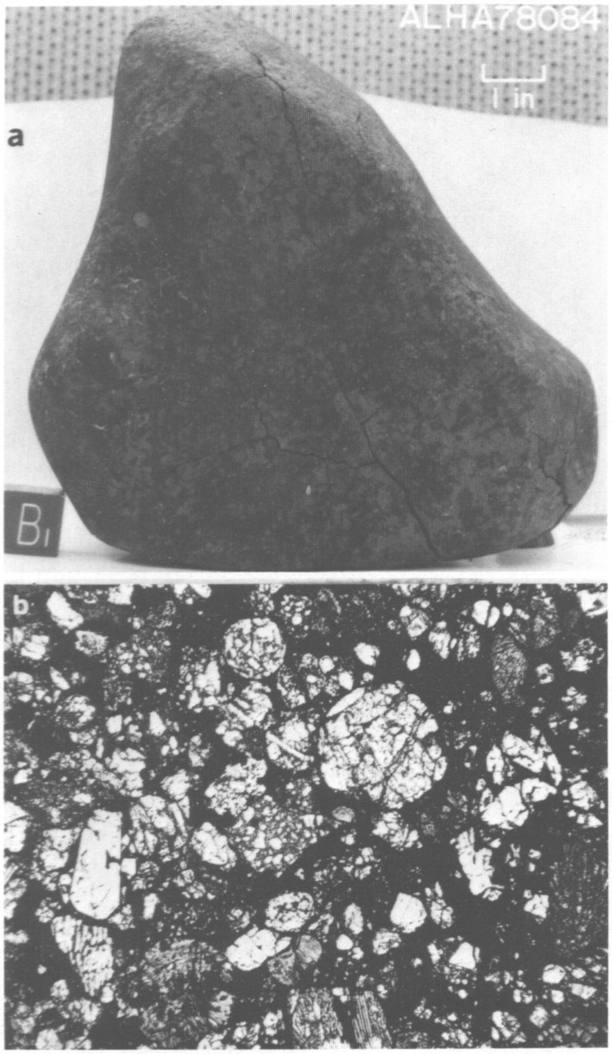

FIGURE 15.—ALHA78084, H3 chondrite: *a,* fusion crust coats the stone, which shows several penetrating fractures; *b,* photomicrograph of thin section (area of field is 3 × 2 mm); closely packed aggregate of chondrules and angular enclaves set in minor amount of dark matrix.

three commonest being granular olivine and olivine-pyroxene, porphyritic olivine, and fine-grained pyroxene. Most of the pyroxene is polysynthetically twinned. Many of the chondrules have dark rims. Troilite is present in minor amounts in the matrix. Weathering is extensive. The section is rimmed and veined with brown limonite, and little nickel-iron remains. Microprobe analyses show olivine ranging from Fa_4 to Fa_{19}, with a mean of Fa_{22}; pyroxene ranges from Fs_2 to Fs_{19}, with mean of Fs_8, and CaO ranging from 0.1 to 1.3 weight percent. The low content of nickel-iron and troilite suggests L group, and the meteorite is tentatively classified as L3 chondrite.

ALHA78188 (0.8 g).—The thin section shows a close-packed aggregate of chondrules, 0.3–1.2 mm across, with a relatively small amount of matrix. Porphyritic olivine chondrules contain intergranular glass, some of which is transparent brown but much is turbid from partial devitrification. Other chondrules consist of granular olivine and polysynthetically twinned low-Ca clinopyroxene. Many chondrules have dark rims consisting largely of troilite. A little nickel-iron is present. Weathering is extensive, with veins and patches of brown limonite throughout the section. Microprobe analyses show variable composition for both olivine and pyroxene: olivine, Fa_{1-34}, average Fa_{15}; pyroxene, Fs_{5-29}, average Fs_{17}.

ALHA79001 (32.3 g).—The polished thin section shows a closely packed aggregate of chondrules, 0.2–2.0 mm in diameter, and irregular crystalline aggregates, set in a small amount of dark, fine-grained matrix that includes minor subequal amounts of nickel-iron and troilite. A considerable variety of chondrules is present, the most common being granular olivine with or without polysynthetically twinned clinopyroxene, porphyritic olivine, and fine-grained pyroxene. Some chondrules have intergranular, transparent, pale brown glass, in others the glass is turbid and partly devitrified. Some weathering is indicated by the presence of a moderate amount of brown limonite as veins and patches. Microprobe analyses show a wide range in the composition of olivine (Fa_{6-39}) and pyroxene (Fs_{2-31}); the pyroxene is a low-calcium clinopyroxene (CaO = 0.2–1.8%). This range of composition, together with the presence of glass and twinned clinopyroxene, indicates type 3, and the small amount of nickel-iron suggests L group; the meteorite is therefore tentatively classed as an L3 chondrite.

ALHA79003 (5.1 g).—The section is texturally identical and the olivine and pyroxene show a

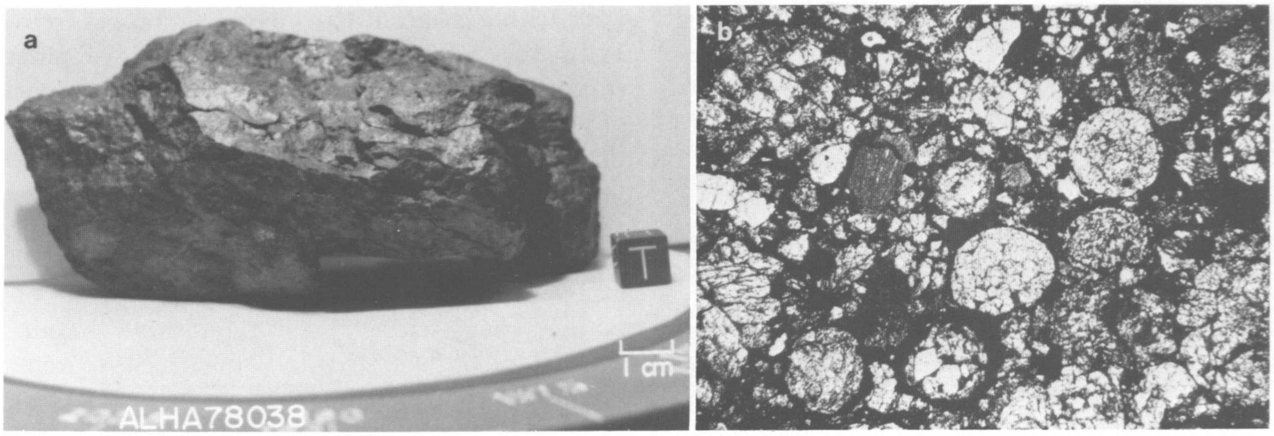

FIGURE 16.—ALHA78038, L3 chondrite: *a*, surface bounded by fractures and little or no fusion crust remains; *b*, photomicrograph of thin section (area of field is 3 × 2 mm); round chondrules and irregular enclaves in dark, fine-grained matrix.

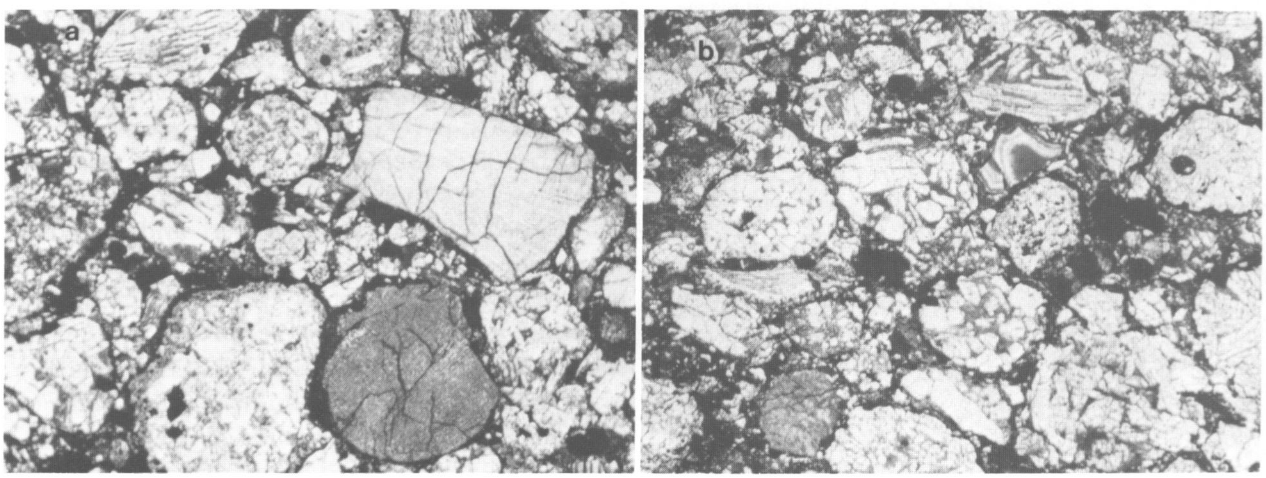

FIGURE 17.—Photomicrographs of thin sections of L3 chondrites (area of fields is 3 × 2 mm): *a*, ALHA79001; *b*, ALHA79003. (Closely packed aggregates of chondrules and angular enclaves set in minor amount of dark matrix).

similar range of composition to these minerals in ALHA79001; hence these two specimens are probably pieces of a single meteorite.

ALHA79022 (31.4 g).—This stone (3.5 × 2.5 × 2 cm) is mostly covered with dull black fusion crust. The areas devoid of fusion crust appear to have been spalled off or preferentially plucked off because they occur along ridges. Chipping the stone exposed a relatively fresh, light gray interior, with many inclusions of various colors from black to white. The largest inclusion is white and 7 mm in longest dimension. A narrow (<1 mm) weathering rind is present.

The thin section shows well-developed chondritic structure, with chondrules ranging up to 1.8 mm in diameter; some have dark rims consisting largely of troilite. The commonest chondrules are granular and porphyritic olivine, with intergranular glass; some of the glass is brown and transparent, but most is turbid and partly devitrified. The groundmass consists largely of fine-grained olivine and pyroxene, with minor amounts of nickel-iron and troilite; limonitic staining is present around the metal grains. Much of the pyroxene is polysynthetically twinned. Microprobe analyses show olivine and pyroxene of variable composition: olivine, Fa_{1-28}, average Fa_{17}; pyroxene, Fs_{9-22}, average Fs_{16}.

ALHA79045 (115 g).—This specimen (5.5 × 4.5 × 3 cm) has a small patch of weathered fusion crust on one surface; an iridescent, reddish-brown coating on other areas may be remnant fusion crust. The rest of the stone is dull red-brown, but its clastic nature is clearly visible. One clast is 4 mm across and yellow. The thin section shows a close-packed aggregate of chondrules, 0.3–2.1 mm across, and irregular clasts (some of them chondrule fragments), with a relatively small amount of matrix material. Chondrule types include porphyritic and granular olivine and olivine-pyroxene, barred olivine, and fine-grained pyroxene. Some chondrules have black, troilite-rich rims. Intergranular glass in chondrules may be transparent and pale brown, but is usually turbid and partly devitrified. Only a small amount of nickel-iron is present. Most of the pyroxene shows polysynthetic twinning. Brown limonitic staining pervades the section. Microprobe analysis show variable composition for both olivine and pyroxene: olivine, Fa_{2-38}, average Fa_{23}; pyroxene Fs_{2-29}, average Fs_{8}.

RKPA79008 (72.9 g).—Black fusion crust covers about half of the stone. Areas devoid of fusion crust are greenish black and show numerous rounded and irregular clasts, up to 2 mm across, and cream to black in color; two larger cream-colored clasts, 7 and 15 mm in largest dimension, are also visible. The stone is extensively fractured.

The thin section shows abundant chondrules, 0.3–1.8 mm in diameter; a wide variety of types is present, the three commonest being granular olivine and olivine-pyroxene, barred olivine, and fine-grained pyroxene. The granular chondrules have intergranular glass, sometimes pale brown and transparent, but commonly turbid and partly devitrified. Irregular clasts, some of them chondrule fragments, are also present. Some of the pyroxene in the chondrules is polysynthetically twinned clinoenstatite or clinobronzite. The matrix is fine-grained olivine and pyroxene, with minor subequal amounts of nickel-iron and troilite. Remnants of fusion crust, up to 0.3 mm thick, are present along one edge. Minor weathering is indicated by brown limonitic staining in association with the fusion crust and nickel-iron grains. Microprobe analysis show that most of the olivine has composition Fa_{23}, but a range of composition Fa_{1-29} is present; pyroxene composition is variable, Fs_{2-28}, average Fs_{15}.

Class H4

Figures 18, 19

ALHA77221 (229 g).—All surfaces of the meteorite, except the S surface, have remnant patches of thin, dull black fusion crust. The exterior surfaces, devoid of fusion crust, are stained by iron oxidation. Several clasts, approximately 1 mm in diameter, are apparent on the S surface. The specimen is fractured. Chipping revealed no unweathered material in the interior of the sample.

ALHA77223 (207 g).—The T surface of this specimen has patches of dull black fusion crust. The remainder of the sample is stained reddish brown by iron oxidation. The surfaces devoid of fusion crust are fracture surfaces. Several cracks penetrate the sample.

ALHA77225 (5878 g).—This stone (20 × 19 × 11 cm) has no fusion crust and is uniformly weathered and stained reddish brown; however, some surfaces are more shiny than others. It is extensively fractured. One brassy colored clast, possibly a troilite nodule, is present on the T surface. The B surface has what appear to be slickensides, but because of the severe weathering of the specimen it is impossible to determine this unambiguously. No unweathered material is present on the exterior of the sample. When the specimen was cleaved it fell into many pieces. No unweathered material was exposed.

ALHA77226 (15323 g).—A small patch of dull black fusion crust is present on the S surface. The

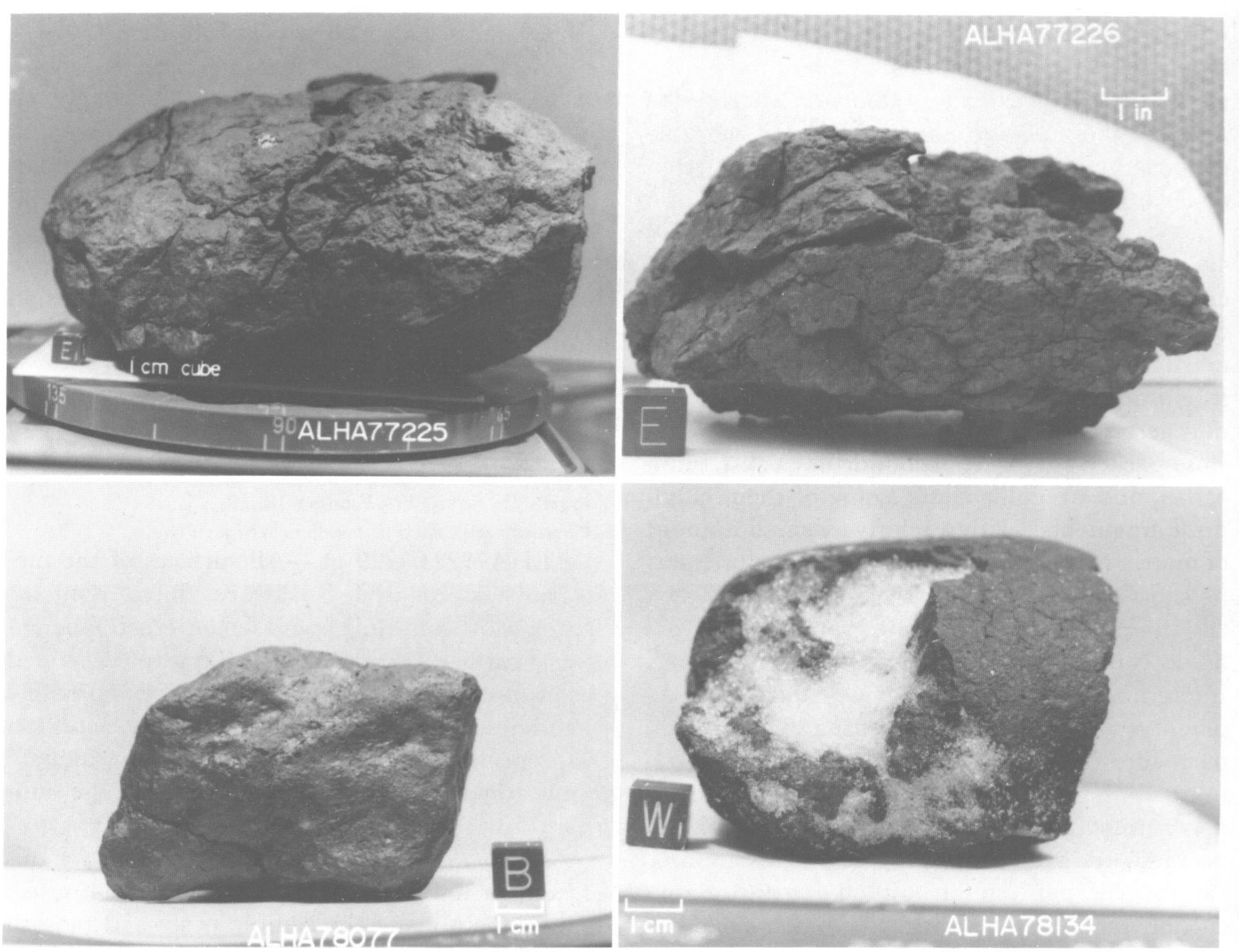

FIGURE 18.—H4 chondrites. (Note snow and ice on ALHA78134, present when specimen was unpacked at Johnson Space Center).

W surface is concave and flow bands are present in the T-B direction. The specimen is severely fractured and crumbled into many pieces during processing. Except for a few, small, light gray areas, nearly all the material exposed is extensively stained by iron-oxides.

ALHA77232 (6494 g).—The stone (20 × 19 × 14 cm) is rounded, and only small patches of remnant fusion crust remain on the exterior surface. It is severely weathered, uniformly stained reddish brown, and fractured. When the sample was sawed it crumbled into many pieces. No fresh, unoxidized surfaces were exposed during processing. White deposits developed on some surfaces of the meteorite while it dried in the nitrogen cabinet.

ALHA77286 (245 g).—The B surface and portions of the N surface are devoid of fusion crust. The remaining surfaces have remnants of a thin black fusion crust. The surfaces lacking fusion crust are rough on a small scale. It appears that many ~1-mm inclusions produce the roughness. Chondrules and lithic clasts are present. No unweathered material was exposed when the stone was sawed.

ALHA78053 (179 g).—This 8.0 × 6.0 × 2.5 cm specimen has a small amount of thin, shiny black fusion crust on the B face. The remainder of the

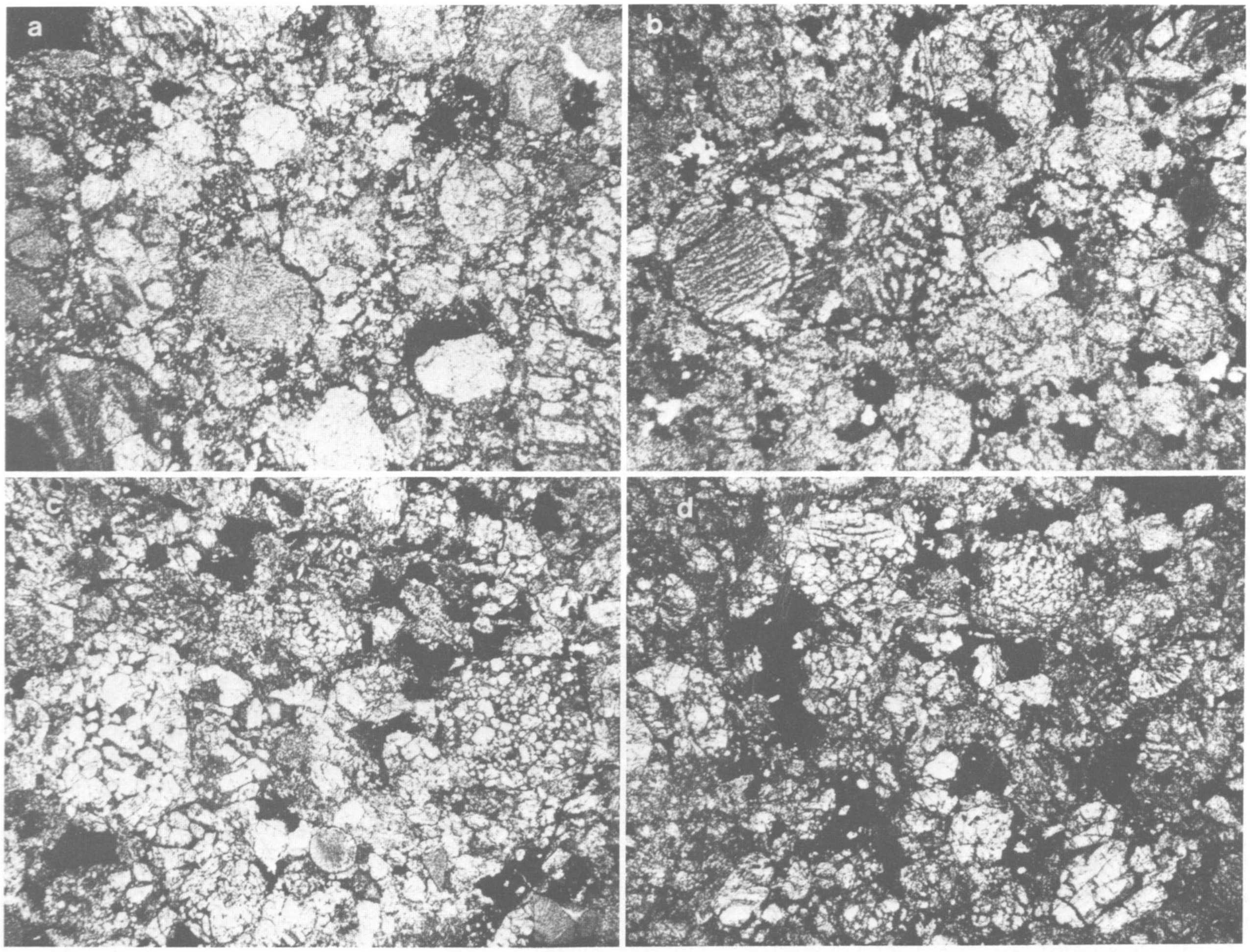

FIGURE 19.—Photomicrographs of thin sections of H4 chondrites (area of fields is 3 × 2 mm): *a*, ALHA77221; *b*, ALHA77223; *c*, ALHA77232; *d*, ALHA78134. (Chondritic structure well developed, but some chondrule margins tend to merge with granular matrix.)

sample is smooth, weathered, and stained reddish brown by iron oxidation. Fractures are present on the T and B surfaces. No unweathered material was exposed during processing.

ALHA78077 (330 g).—Thin, shiny black fusion crust covers this 6.5 × 6.0 × 5.0 cm stone. In spots the fusion crust is weathered away, revealing a smooth, brownish-red surface. Several deep cracks penetrate the sample. During processing the sample cleaved along one of these fractures, revealing no unoxidized material.

ALHA78134 (458 g).—The stone (7.0 × 5.0 × 7.5 cm) has dull black fusion crust on about 40% of the surface. The remaining surfaces are weathered and stained by iron oxidation. On the S surface the inclusions in the meteorite have a higher relief then the surrounding matrix, probably as a result of preferential weathering. Inclusions (chondrules and lithic fragments) are visible on the other fracture surfaces but have not experienced any preferential weathering. Several large fractures penetrate the meteorite. When it was divided during processing, 60% of the interior was stained reddish brown. The remaining 40% is light gray and contains many clasts 1 mm or less in size.

ALHA79030 (108 g).—This 6 × 5 × 2.5 cm stone is totally covered with thin, black fusion crust that has a blistery texture on the B surface. The T surface is concave and the B surface is flat. Most of the interior is somewhat weathered, although areas of light gray material are present.

META78001 (624 g).—This stone (14.5 × 8 × 3 cm) is shaped like a boomerang and is entirely covered with fusion crust. The fusion crust on the B surface has an iridescent sheen, is much thinner than the fusion crust on the remainder of the sample, and has a well-defined area of weathering 1 cm from the edge of the sample. Remaining surfaces have dull, brownish-black fusion crust. Small regmaglypts are apparent on the T and N surfaces and flow bands are present on the B surface at the E and W ends. Small fractures exist on the T and B surfaces, but they do not appear to penetrate the stone. The interior material ranges from being completely weathered and iron-oxide stained to unweathered. The weathered portions are massive and are preferentially located in the T half of the sample. The unweathered areas are light grayish green and contain unoxidized metal grains.

RKPA78002 (8483 g).—This tabular-shaped meteorite (17 × 13.5 × 17 cm) has two flat and two semi-rounded surfaces with sharp ridges. Black, polygonally fractured fusion crust, 0.5 mm thick, covers the entire specimen except for areas along the ridges where it has broken off. The areas without fusion crust are greenish brown and contain numerous inclusions. One fraction penetrates the interior of the meteorite. After drying for several days in the nitrogen cabinet, minute amounts of white deposit appeared along the polygonal fractures. The cut face reveals a weathering rind 1–4 mm thick. Abundant metal blebs are obvious, with most of the metal having oxidation halos around them.

RKPA78004 (166 g).—All but one surface is covered with thin, dull black fusion crust, although portions of the fusion crust on another surface appear to have been physically plucked away. The portions devoid of fusion crust are shiny reddish brown. Chipping this small stone was impossible. Sawing revealed an interior with many clasts discernible in the dark gray matrix. Metallic grains are present. On the cut face it appears that the inclusions in the meteorite have a more dense population around the circumference, from the exterior margin to a depth of approximately 1 cm.

H4 chondrites weighing less than 100 g are ALHA78193, 13.3 g; 78196, 11.1 g; 78223, 6.4 g; 79023, 68.1 g; 79035, 37.6 g.

The thin sections of the H4 chondrites resemble each other closely. They all show well-developed chondritic structure, chondrules 0.2–1.8 mm in diameter. (ALHA77221 has some unusually large chondrules, ranging up to 3 mm in diameter.) A variety of chondrule types is seen, the four commonest being porphyritic to granular olivine, barred olivine, fine-grained pyroxene, and granular olivine-pyroxene. The chondrules are set in a fine-grained, granular matrix consisting largely of olivine and pyroxene, with minor amounts of nickel-iron and troilite (nickel-iron in greater amount than troilite). Much of the pyroxene is polysynthetically twinned clinobronzite. All these meteorites except META78001 and RKPA78002 are considerably weathered, with brown limonitic staining throughout the sections, and veins and patches of limonite often associated with the nickel-iron grains. The section of META78001 shows areas of blackening that appear to be due to fine-grained troilite, possibly a shock effect. Microprobe analyses (Appendix Table A) show that the olivine in these meteorites has essentially uniform composition (Fa_{17-18}); pyroxene may have uniform composition (Fs_{15-16}), but in many of these H4 chondrites shows some variability.

Class H5

Figures 20, 21

ALHA77259 (294 g).—This appears to be a nearly complete stone, with only a small area of the T surface not intact; this area is weathered yellowish brown and shows traces of inclusions. The rest of the surface shows remnant patches of dull black fusion crust over a weathered surface stained reddish brown with iron oxide. Regmaglypts are present on the E/S surface.

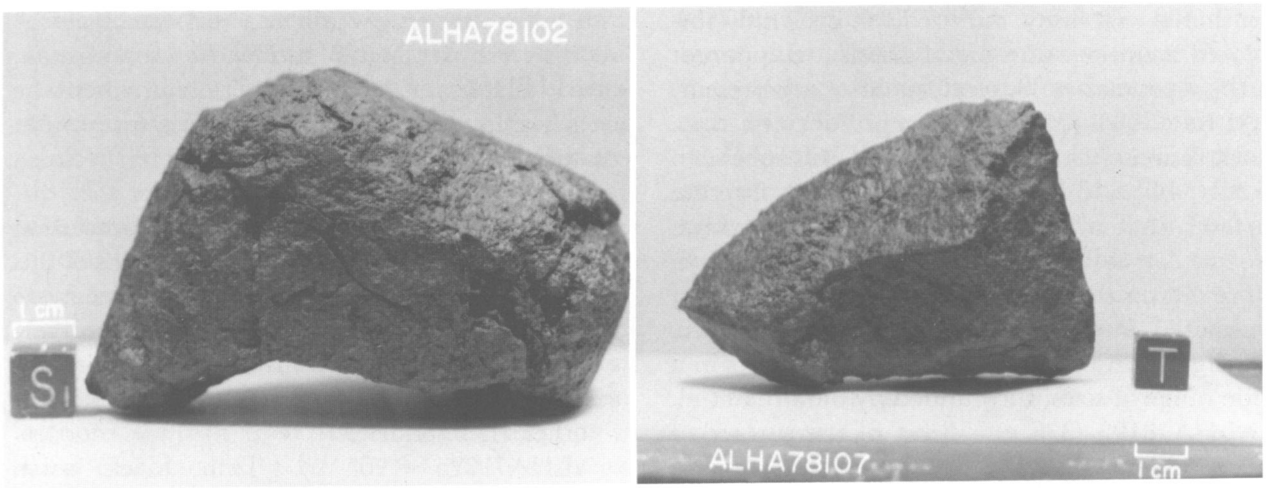

FIGURE 20.—H5 chondrites: ALHA78102, rounded weathered stone with small patches of remnant fusion crust; ALHA78107, angular stone bounded largely by fractures.

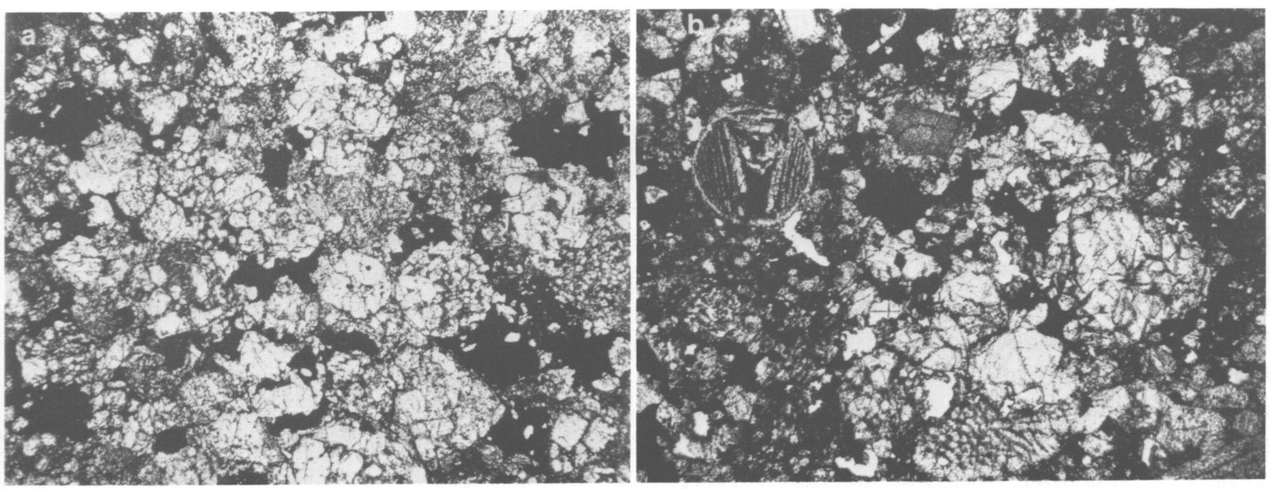

FIGURE 21.—Photomicrographs of thin sections of H5 chondrites (area of fields is 3 × 2 mm): *a*, ALHA77259; *b*, ALHA78107. (Chondritic structure easily discernible, but many chondrules show partial integration with granular matrix.)

ALHA77268 (272 g).—This appears to be a complete specimen with dull black fusion crust on all surfaces. One small area with an iridescent sheen is present on the T surface. A large fracture penetrates the entire stone. No unweathered material was exposed during processing.

ALHA77274 (288 g).—A small patch of black fusion crust remains on the B surface. The other surfaces are devoid of fusion crust and are stained reddish brown with iron oxides.

ALHA77287 (230 g).—Small patches of remnant fusion crust are preserved on the T and B surfaces. The remaining surfaces are smooth and weathered reddish brown. Small areas of the surface have an iridescent sheen. No unweathered material was exposed during processing.

ALHA78075 (280 g).—Thin, shiny fusion crust covers most of this (7 × 6 × 3 cm) specimen, with the exception of portions of the T and W faces. Areas devoid of fusion crust are smooth and weathered to a shiny, dark reddish brown. Light-colored inclusions and metal grains are apparent in the dark matrix. Several fractures are present.

ALHA78085 (219 g).—Except for very thin, black fusion crust on the B surface, this specimen (6.5 × 4.5 × 3.5 cm) is bounded by fracture surfaces that are weathered to a dark reddish brown. A small clast (~2 mm), possibly troilite, is present on the T surface. Processing revealed a brecciated interior with a light-dark structure. The light portion consists of numerous clasts in a wide range of sizes, surrounded by dark material.

ALHA78102 (336 g).—Most of the surface of this specimen (9 × 6 × 6 cm) is weathered and stained by iron oxidation and spotted with small patches of black fusion crust. The specimen is totally weathered except for the innermost material, which contains many small (up to 3 mm) dark clasts.

ALHA78107 (198 g).—The B, S, and portions of the E surfaces are covered with thin, black, polygonally fractured fusion crust that is slightly stained by iron oxides. Shallow regmaglypts are present on the S surface. Other surfaces are fractured and are weathered and stained reddish brown. No unweathered material was seen during processing.

ALHA78108 (172 g).—Remnants of fusion crust are present on the T and N surfaces, the specimen (6.0 × 5.5 × 4.0 cm) being elsewhere bounded by weathered, red-brown fracture surfaces. The specimen appears to be severely shocked and brecciated. Many slickensided surfaces were exposed during processing. Two black veins (~1 mm wide), with higher relief than the surrounding material, are present in the interior.

ALHA78110 (160 g).—The stone (7.0 × 5.0 × 2.5 cm) is covered with thin, patchy black fusion crust except on the B surface, which is stained reddish brown with iron oxides and shows two protruding chondrules. Small, rounded, and irregular inclusions are visible through the fusion crust. The matrix is reddish brown and shows many inclusions and chondrules (up to 2 mm in diameter), as well as metal grains.

ALHA78128 (154 g).—Fusion crust is absent, this specimen being weathered and stained a dark reddish brown. The B surface has some small, nearly black spots, and in other areas, where the weathering is less severe, chondrules (maximum diameter 2 mm) can be recognized. The specimen is extensively fractured.

ALHA79012 (191 g).—Thin patches of fusion crust are present over all but the B surface of this stone (9.0 × 5.5 × 3.5 cm). Fractures penetrate the interior of the meteorite, which is extensively weathered to a deep reddish brown. Field notes state that this stone was found near ALHA79029, another H5 chondrite.

ALHA79025 (1208 g).—Thin, black fusion crust covers the S and B faces of this specimen (10 × 13 × 7 cm). Otherwise it is bounded by fractures that are weathered to a dark reddish brown; remnants of fusion crust are present on the E surface.

ALHA79026 (572 g).—This 9 × 6 × 5.5 cm specimen is angular with flat surfaces covered with a very thin, black to brown fusion crust. The fusion crust has been lost from the T and a corner of the N face, exposing a rough, irregular surface, weathered reddish brown. A few small white clasts are visible. The interior is friable and fractured. The matrix is gray with oxidation haloes around metal grains.

ALHA79029 (505 g).—This 10 × 7 × 4.5 cm stone has a very thin, patchy fusion crust on the T, E, N, and S faces. Where the fusion crust has been worn away, the surfaces are dark reddish brown. Fusion crust and weathered surfaces are smooth and shiny with an iridescent appearance. The stone is extensively fractured.

EETA79007 (199 g).—When this meteorite was received, it was numbered as two different samples; however, they fit together perfectly and are therefore numbered as a single specimen. The specimen (8 × 4.5 × 3.5 cm) is covered with black fusion crust except for a few spalled areas. The fracture surface between the two pieces has a 5-mm thick weathering rind of reddish-brown color. Many chondrules are visible. An area exposed by chipping is relatively fresh and gray.

META78010 (233 g).—Smooth, black fusion

crust covers this specimen (8.5 × 5 × 4.5 cm). Cleaving the stone into two approximately equal parts revealed a light-dark structure. Dark, vein-like areas, which contain small light-colored clasts (1–2 mm), surround large lighter-colored clasts up to 1 cm across. Some areas of the stone are weathered to a dark reddish brown.

RKPA79004 (370 g).—When the Reckling Peak meteorites were initially processed, it was found that six stones appeared identical. Field notes state that the six stones were found within 49 meters of each other. Examination of thin sections confirm their identity, and they have been combined as RKPA79004. All six stones have brown-black fusion crust on at least one surface. No stone was completely covered with fusion crust, but two stones have fusion crust on a fracture surface, indicating that the meteorite broke up during flight in the upper atmosphere. Fracture surfaces have all weathered to a reddish brown and have uniformly pitted surfaces where chondrules and inclusions have been plucked away. Chondrules, <1 to 3 mm in diameter, are visible on weathered surfaces.

H5 Chondrites Weighing Less Than 100 g.—ALHA78209, 12.1 g; 78221, 5.4 g; 78225, 4.5 g; 78227, 2.4 g; 78233, 1.2 g; 79004, 34.9 g; 79006, 40.9 g; 79008, 12.0 g; 79009, 75.6 g; 79010, 25.1 g; 79011, 14.0 g; 79013, 28.3 g; 79014, 10.8 g; 79015, 63.9 g; 79021, 29.4 g; 79031, 2.7 g; 79032, 2.6 g; 79036, 20.2 g; 79038, 49.6 g; 79040, 13.2 g; 79041, 20.1 g; 79042, 11.4 g; 79046, 89.7 g; 79047, 19.3 g; 79048, 36.7 g; 79050, 27.0 g; 79051, 24.0 g; 79053, 86.0 g; 79054, 36.0 g; RKPA79014, 77.7 g.

In thin sections all the H5 chondrites show a generally well-developed chondritic structure, with a variety of chondrule types, the four commonest being barred olivine, granular and porphyritic olivine and olivine-pyroxene, and fine-grained pyroxene. The groundmass is fine- to medium-grained, and consists largely of olivine and pyroxene, with minor amounts of nickel-iron and troilite; small grains of sodic plagioclase can sometimes be seen. The compositions of the olivine (Fa_{16-18}) and orthopyroxene (Fs_{14-17}) are essentially uniform within the individual specimens. ALHA79004 contains an enclave of granular polysynthetically twinned clinopyroxene that appears to be of a lower petrographic type. ALHA79008 contains a granular olivine-pyroxene enclave, 3 mm across, with the same olivine and pyroxene compositions as the main mass of the meteorite. ALHA79026 contains some unusually large chondrules, up to 3 mm across.

Class L5

Figure 22

EETA79009 (140 g).—This stone (6 × 5 × 3 cm) was received as two different samples, consisting of three pieces. The three pieces fit perfectly together and are therefore numbered as a single specimen. Dull black fusion crust covers most of the surface. A weathering rind up to 4 mm thick is present. The interior is whitish gray and shows numerous dark gray, fine-grained inclusions up to 14 mm in maximum dimension. The thin section shows moderately abundant chondrules, many of which are deformed or fragmented. The matrix consists of fine-grained olivine and pyroxene, with minor amounts of nickel-iron and troilite; much of the nickel-iron and troilite is finely dispersed through the silicates, possibly a shock effect. Brown limonitic staining pervades much of the section. Microprobe analyses give the following compositions: olivine, Fa_{24}; pyroxene, Fs_{20}.

RKPA79013 (11.0 g).—This small stone (2.5 × 1 × 1.5 cm) is completely covered with dull brown to black fusion crust. Chipping revealed a weathered interior with two gray, rounded inclusions, 2 mm in diameter. The thin section shows well-developed chondritic structure, with chondrules ranging from 0.3 to 2.2 mm across. Fusion crust, up to 0.5 mm thick, rims most of the section. Brown limonitic staining is concentrated around nickel-iron grains and below the fusion crust. Microprobe analyses give the following compositions: olivine, Fa_{23}; pyroxene, Fs_{20}; accessory merrillite was identified with the microprobe.

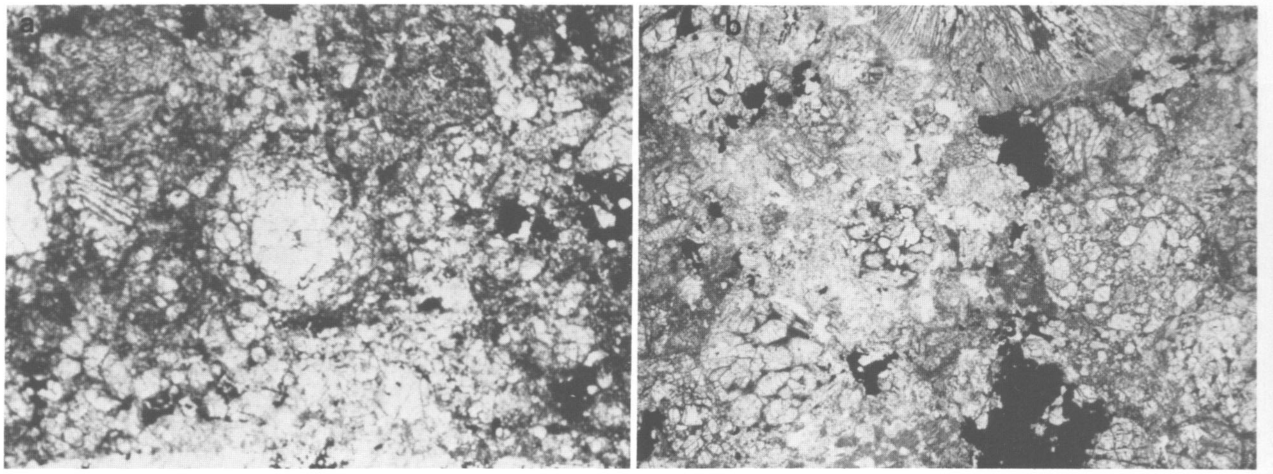

FIGURE 22.—Photomicrographs of thin sections of L5 chondrite (area of fields is 3 × 2 mm): *a*, EETA79009; *b*, RKPA79013. (Chondrules discernible, but their margins tend to be poorly defined and to merge with granular matrix.)

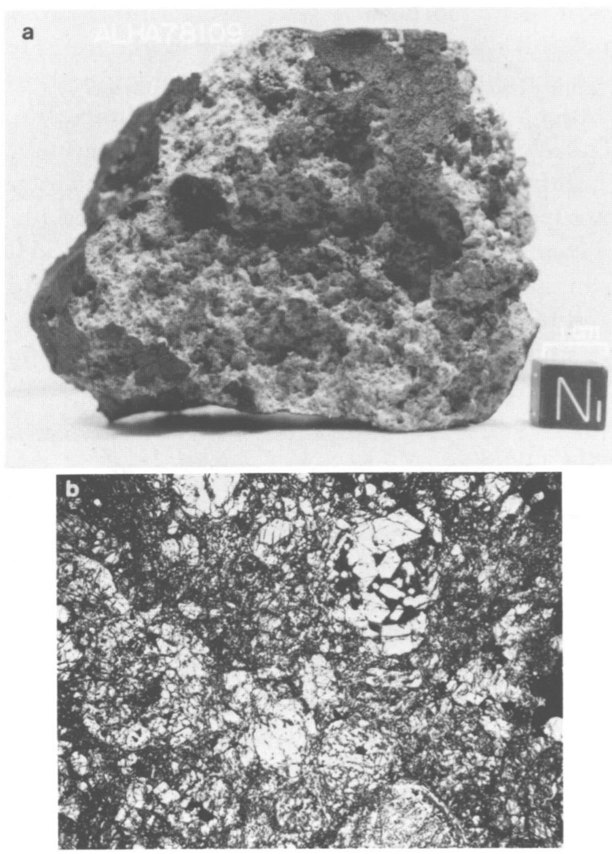

FIGURE 23.—ALHA78109, LL5 chondrite: *a*, fusion crust (black) broken away over parts of stone and exposed light gray interior; *b*, photomicrograph of thin section (area of field is 3 × 2 mm); well-defined chondrules, some broken and deformed, in fine-grained granular matrix.

CLASS LL5

FIGURE 23

ALHA78109 (233 g).—Approximately 75% of this stone (7.0 × 5.5 × 3.5 cm) is covered with dull black fusion crust. Areas without fusion crust are light gray and show abundant dark gray chondrules up to 2 mm in diameter. Chondrules are easily removed from the matrix, many falling out on handling. Troilite nodules, 3–10 mm across, and gray clasts are also present. The thin section shows prominent and well-defined chondrules, some broken and deformed. A variety of types is present, the three commonest being granular olivine, barred olivine, and fine-grained pyroxene. The matrix is dominantly olivine with lesser amounts of pyroxene, and a little nickel-iron and troilite; plagioclase is present as very small grains difficult to recognize. Some limonitic staining occurs in association with the nickel-iron grains. Microprobe analyses gave the following compositions: olivine, Fa_{28}; orthopyroxene, Fs_{23}; plagioclase, An_{11}.

CLASS H6

FIGURES 24, 25

ALHA77183 (288 g).—This is a well-rounded specimen, except for a flat B surface. Fusion crust

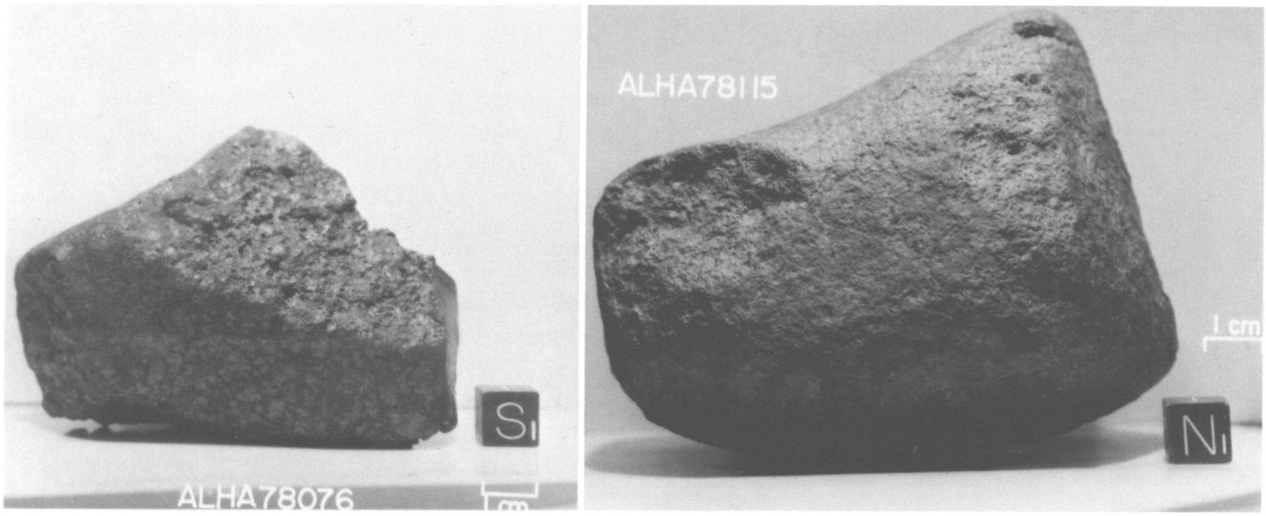

FIGURE 24.—H6 chondrites: Fusion crusts coats most of surface of ALHA78076, whereas on ALHA78115 much of fusion crust has been removed by weathering.

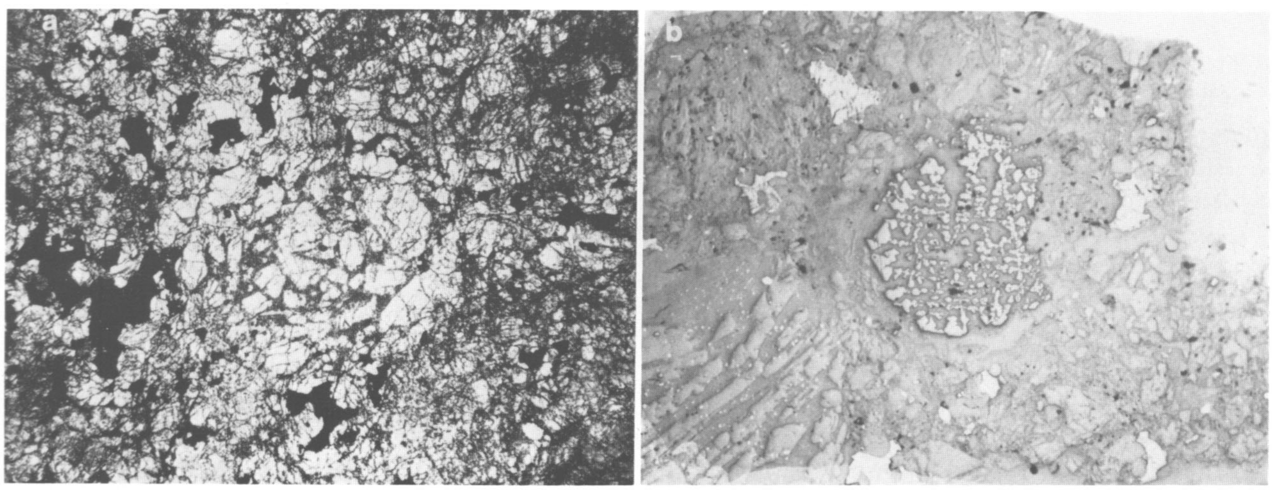

FIGURE 25.—Photomicrographs of thin sections of H6 chondrites (area of fields is 3 × 2 mm): *a*, META78007; chondritic structure barely discernible, chondrules merging with granular matrix; *b*, ALHA78076 (reflected light); rounded intergrowth (possibly chondrule) of chromite (white) and plagioclase (light gray) occupies center of field.

is absent, and all surfaces are stained a uniform reddish brown. Small inclusions are visible on the T surface. No unweathered material was seen when the stone was cleaved.

ALHA78076 (275 g).—Thin, black fusion crust covers most of the stone (8.0 × 5.0 × 4.5 cm). Where the fusion crust is absent, the surface is stained reddish brown with iron oxides and 1–2 mm clasts are visible. Polygonal fractures are present on the T and N surfaces. Cleaved surfaces shows clasts up to 3 mm across, in gray matrix. Minor amounts of iron oxides are present around metal grains.

ALHA78115 (847 g).—This is a smooth, rounded stone with scattered fusion crust on the B and E surfaces, and a very small amount on the W surface. The fusion crust is black, thin, and pitted. Where fusion crust is absent the surface is weathered reddish brown. Clasts and chondrules, as much as 9 mm across, are present. The interior, exposed during processing, contains metal particles and is moderately weathered.

ALHA79002 (222 g).—A small, thin patch of black fusion crust and remnant red-brown fusion crust cover the stone (8 × 5 × 4.5 cm). Several fractures penetrate the interior. No unweathered material was exposed by chipping.

ALHA79016 (1146 g).—This stone (13 × 8 × 6.5 cm) is covered with smooth, black fusion crust, except for small patches on the T and E surfaces; these patches are weathered to a reddish brown color. Shallow regmaglypts are present on several faces. The S and B faces appear to have been fracture surfaces that have been covered with fusion crust. The interior has a yellowish color, is friable, and shows metallic particles; no chondrules are visible.

META78006 (409 g).—This specimen is completely covered with fusion crust. Cleaving revealed that the interior is considerably stained with iron oxides; unstained areas are light gray; a few darker-colored inclusions are present.

META 78007 (174 g.)—Fusion crust, ranging from dull black to iridescent red-brown, totally covers this irregular-shaped meteorite. The interior of the stone is 75% weathered; the unweathered part appears to have many clasts, up to 5 mm across. This stone was magnetically oriented in Antarctica and the orientation has been kept throughout processing.

RKPA79003 (182 g).—This semi-rounded stone (7 × 4.5 × 3.5 cm) is covered with black fusion crust. Small areas where the crust has been plucked off reveal a reddish-brown interior with many inclusions.

H6 chondrites weighing less than 100 g: ALHA78211, 11.4 g; 78213, 9.5 g; 78215, 6.3 g; 78229, 1.9 g; 78231, 1.8 g; 79005, 60.0 g; 79019, 12.1 g; 79020, 4.2g; 79024, 21.6 g; 79028, 16.2 g; 79034, 12.6 g; 79037, 14.8 g; 79049, 54.0 g; 79055, 15.2 g; RKPA79009, 54.6 g; 79012, 12.8 g.

In thin sections all the H6 chondrites show very similar petrographic features. Chondrules are sparse and poorly defined, tending to merge with the granular groundmass, which consists mainly of olivine and pyroxene, with minor amounts of nickel-iron, troilite, and sodic plagioclase, and accessory chromite. Compositions of the olivine (Fa_{17-19}) and pyroxene (Fs_{15-17}) are uniform within the individual specimens. The thin section of ALHA78076 showed a rounded aggregate of closely-packed chromite grains with interstitial plagioclase, possibly a chondrule of unusual composition. A vein of nickel-iron up to 0.5 thick is present in ALHA79016.

Class L6

Figures 26, 27

ALHA77180 (190 g).—This stone has remnant fusion crust on three surfaces; other surfaces are fractures and stained reddish brown with iron oxides. Processing revealed a light gray, fine-grained interior and one fine-grained inclusion approximately 10 mm in diameter.

ALHA77292 (199 g).—This is an incomplete stone. The T surface is less severely weathered than the other surfaces; the N surface has remnants of dull black fusion crust. Surfaces devoid of fusion crust are rough and stained reddish brown with iron oxides. Fractured surfaces show rounded and irregular inclusions.

ALHA78039 (299 g).—This specimen (8 × 4 × 5 cm) is totally covered with black fusion crust except for a 4.0 × 2.5 cm area that shows a light gray interior. Cleaving the stone revealed a light gray matrix with light gray clasts. A well-defined weathering rind penetrates the stone to a depth of 1–10 mm. Scattered areas of partly oxidized metal are present throughout the meteorite.

ALHA78042 (214 g).—The T surface of this 5.5 × 4.0 × 5.0 cm specimen has a 4 × 3 cm area of reddish-black fusion crust; the remaining surfaces are fractures that are weathered reddish brown. The sawed specimen revealed a relatively fresh interior with a light gray matrix and rounded and irregular inclusions up to 1 mm in diameter.

ALHA78043 (680 g).—This stone, 10.0 × 8.5 × 6.0 cm, is covered with black fusion crust, ~1

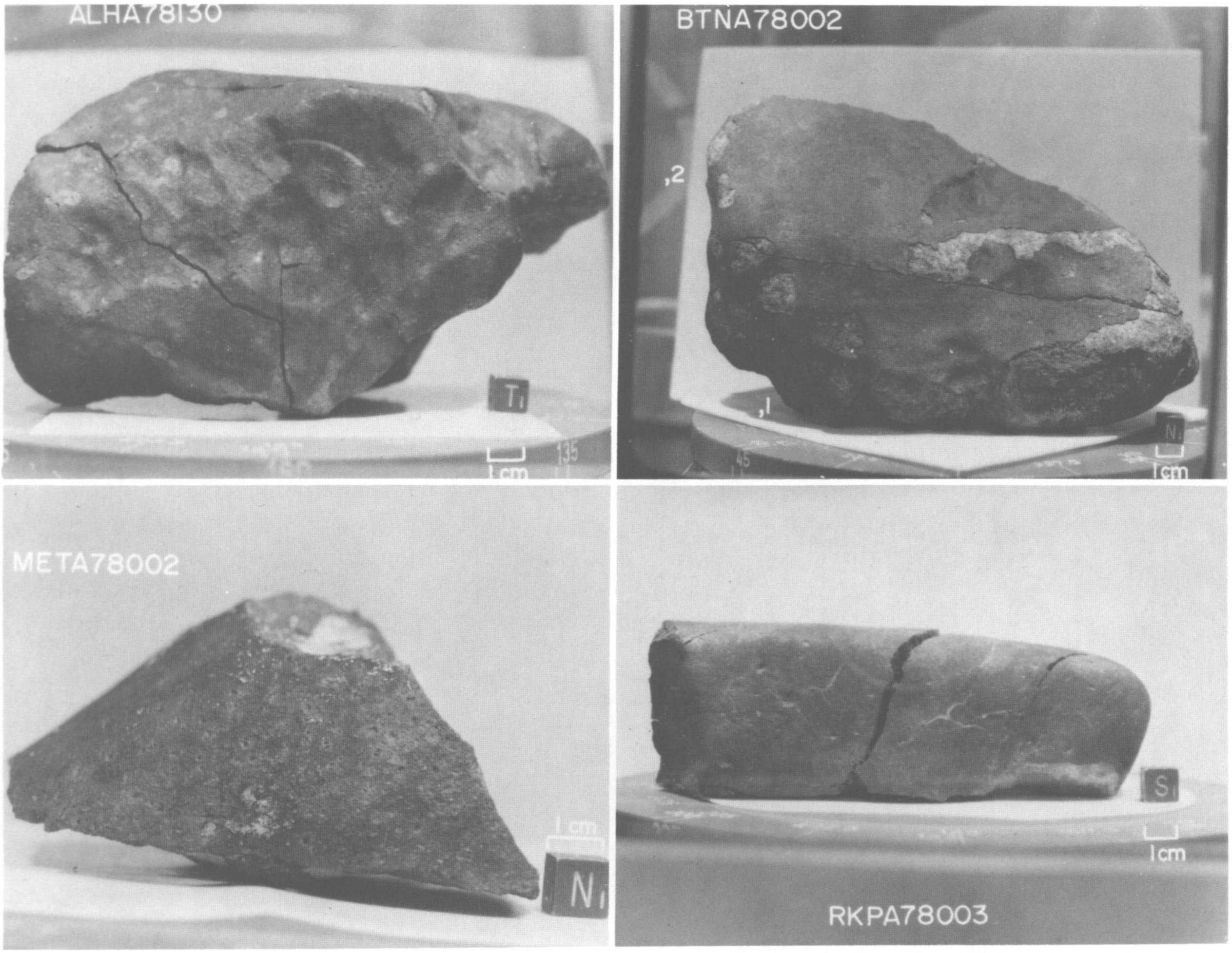

FIGURE 26.—L6 chondrites.

mm thick, that shows some weathering; the W surface appears to be less weathered than the other surfaces. A large chondrule is present on the B surface. The T surface is a fracture with some remnant fusion crust. During processing the stone broke along fractures that were weathered and stained with iron oxides. The matrix is yellowish green and contains some small (<3 mm) clasts. A few metallic flakes are present in the matrix.

ALHA78045 (396 g).—This tabular specimen, (8.0 × 5.0 × 5.0 cm) is covered with blackish brown fusion crust except for a 2.5 × 3.5 cm area on the T/E surfaces that is very smooth and highly polished. Three large fractures penetrate the specimen. During processing the specimen broke into two approximately equal pieces along one of the fractures. The matrix is weathered to a reddish yellow.

ALHA78048 (190 g).—This specimen is partly covered with brown to black fusion crust. Where fusion crust is absent, a light gray matrix with some iron-oxide staining is seen. Shallow regmaglypts are present on all surfaces. When the stone was cleaved a thin (1–2 mm) weathering rind was exposed. The interior is light gray with darker gray inclusions and shows some unoxidized metal grains.

ALHA78050 (1045 g).—This 15 × 8 × 6 cm specimen is an incomplete stone, being bounded by fractures on the N, T, and B surfaces; these surfaces are stained reddish brown with iron oxides. Inclusions are apparent on these surfaces,

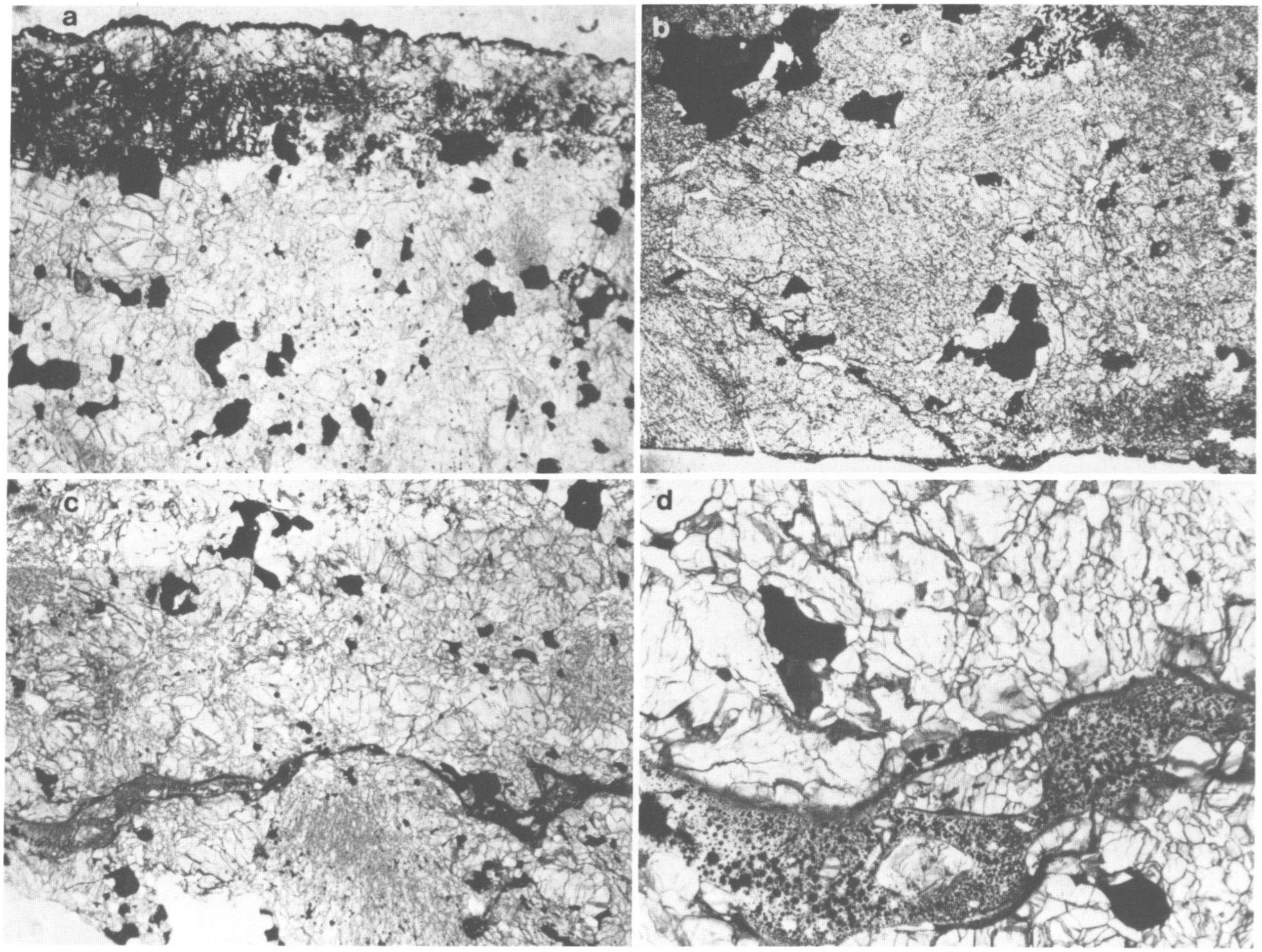

FIGURE 27.—Photomicrographs of thin sections of L6 chondrites (area of fields is 3 × 2 mm in *a*, *b*, *c*; 0.9 × 0.7 mm in *d*): *a*, ALHA78106; *b*, BTNA78002; *c* and *d*, RKPA78003. (Chondritic structure barely discernible in these sections, chondrules almost completely integrated with granular matrix; ALHA78106 has thick fusion crust (top of section); *d*, enlargement of *c*, with shock vein containing ringwoodite and majorite (tentative determinations).)

and patches of remnant fusion crust, mottled brown and black, remain on the B surface. Sawed surfaces show metallic grains, some with oxidation halos, and small irregular inclusions.

ALHA78074 (200 g).—This is an incomplete stone, with shiny fusion crust (1–2 mm thick) on the B, W, and parts of the S, N, and E surfaces; polygonal fractures are present on the B and N surfaces. Fracture surfaces are rough, slightly weathered, and stained with iron oxides. The matrix is light gray, it includes darker gray clasts and chondrules.

ALHA78078 (290 g).—This 6.0 × 4.5 × 8.0 cm stone is covered with thin black fusion crust except at the corners. Processing revealed a light gray matrix speckled with light and dark clasts and metallic grains.

ALHA78103 (589 g).—This rounded specimen (11 × 7 × 4 cm) is weathered and stained with iron oxides, except for a small patch of remnant fusion crust on the E surface. The B surface, which is least weathered, displays several chondrules, 3–5 mm in diameter. The stone broke along fractures during processing, showing a greenish-gray matrix with some metallic grains and oxidation halos. A weathering rind, ~3 mm thick, is present on the T surface.

ALHA78104 (672 g).—The W surface is partly covered with black fusion crust, but the remainder of the surface is weathered and stained with iron oxides. A large clast (~7 mm) is exposed on the N surface, and a smaller (~3 mm) possibly metallic clast on the T surface. A number of smaller clasts that appear to be metallic are scattered over the surface. Processing revealed a light gray matrix with metallic particles. Weathering rind, ~5 mm thick, is present on some surfaces.

ALHA78105 (941 g).—The surface of this stone (11 × 7 × 6 cm) is rough and irregular on a mm scale, apparently as a result of the weathering of the fusion crust, of which small patches remain on the B and N surfaces. The interior shows a light to medium gray matrix with chondrules, lithic clasts, and sparse metal grains.

ALHA78106 (464 g).—This semi-pyramidal specimen appears to be completely unweathered (a recent fall?). It is covered with a spotted, brown to black, polygonally fractured fusion crust, ~1 mm thick. Shallow regmaglypts are present on all surfaces. The interior shows a light gray matrix with dark and light clasts up to 2 mm across.

ALHA78112 (2485 g).—This stone (14 × 13 × 13 cm) is covered with fusion crust, 0.5–1 mm thick, on four surfaces; on one surface the fusion crust has weathered to a brown color, on the other surfaces it is black. The S surface is a fracture, and 80% is weathered and stained with iron oxides. Sawing the specimen revealed light gray matrix with oxidation halos around most of the metal grains; clasts up to 3 mm across are present.

ALHA78114 (808 g).—The B surface of this meteorite is planar and has small patches of dull black fusion crust on a shiny reddish-brown background, which may possibly be severely weathered fusion crust. All other surfaces are covered with dull black fusion crust except for small areas on the S surface. Small regmaglypts are present on this surface. Many shallow voids are present on the exterior. The stone was cleaved along a large crack, exposing mostly weathered material. Unweathered material is light gray and flecked with light and dark clasts (~1 mm).

ALHA78126 (606 g).—Thin black fusion crust, weathering brown in some areas and polygonally fractured on the B surface, covers this specimen (12 × 8 × 5 cm) except on the NE corner. Matrix material exposed during processing is greenish gray, with several darker veins penetrating it; small metallic particles were also apparent in this friable specimen.

ALHA78127 (194 g).—The stone is covered with very thin shiny fusion crust on the T, B, N, and W surfaces; remnants of fusion crust are present on the S surface, and the E surface is a fracture surface. Where fusion crust is absent, the specimen is reddish brown. Processing showed that nearly all of the specimen is severely weathered.

ALHA78130 (2733 g).—This meteorite (18 × 9 × 9 cm) is covered with a thin, dull black fusion crust, except along the edges and a 4 × 4 cm area on the W surface. There is preferential weathering of the fusion crust around clasts. The stone is covered with shallow regmaglypts and is extensively fractured. Processing revealed that about 70% of the interior is severely oxidized. The unweathered portion is light gray and speckled with light and dark clasts, some up to 5 mm across. Small veins of darker material, 20–30 mm long and 3 mm wide, are present in the matrix.

ALHA78131 (268 g).—Thin, shiny black fusion crust covers the specimen except for most of the T surface and portions of the B and N surfaces. Shallow regmaglypts are present on the S, W, and T surfaces. Surfaces devoid of fusion crust are weathered and stained with iron oxides; several light-colored clasts were noted on these surfaces. Processing exposed only a small amount of unweathered material.

ALHA78251 (1312 g).—This specimen (12 × 7.5 × 10 cm) is completely devoid of fusion crust and the surface is rough and irregular. The interior is fine-grained and greenish gray, and shows metal grains surrounded by oxidation halos. Fractures are present with iron oxides along their margins.

ALHA79007 (142 g).—Dull black fusion crust covers 50% of this stone (6 × 4 × 4 cm). Areas devoid of fusion crust range from light gray to yellowish brown in color; many clasts are visible, one of which is 6 × 10 mm, greenish yellow, and very fine-grained. The interior is relatively fresh; with a thin weathering rind in some areas and a small amount of oxidation around metal grains in the light gray matrix.

ALHA79018 (120 g).—This stone (4.5 × 5 × 3.5 cm) is covered with thin, brown to black, patchy, fusion crust on all but one surface; this surface has a yellow to deep reddish-brown color and shows several inclusions. The interior is mainly weathered but has small areas of fresh material. Several black veins are present (infilled cracks ?), as are rounded inclusions up to 3 mm in diameter.

ALHA79027 (133 g).—Dull black fusion crust coats most of this stone (5.5 × 4.5 × 3 cm). A fracture surface has patches of fusion crust, which suggests that the stone broke during passage through the atmosphere. Many inclusions are visible, with the largest being 4 mm in greatest dimension.

ALHA79033 (208 g).—All but the T surface of this stone (7.5 × 6.5 × 3.5 cm) is covered with dull brown to black fusion crust. The T surface is a fracture that has weathered reddish brown; a number of mm-sized inclusions were noted. Fresh interior material is light gray with darker gray inclusions; metal grains surrounded by oxidation halos are present. A weathering rind 1–5 mm thick is visible.

BTNA78001 (160 g).—The specimen is shaped like a flat plate, 10 × 6 × 1 cm, and is covered with black fusion crust except on the B and portions of the W surface; the B surface is polished and has a mottled, yellowish-red-brown appearance. Processing revealed a medium gray matrix with inclusions (~1 mm). The specimen has a prominent (1 mm) weathering rind.

BTNA78002 (4301 g).—This specimen consists of two separately collected pieces that fit together. The complete stone (20 × 12 × 14 cm) is almost entirely covered with thin, dull brown fusion crust (apparently weathered) that is dotted with black fusion crust. An approximately 7 × 10 cm area on the S surface appears to have been broken away (this may be BTNA78001, which is petrologically identical to BTNA78002). Areas devoid of fusion crust are light grayish green except where flecked with iron oxides around metal grains. The T surface shows flow bands in the E-W direction, and regmaglypts are present on the B surfaces.

EETA79003 (435 g).—This 7.5 × 6 × 5 cm stone is covered with thin, shiny black fusion crust that is pitted and weathered, leaving a brown surface in some areas. The interior is gray and very friable, with numerous oxidation halos around metal grains.

EETA79010 (287 g).—The exterior of this stone (8.5 × 6 × 4 cm) has weathered yellow-brown to red-brown. One small patch of black fusion crust remains. The interior is whitish gray with brown limonitic staining around nickel-iron grains. A thin weathering rind was noted.

META78002 (542 g).—Thin, dull black fusion crust is present on three surfaces of this pyramidal specimen; the fusion crust is pitted, apparently the result of preferential weathering of small inclusions. The T, W, and B surfaces are fractures that are stained reddish brown. Many clasts, up to 3 mm across, can be seen on the T and W surfaces. Processing revealed a greenish-gray matrix containing metal grains, some of which have oxidation halos.

META78003 (1726 g).—The E, T, and W surfaces of this meteorite (15.0 × 7.5 × 8.0 cm) are covered with thin, dull black fusion crust. The other surfaces are fractures that are weathered to a reddish color; light-colored inclusions are visible on these surfaces. Processing revealed a greenish-gray matrix with oxidation halos around metal grains.

META78005 (172 g).—Three surfaces of this stone (6.5 × 5.5 × 4.0 cm) are covered with dull black polygonally fractured fusion crust. Surfaces devoid of fusion crust are fractures, are weathered to a reddish yellow, and contain many inclusions with greater relief than the surrounding matrix. Processing revealed a light gray matrix with small clasts and non-oxidized metallic particles.

RKPA78001 (234 g).—Thin dull black fusion crust covers two surfaces of this angular stone (9 × 5 × 4.5 cm). The other surfaces are fractures that are stained reddish brown by iron oxidation. Processing revealed only a small amount of grayish unweathered material. No inclusions were seen.

RKPA78003 (1276 g).—This specimen was found as two pieces, which fit together perfectly. Most of it is covered with thin, dull black fusion crust. Surfaces devoid of fusion crust have weathered to a deep reddish brown, as have the two surfaces that fit together. The W butt end has a clast, 10 mm across, that appears to be troilite. Chipping revealed surfaces composed of very dark gray and very light gray matrix material, possibly the result of weathering processes.

RKPA79001 (3006 g).—Small patches of shiny black fusion are present; the remaining surfaces are fractured, rough, and yellowish brown. Chondrules can be distinguished; most are small, but the largest one is 6 mm in diameter. Indentations in the surface indicate chondrules may have been plucked out. There is a vein of dark material, 1–3 mm thick, on one surface, probably indicating weathering along a fracture. A small amount of white powdery deposit is present on the fusion crust. The interior matrix is light gray to yellow, with oxidation halos around metal grains; gray and cream-colored chondrules, ~2 mm in diameter, are visible.

RKPA79002 (203 g).—Dull black fusion crust partly covers three surfaces of this stone (8.5 × 5.5 × 3.5 cm). The B surface is highly polished in areas of fusion crust. Clasts up to 3 mm are visible on the surface and are identical to those seen in RKPA79001. Surfaces devoid of fusion crust are weathered from brownish yellow to reddish brown. The interior is whitish gray with oxidation halos around metal grains. A small weathering rind was noted.

All the RKPA L6 meteorites are petrologically identical, with maskelynite and shock veins containing majorite and ringwoodite; it is reasonable to conclude that they are all pieces of a single meteorite.

L6 chondrites weighing less than 100 g: ALHA79043, 62.2 g; 79052, 22.6 g.

The L6 chondrites are all very similar in their petrographic characters. Polished thin sections show sparse, poorly defined chondrules that tend to merge with the granular groundmass. Principal minerals are olivine and orthopyroxene in subequal amounts, together with minor quantities of plagioclase (or maskelynite), nickel-iron, troilite, diopside, and accessory chromite and merrillite. Microprobe analyses (Appendix Table 1) show essentially uniform compositions for the principal minerals: olivine, Fa_{23-25}; orthopyroxene, Fs_{19-21}; plagioclase, An_{10-12}. The following meteorites contain maskelynite: ALHA78039 (in part), 78048 (in part); 79018; 79043; 79052; BTNA78001, 78002; RKPA78001, 78003, 79001, 79002. Ringwoodite and majorite were tentatively identified in shock veins in ALHA79018, BTNA78001 and 78002, and RKPA78001, 78003, and 79002.

Class LL6

Figure 28

ALHA78153 (151 g).—Thick (1–2 mm), dull, brownish-black fusion crust, with a blistery texture, covers the N, B, and parts of the E surface. A weathering rind, up to 5 mm thick, is present in some areas. Fracture surfaces are dark brown in isolated areas, but the overall color is greenish yellow. It appears that some large clasts have been plucked from the surface. This stone shows an unusual weathering pattern. Dark reddish-brown veins adjoin areas of yellowish material; areas of less severely weathered gray matrix were exposed during processing. In thin section chondritic structure is barely discernible, the meteorite showing a rather uniform granular aggregate of olivine and pyroxene, with minor amounts of troilite and plagioclase, a little nickel-iron, and accessory chromite. Limonitic staining is present in association with the metal grains. Microprobe analyses gave the following compositions: olivine, Fa_{29}; orthopyroxene, Fs_{24}; plagioclase, An_{11}.

BTNA78004 (1079 g).—This stone (12 × 7 × 7 cm) is covered with thin, dull black fusion crust except on one fracture surface. Regmaglypts are present on the N and S surfaces. The meteorite appears to be composed of angular, light-colored clasts surrounded by greenish-brown to gray in-

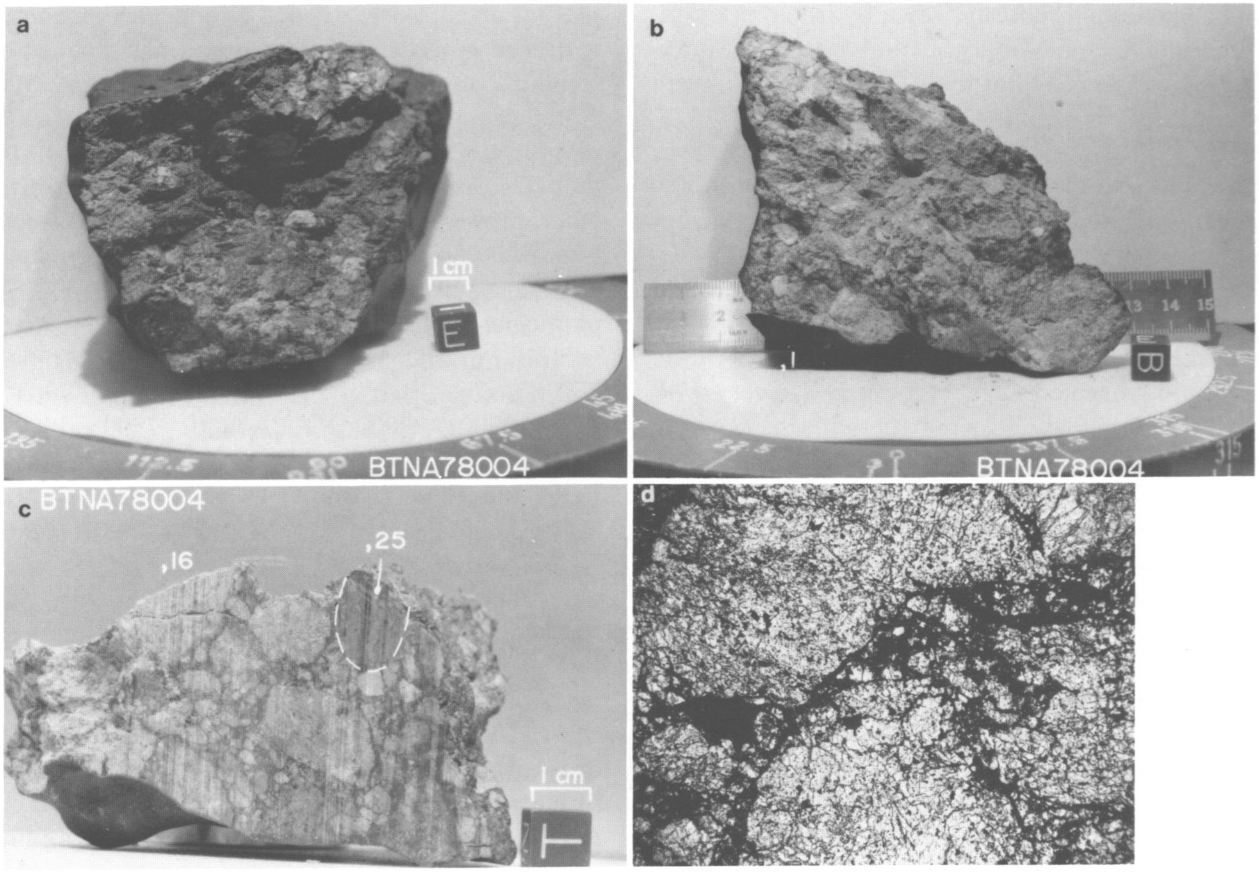

FIGURE 28.—BTNA78004, LL6 chondrite: *a*, fusion crust (black) coats part of surface; *b*, fracture surface showing brecciated structure; *c*, sawn surface showing brecciated structure with light and dark clasts; *d*, photomicrograph of thin section (area of field is 3 × 2 mm), showing granular clasts bounded and penetrated by black glassy veinlets.

terstitial material. The clasts comprise approximately 70% of the surface area and have a wide range in size; some are as much as 2.0 cm across. A thin section shows a granular aggregate consisting mainly of olivine and pyroxene (average grain size 0.1–0.2 mm), with minor amounts of plagioclase, nickel-iron, troilite, and accessory chromite. Chondritic structure is barely visible in a few places, and the chondrules are somewhat fragmented. Many of the silicate grains show undulose extinction. The meteorite has a brecciated structure, and the breccia fragments are outlined by an anastomosing network of black, glassy veinlets that contain numerous minute troilite globules. A small amount of limonite staining is present around some of the nickel-iron grains. Microprobe analyses show olivine (Fa_{30}) and orthopyroxene (Fs_{24}) of essentially uniform composition; plagioclase is somewhat variable in composition, An_{13}-An_{22}, average An_{19}. The black glass is quite variable in composition, as follows (range and average, in weight percent): SiO_2 31.5–49.9, 40.4; Al_2O_3 0–6.3, 2.8; FeO 17.5–40.9, 23.9; MgO 16.7–31.3, 27.3; CaO 0–3.3, 1.6; Na_2O 0–2.4, 1.1; TiO_2 0–0.15, 0.09; MnO 0.3–0.5, 0.4. The meteorite shows to a high degree the brecciation characteristic of many LL chondrites.

Achondrites

EUCRITES

FIGURES 29, 30

Eucrites and howardites are pyroxene-plagioclase achondrites, but different authorities have

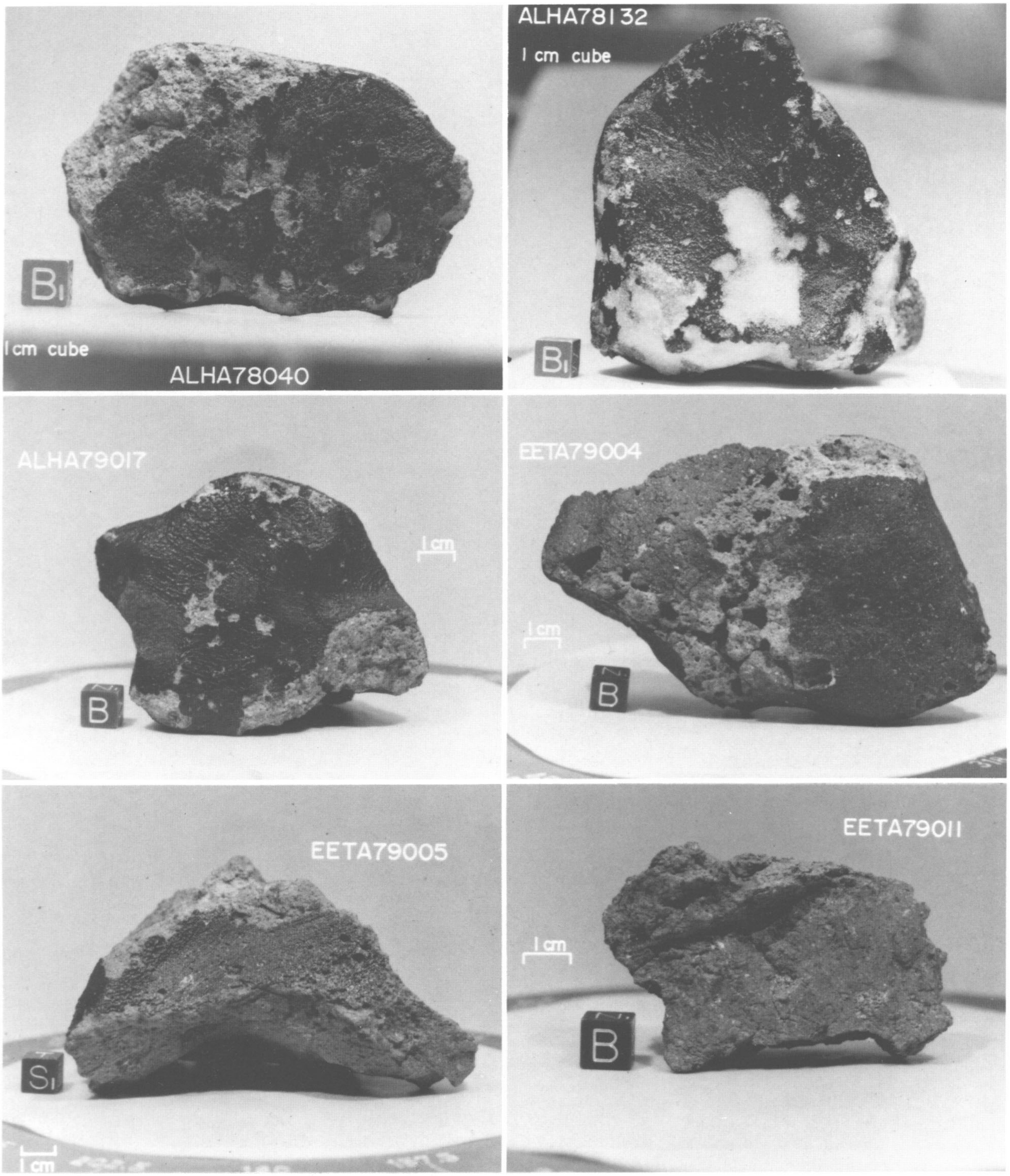

FIGURE 29.—Eucrites; black glassy fusion crust coats most of specimens, except EETA79011; note snow and ice still present on ALHA78132 when unpacked at Johnson Space Center.

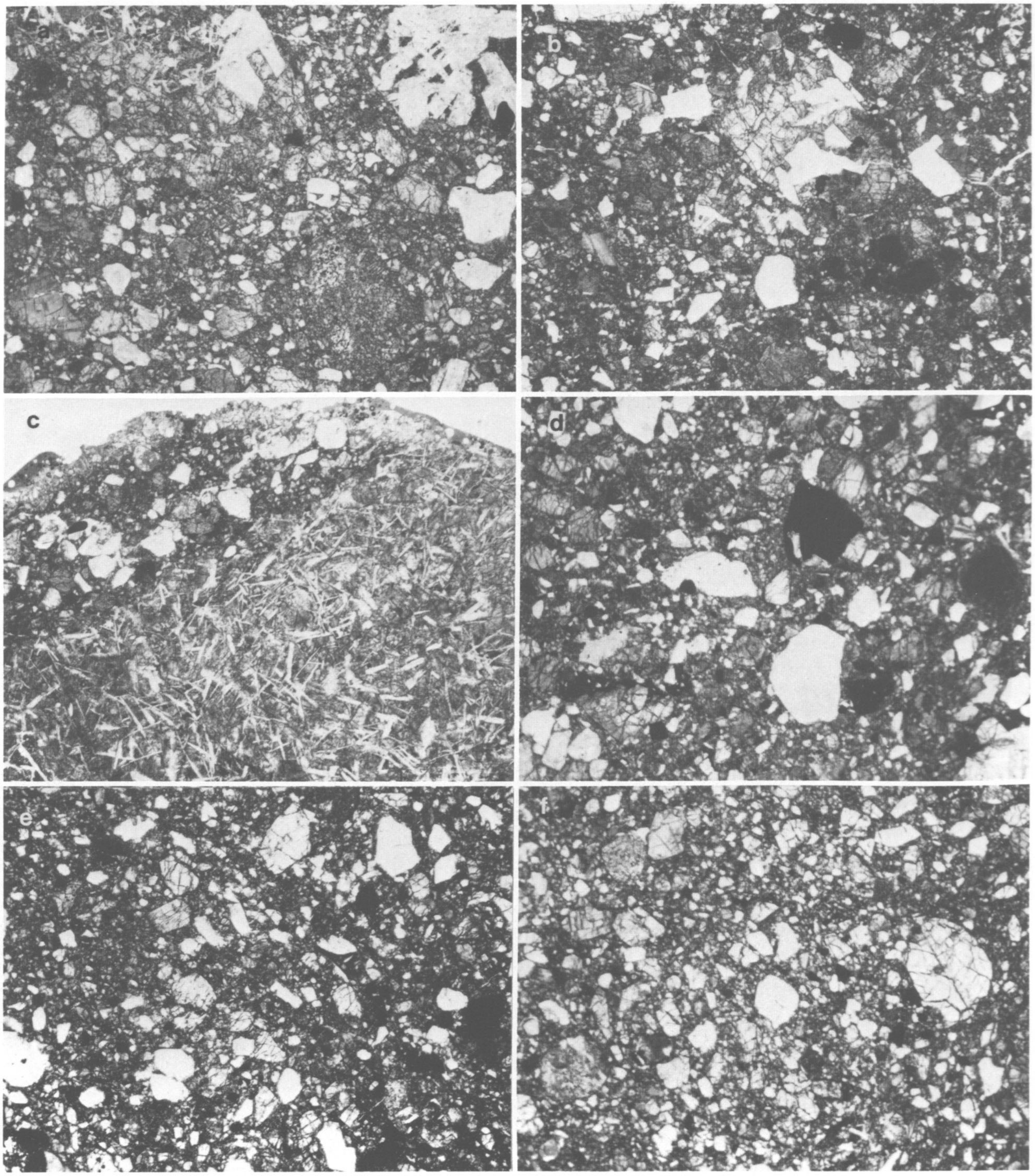

FIGURE 30.—Photomicrographs of thin sections of eucrites (area of fields is 3 × 2 mm): *a*, ALHA78132; *b*, ALHA78158; *c*, ALHA78165; *d*, ALHA79017; *e*, EETA79005; *f*, EETA79011. (Photomicrographs show typical brecciated structure of eucrites, with clasts of plagioclase (white), pyroxene (light gray), and chromite (black) in fine-grained comminuted matrix of these minerals; (*c*) has area showing ophitic intergrowth of plagioclase (white laths) and pyroxene.)

proposed different criteria for distinguishing between the two classes. Duke and Silver (1967) discussed previous classifications, and adopted the definition of eucrites as monomict breccias and howardites as polymict breccias. Takeda, Miyamoto, Duke, and Ishii (1978:1159), however, described the Yamato-74159 meteorite as a eucrite that "clearly is polymict in terms of lithic variability but carries no magnesian orthopyroxene of the type found in howardites," and the term polymict eucrite has been applied quite widely since. We accept this term and the definition thereof. Howardites are then polymict pyroxene-plagioclase achondrites containing magnesian orthopyroxene. Our experience is that these orthopyroxenes have compositions $En_{>70}$, and some have compositions indicating admixture of a diogenitic component, although the range of compositions may be considerably greater than in analysed diogenites.

ALHA78040 (211 g).—This is a complete unweathered specimen (~9.0 × 5.0 × 3.0 cm). Black, shiny fusion crust 0.5 mm thick covers all the surfaces of the stone. The crust has been removed from the edges by spallation and has been preferentially weathered away on the surfaces in small circular areas. The B and T surfaces have had the most fusion crust removed, thus revealing light to medium gray matrix material that contains small (<1 mm), elongated, white grains, probably feldspar. The T and S surfaces each have a 1.0 cm clast present. These clasts have a slightly lighter color than the surrounding fusion crust. On the N surface an oval vug is present. Inside this vug is a weathered yellowish-brown inclusion ~0.5 cm diameter that has a coarser texture than the surrounding matrix material.

ALHA78132 (656 g).—This appears to be a complete specimen (11 × 10 × 8 cm) with vitreous black fusion crust on all sides. The overall shape is pyramidal with the B surface being flat. The fusion crust on the T surface has flow bands, most prominent in the N-S direction and less prominent in the W-E direction. The B surface has radial flow lines in a concave area. The fusion crust on the S surface is much duller than on the rest of the stone. The crust has been spalled or chipped in some areas, revealing a medium gray interior material. Small (<1 mm) inclusions, both lighter and darker than the matrix, are apparent. Several holes (voids) that penetrate the fusion crust by as much as ~1 cm were noted over the entire stone. One in particular is ~9 mm in diameter and ~1 cm deep and contains a yellowish grain (?) ~2 mm long. The cut face shows a light gray matrix dotted with rounded and irregularly shaped grains(?) that are both lighter and darker than the matrix. The largest grain is ~0.5 cm in diameter. The voids on the exterior of this specimen did not appear in the interior. A vein(?) of white grains extends for 6 cm across the cut face in the W-E direction.

ALHA78158 (15.1 g).—This is not a complete specimen. Shiny black fusion crust is present on one surface. All other surfaces are fractures that show a medium gray matrix with white flecks. Some clasts (<1 mm) are oxidized to a yellow color. An area ~0.5 cm diameter on the B surface is a darker gray and appears very homogeneous—this appears to be a rounded clast. One fracture goes completely across the sample. Overall dimensions are 3.0 × 2.5 × 2.0 cm.

ALHA78165 (20.9 g).—This is not a complete specimen (~3.5 × 3.0 × 1.5 cm). Shiny black fusion crust covers only one surface. The other surfaces are fracture surfaces that have a medium gray matrix with <1 mm white clasts. A few of these clasts are weathered and yellow. When this stone was cleaved in half, a dark gray clast (~0.5 cm) was exposed.

ALHA79017 (310 g).—This meteorite is mostly covered with a shiny black fusion crust with flow bands on all surfaces. The areas devoid of fusion crust are medium gray and speckled with light and dark clasts that are <1 mm in diameter. Some clasts are up to 0.5 cm long. The interior exposed through chipping is lighter gray than the exterior. Several large clasts of up to 1.2 cm are visible on the fresh fractures.

Reid and Schwarz (1980:353) have studied the Allan Hills eucrites and give the following description:

The basaltic achondrite meteorites collected in the Allan Hills region of Antarctica (76005, 77302, 78040, 78132, 78158 and 78165) are all petrographically similar and could even be pieces from a single fall. They are breccias with abundant but small (from fine dust to a maximum diameter of approximately 1 cm) angular clasts of rock and mineral fragments. The lithic clasts are basaltic, consisting of subequal amounts of pyroxene and feldspar with a range of igneous textures. The diverse clast types correspond to a range of thermal histories and to a limited range of basaltic compositions. Rock and mineral fragments studied to date correspond in texture and in mineral composition to the known range of eucrites, including both unequilibrated and equilibrated types. The range in pyroxene compositions is wide (Wo_4En_{69} to $Wo_{13}En_{33}$) but pyroxenes with the compositions of those in diogenites are absent or rare.

The Allan Hills basaltic achondrites are unlike previously described eucrites and howardites (with the possible exception of Macibini) in that they contain a series of fragments covering a range of eucrite types and are thus polymict but they do not appear to contain a diogenite component as in typical howardites. The name polymict eucrite seems appropriate. Very similar polymict eucrites are common in the suite of achondrites collected in the Yamato region of Antarctica, almost 3000 km from Allan Hills.

Petrographic examination of ALHA79017 has shown that it is a polymict eucrite similar to the previously collected Allan Hills eucrites, and thus possibly another piece of a single fall.

Takeda et al. (1980b) have published chemical analyses of ALHA76005 and ALHA78132 that show their near-identity in composition. Delaney et al. (1980) have provided detailed descriptions of eucritic clasts in ALHA78040 and ALHA 77302.

EETA79004 (390 g).—This oblong achondrite (11 × 6.5 × 4 cm) is covered with a thin, dull fusion crust on all but two surfaces. The exterior matrix appears medium to dark gray and contains numerous clasts as large as 2 cm in diameter. Most of the larger clasts are dark, though light clasts do exist. Vugs occur in this meteorite. Most are concentrated on a surface in an area devoid of fusion crust. These vugs are as deep as 1 cm, as wide as 0.5 cm. The interior matrix is light gray with many inclusions. Many of the clasts in this achondrite will be easily plucked out. Several spots of severe oxidation are visible.

The thin section shows a breccia dominantly made up of monomineralic pyroxene and feldspar fragments in a fine-grained matrix. Much of the matrix is dark and may be recrystallized. The clasts are generally angular but some have poorly defined outlines and may have been reheated. Mineral fragments range up to 1.3 mm. They are pyroxene (some showing exsolution), feldspar, and minor opaques. Pyroxene compositions show a range in Ca contents with little variation in Mg/Fe, ($Wo_2En_{45}Fs_{53}$ to $Wo_{40}En_{36}Fs_{24}$ with low Ca compositions most abundant, in the few grains analyzed). Feldspars range from $Or_1Ab_6An_{93}$ to $Or_1Ab_{14}An_{85}$.

Two major types of lithic clasts are present: (1) angular fragments up to 2.5 mm in size of fine grained eucrites with igneous textures; (2) fragments up to 1.6 mm across of dark aphanitic material that appears to consist of extremely fine pyroxene and feldspar in a subparallel growth. The overall texture and nature of the clasts resemble those of the Allan Hills polymict eucrites. The small number of pyroxenes analyzed shows essentially no variation in Mg/Fe. On this evidence EETA79004 is classified as a monomict equilibrated eucrite rather than a polymict eucrite.

EETA79005 (450 g).—One surface of this achondrite (10.5 × 8 × 7 cm) is concave; the rest of the meteorite is convex. Fusion crust is visible only on one surface and it is very shiny and polygonally fractured. The matrix is medium gray in color and is speckled with light and dark clasts up to 3 mm in diameter. Vugs are apparent all over the sample. Chipping a corner off the meteorite revealed one fine-grained, black clast 0.5 cm in diameter. The color of the interior matrix is considerably lighter gray than the exterior.

EETA79011 (86.4 g).—A patch of dull black fusion crust appears only on one surface. The rest of this achondrite is medium gray. Several types of clasts are visible on the exterior with the largest one being ~0.7 cm in its longest dimension. The interior revealed through chipping is lighter gray in color than the exterior and contains many clasts.

Petrographically these two meteorites are so similar that the following descriptions of thin section EETA79011 can serve for both. It shows a fine breccia with highly angular, small, monomineralic pyroxene and feldspar clasts predom-

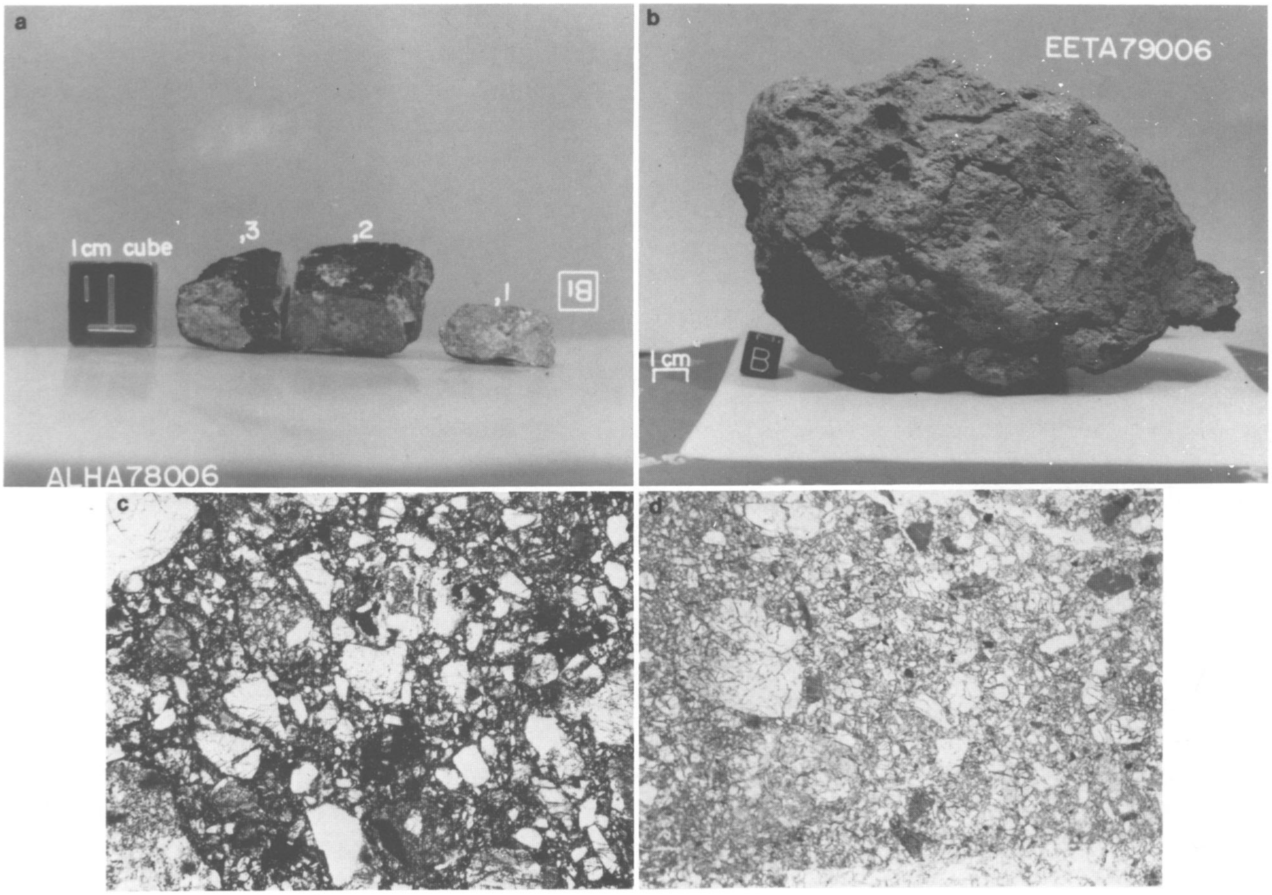

FIGURE 31.—Howardites: *a*, ALHA78006; black fusion crust coats most of surface; *b*, EETA79006; fusion crust coats part of surface, but mostly fracture exposing vuggy interior; *c*, photomicrograph of thin section of ALHA78006 (area of field is 3 × 2 mm) showing brecciated structure and variety of clasts; *d*, photomicrograph of EETA79006 showing brecciated structure and variety of clasts.

inating. Pyroxene grains range up to 2.5 mm, with the large fragments showing evidence of deformation. Some single pyroxene fragments show exsolution textures. Among the small lithic clasts are: (1) fragments of brown, devitrified glass, up to 1.6 mm; (2) fine-grained eucrite clasts with granoblastic texture, up to 0.6 mm; (3) fine-grained eucrite fragments, up to 0.7 mm; and (4) medium-grained eucrite up to 1.6 mm. Pyroxenes have a range of compositions from $Wo_4En_{66}Fs_{30}$ to $Wo_2En_{37}Fs_{61}$. The more magnesian pyroxenes all have low Ca contents but the more Fe-rich varieties range from $Wo_2En_{37}Fs_{61}$ to $Wo_{35}En_{27}Fs_{38}$. Feldspar ranges in composition from $\sim Or_{0.2}Ab_7An_{93}$ to $Or_{1.5}Ab_{19}An_{80}$.

These two meteorites from Elephant Moraine are classified as polymict eucrites. Their petrological similarity and the fact that they were found within 400 m of each other, as shown on the sketch map of Figure 7B (Cassidy and Rancitelli, this volume), strongly suggest that they are individual pieces of a single fall.

HOWARDITES

FIGURE 31

ALHA78006 (8.0 g).—This is a nearly complete specimen (3.0 × 1.5 × 2.0 cm). Shiny black fusion crust covers all of the stone except portions of the E, W, and S surfaces. Where the sample is devoid of fusion crust, light to dark gray interior material is exposed. Cleaving this stone in half revealed an unweathered, brecciated surface.

The thin section shows a complex breccia of angular fragments, up to 1 mm long, of pyroxene (orthopyroxene and pigeonite) and plagioclase, with numerous polymineralic enclaves, set in a matrix of comminuted pyroxene and plagioclase. Accessory chromite and ilmenite and trace amounts of troilite and nickel-iron are present. The enclaves are holocrystalline pyroxene-plagioclase aggregates, and range considerably in texture from coarse-grained gabbroic to fine-grained basaltic types. A slight amount of weathering is indicated by small areas of rusty staining, usually in association with metal grains. Microprobe analyses show a wide range in pyroxene composition: $Wo_{2-12}En_{31-72}Fs_{25-61}$; a number of grains with uniform composition $Wo_3En_{11}Fs_{26}$ suggests the presence of a diogenitic component. Plagioclase averages An_{91}. A single grain of iron-rich olivine (Fa_{81}) was analyzed.

Takeda, Yanai, and Shiraishi (1980) have published analyses of orthopyroxene and inverted pigeonite from ALHA78006.

EETA79006 (7167 g).—This meteorite (14 × 8.5 × 4.5 cm) is partly covered with dull to shiny black fusion crust. Many vugs are present, some with interior clasts. The medium gray matrix contains a variety of clasts (dark gray, yellow, white), the largest being 1 cm in its longest dimension. Several rounded spots of oxidation are obvious and several cracks appear to penetrate the sample. The interior of the meteorite is lighter gray than the exterior. Several clasts (~3 mm diameter) were revealed by chipping the specimen.

The thin section shows a fine-grained breccia with angular pyroxene and feldspar fragments and minor opaques. The larger pyroxene fragments, up to 1 mm, are commonly deformed and some show exsolution. A variety of clast types include the following: (1) fine grained eucritic fragments, up to 2 mm; (2) polymineralic pyroxene-feldspar intergrowths; (3) fragments of brown devitrified glass, up to 1 mm; (4) one fragment, 2 mm, with feldspar ≫ pyroxene; (5) one fragment, 2 mm, with pyroxene ≫ feldspar; and (6) one 4.5 mm recrystallized eucrite clast with mosaic texture. Analysis of pyroxenes yields a wide range of compositions from $Wo_1En_{80}Fs_{19}$ to $Wo_{15}En_{28}Fs_{57}$.

Shergottite

Figure 32

EETA79001 (7942 g).—All but one surface of this achondrite (22 × 17 × 14 cm) is covered with black fusion crust, but there are areas on all surfaces where the fusion crust has been plucked away. One surface has a deep regmaglypt that is covered with fusion crust. The areas void of fusion crust are white-gray and the matrix appears porous. Veins (~0.5 mm wide) of dark material criss-cross each other. Whitish-yellow clasts (~3 mm diameter) are scattered all over this achondrite. Most of the specimen appears very fine-grained but a small part near the E surface has a different lithology. Sawing exposed a light interior with rounded white clasts, as large as 0.5 cm in diameter. Several large, black, fine-grained clasts, as large as 2.5 cm, are scattered over the cut face. Some of these black clasts contain vugs with glass in their interior. Upon chipping one of these clasts containing a vug, the entire clast popped out easily without adhering matrix. Numerous veins of black material criss-cross each other. Most of these veins run through a black clast. The longest vein is ~14 cm long. Near the W end of the cut face are brownish clasts that may be pyroxene. Ninety percent of the cut face is fine-grained. Ten percent (near the E end) of the cut face consists of intergrown pyroxene and feldspar in a basaltic texture.

Thin sections were cut from the three different lithologies: (1) the main mass of the meteorite; (2) the material with basaltic texture at one end of the sample; and (3) the dark clasts included in the main mass. The main mass is a shocked but unbrecciated pyroxenite with pyroxene as the major phase but also containing maskelynite, Mg-Al chromite, iron sulfide, and ilmenite(?). The major pyroxene is polysynthetically twinned pigeonite(?) resembling twinned clinobronzite,

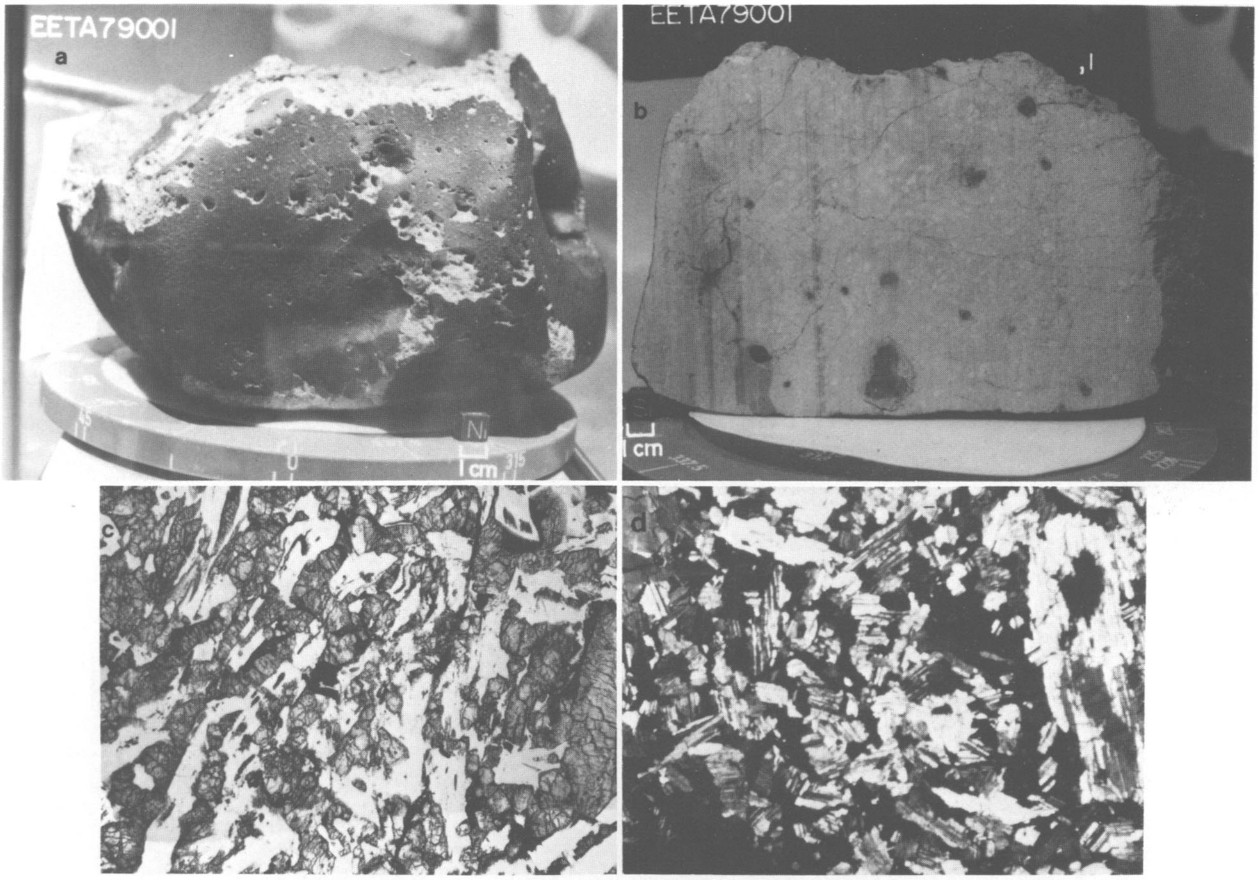

FIGURE 32.—EETA79001, shergottite: *a*, black fusion crust spalled off in some areas, exposing light gray interior; *b*, sawn surface showing black glassy clasts; *c*, photomicrograph (area of field is 3 × 2 mm) showing typical shergottite structure with maskelynite (white), pyroxene (gray), and accessory chromite (black); *d*, photomicrograph (area of field is 3 × 2 mm) showing twinned clinopyroxene (crossed polars).

ranging in composition from $Wo_5En_{70}Fs_{25}$ to $Wo_{12}En_{50}Fs_{38}$. Orthopyroxene forms the cores of larger pyroxene grains and ranges in composition from $Wo_{1.5}En_{83}Fs_{16}$ to $Wo_3En_{78}Fs_{19}$. The larger pyroxene grains, up to 3.5 mm, comprise untwinned cores zoned outward to polysynthetically twinned rims. The smaller pyroxenes, 0.3 to 1 mm, are twinned clinopyroxenes and are intergrown with maskelynite laths. The maskelynite ranges in composition from $Or_1Ab_{39}An_{60}$ to $Or_{1.5}Ab_{44}An_{55}$. A few large olivines, Fo_{77} to Fo_{73}, range to 2.5 mm. The less abundant lithology closely resembles Shergotty in texture but is finer grained. The major minerals are clinopyroxene and maskelynite; calcium phosphate, SiO_2, ilmenite(?), and magnetite(?) are also present. Elongate clinopyroxene and laths of maskelynite are about one mm long and generally subparallel; many of the maskelynite grains contain pyroxene inclusions. Analysed pigeonites range from $Wo_{10}En_{52}Fs_{38}$ to $Wo_{18}En_{15}Fs_{67}$. The maskelynite also shows a range in composition from $Or_{0.5}Ab_{38}An_{62}$ to $Or_4Ab_{50}An_{46}$. The dark clasts are apparently loci of melting; in many cases they connect with the thin, black, glassy(?) veinlets that traverse much of the meteorite. Thin sections from these dark areas show glass (with relict olivine, pyroxene, and maskelynite inclusions), devitrified glass, areas with mosaic texture, and vesicular areas with quench textures. The dark

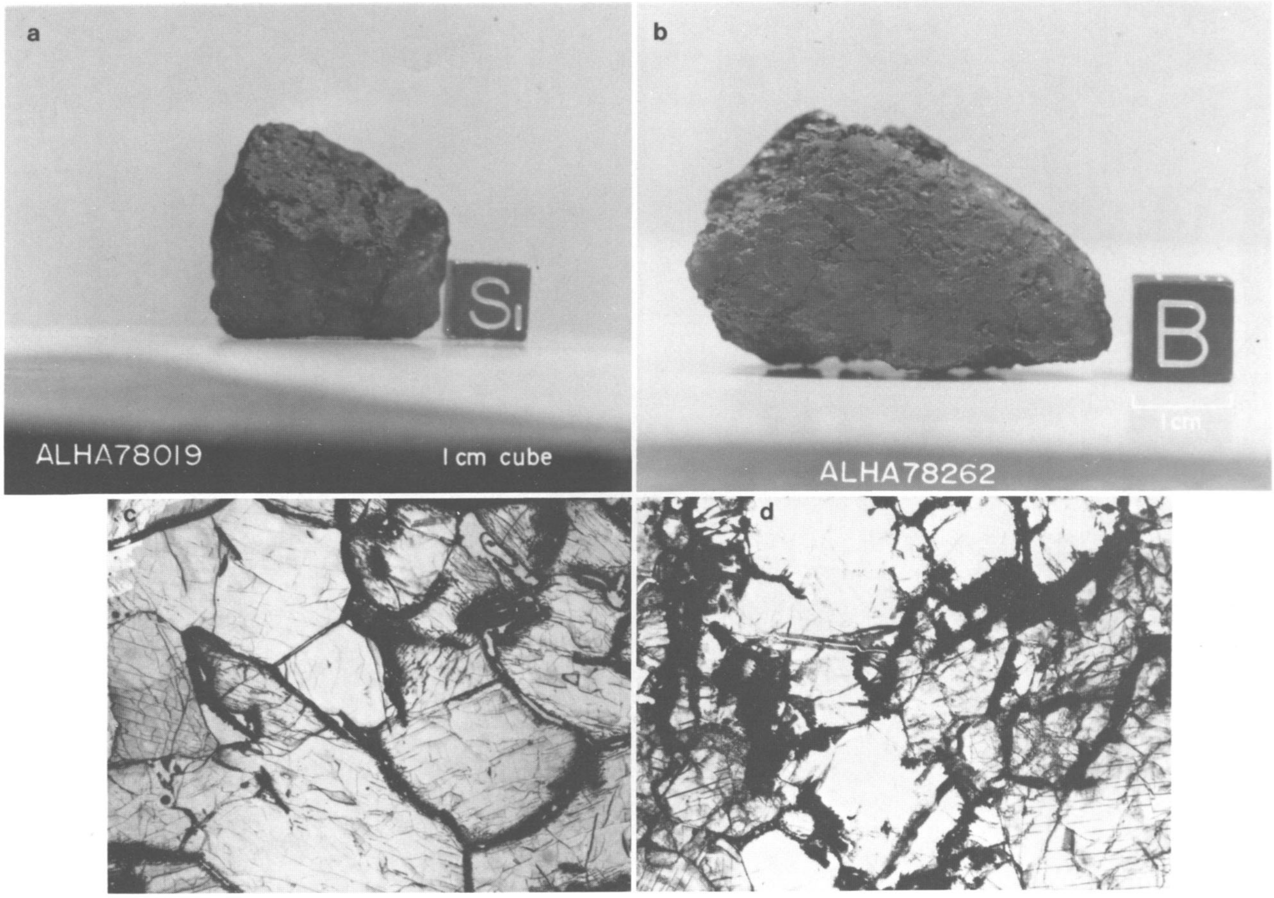

FIGURE 33.—Ureilites: *a*, ALHA78019; patchy fusion crust is present; *b*, ALHA78262; fusion crust coats most of the surface; *c*, *d*, photomicrographs (area of fields is 3 × 2 mm) of ALHA78019 (c) and ALHA78262 (d); olivine (white, without cleavage cracks) and pyroxene (light gray, with cleavage cracks), bordered by black material consisting largely of carbon.

areas appear to be more common in olivine-bearing portions of the main mass.

The meteorite is classed as a shergottite because of the close similarities to the shergottites in texture and mineralogy. Both lithologies, however, are distinct from Shergotty and Zagami.

UREILITES

FIGURE 33

ALHA78019 (30.3 g).—Fusion crust is present on all surfaces but is patchy and does not cover the entire stone. The fusion crust is smooth, dull brownish black, and has polygonal fracture. Where the fusion crust is missing the surface is reddish brown and crystalline. The stone (3.0 × 2.5 × 3.0 cm) was cleaved in half and no unweathered material was exposed. The sample is reddish brown throughout.

The thin section shows an aggregate of rounded to subhedral grains (0.5–3 mm across) of olivine, with minor pyroxene. The grains are rimmed with black carbonaceous material. Trace amounts of troilite and nickel-iron are present, the latter largely altered to translucent brown limonite concentrated along grain boundaries. Microprobe analyses show olivine of uniform composition (Fa_{22}) with notably high CaO (0.4%) and Cr_2O_3 (0.7%) contents; the pyroxene is a pigeonite of composition $Wo_{10}Fs_{18}En_{72}$. This meteorite is a ureilite, with mineral compositions essentially identical to those in the Kenna ureilite

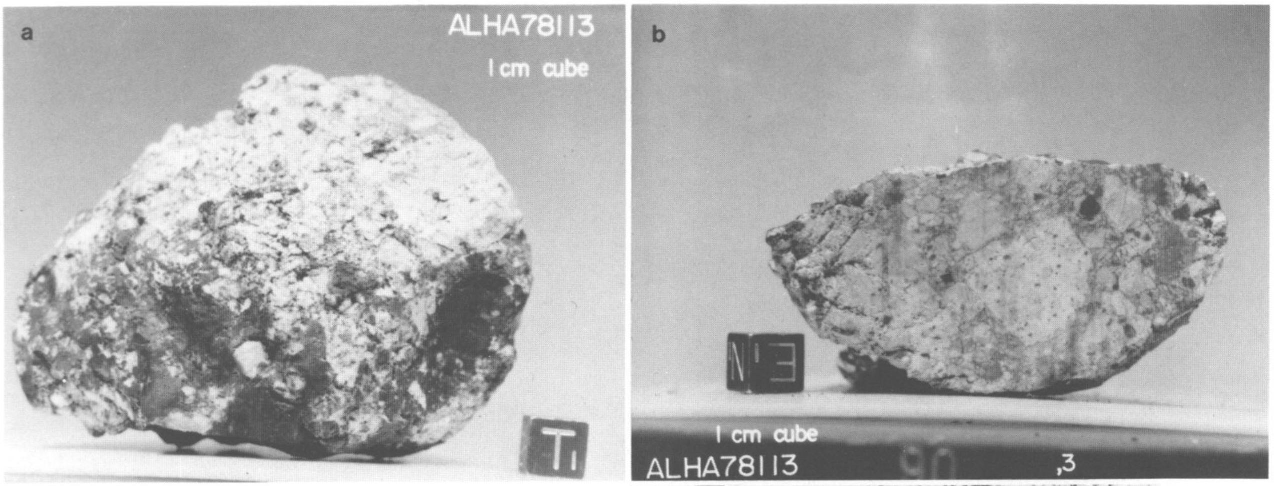

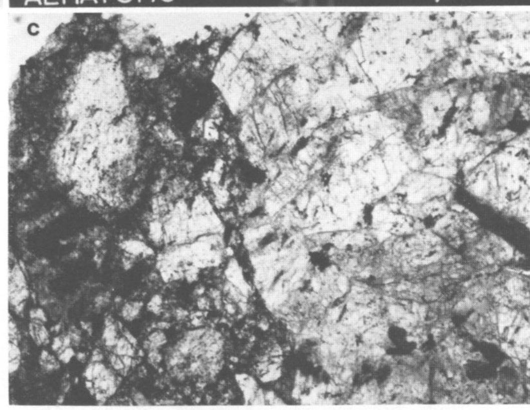

FIGURE 34.—ALHA78113, aubrite: *a*, dark fusion crust spalled off most of surface, exposing interior consisting largely of white enstatite; *b*, sawn surface showing brecciated structure of interior; *c*, photomicrograph of thin section (area of field is 3 × 2 mm) showing brecciated enstatite (white) veined by fine-grained, dark gray material.

(Berkley et al., 1976); it appears to be relatively unshocked compared to most ureilites. ALHA 78019 has been described by Takeda and Yanai (1979).

ALHA78262 (26.1 g).—This specimen (4.0 × 2.5 × 2.0 cm) is triangular and has thin, dull black fusion crust on three surfaces. The remaining surfaces are fracture surfaces that are rough on a small scale, resulting from exposed crystal faces. The overall color is very dark greenish black. The thin section is identical with that of ALHA78019 in all respects, and these two stones are apparently pieces of a single fall.

AUBRITE

FIGURE 34

ALHA78113 (298 g).—This specimen (8.5 × 6.5 × 3 cm) has a brecciated structure, with abundant large enstatite grains (~2.5 × 2.0 cm) and less numerous dark clasts exposed on the surface; patches of very thin, black fusion crust are present. Half of the B surface has thin, yellowish-brown weathering discoloration. Very small spots (<1 mm) of iron oxidation are present on some surfaces. A cut face shows many large, white enstatite clasts, a few containing isolated rounded blebs of metal, some with oxidation halos. The clasts are surrounded and veined by fine-grained, dark gray material.

The thin section consists almost entirely of clasts of orthopyroxene, up to 2 mm long, in a groundmass of comminuted pyroxene. Accessory amounts of sulfides and nickel-iron are present as small grains in the groundmass. The section shows a moderate amount of brown limonitic staining concentrated around the metal grains. Microprobe analyses show that the pyroxene is an iron-free enstatite (FeO 0.1%) with minor and variable amounts of CaO (0.2–0.6, average 0.5%).

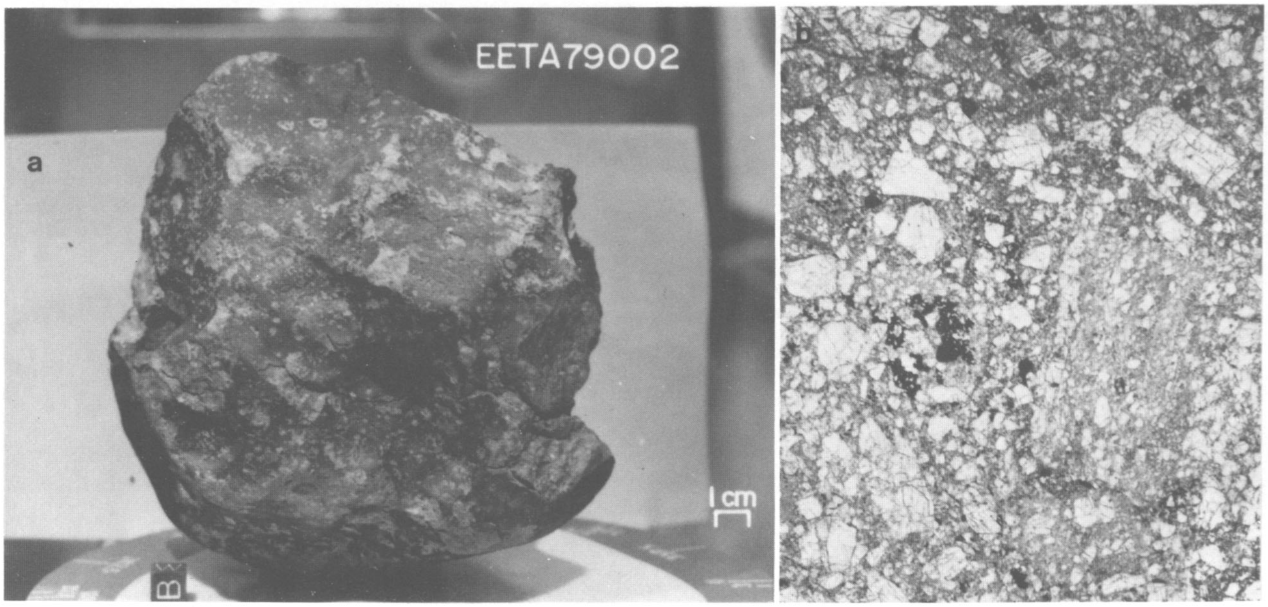

FIGURE 35.—EETA79002, diogenite: *a*, dull black fusion crust coats stone, except in small areas where spalled off to reveal light gray interior; *b*, photomicrographs of thin section (area of field 3 × 2 mm); orthopyroxene clasts (white) in matrix of comminuted orthopyroxene (gray) and a little chromite (black).

Watters et al. (1980) have provided a detailed mineralogical and petrographic description of ALHA78113 and compared it with other aubrites. In addition to the minerals mentioned above, they record the presence of accessory amounts of forsterite (Fo 99.99) albite (An 3.39) diopside (Wo 43.89, En 56.09, Fs 0.02), oldhamite, ferromagnesian alabandite, daubreelite, and schreibersite.

DIOGENITE

FIGURE 35

EETA79002 (2843 g).—This rounded meteorite (15 × 13.5 × 10 cm) is covered with dull fusion crust except on one fracture surface. Fusion crust has been plucked away in places, revealing a medium gray matrix with many light to cream-colored clasts (~0.5 cm diameter). Several areas have been heavily oxidized giving these parts a red-brown color. Many fractures penetrate this meteorite. Chipping revealed an extensive orange-brown weathering rind as wide as 1 cm. The interior matrix is blue-gray with many small (<1 mm) clasts. Two white clasts ~0.5 cm diameter were exposed. No metal was obvious.

The thin section shows a breccia with a very cohesive, fine-grained matrix. Clasts are monomineralic, angular, and range up to 2 mm. One angular lithic clast is polymineralic but extremely fine-grained. The vast majority of the mineral fragments are low-calcium pyroxenes of near-constant composition, $Wo_2En_{76}Fs_{22}$. The only other silicate phase identified is olivine, Fo_{75-76}. Small areas within the breccia are rich in very fine opaque minerals. The meteorite is a diogenite but is texturally distinct from the common diogenites.

Descriptions of Iron Meteorites

Roy S. Clarke, Jr.

This section provides descriptions of the 19 iron meteorite specimens that have been collected in Victoria Land since 1976. Their textural and chemical properties indicate that five irons from the Allan Hills derive from a single shower as do nine from Derrick Peak (plus six more that were collected from the same site by a New Zealand party). Therefore, the total number of iron meteorite falls from Victoria Land is now seven. Descriptions of specimens are given below and in Table 3 in the order of their chemical classification groups. Specimens grouped as members of a single fall are listed by the lowest-numbered specimen retained in United States collections.

Coarse Octahedrites

Group IA

ALHA76002 Group

ALHA76002 (1.51 kg).—This coarse octahedrite was the first iron meteorite to be recovered from the Allan Hills. It was listed by King et al. (1980:42) in the previous Catalog of Antarctic Meteorites (Marvin and Mason, editors, 1980). It was described and given an ambiguous classification by Olsen et al. (1978). Clarke et al. (1980) have re-examined ALHA76002 and found it to be indistinguishable from four other Allan Hills specimens that were collected a year later. All five are typical coarse octahedrites of chemical group IA.

Roy S. Clarke, Jr., Department of Mineral Sciences, National Museum of Natural History, Smithsonian Institution, Washington D.C. 20560.

ALHA77250 (10.5 kg; 26 × 15 × 8 cm).

ALHA77263 (1.68 kg).—This specimen was described with a photograph by King et al. (1980:42).

ALHA77289 (2.19 kg).—This specimen was described with a photograph by King et al. (1980:42).

ALHA77290 (3.78 kg; 16 × 13 × 6 cm).

All five specimens have generally similar reddish-brown iron oxide coatings. Surfaces that were probably initially at least partially regmaglypt-covered have undergone severe weathering. No fusion crust remains. Surfaces of the under side of specimens are more severely weathered than those that were exposed to the atmosphere. An occasional troilite inclusion is visible at the surface.

Macroetched surfaces reveal the same basic metallography for all five specimens. They all have surficial patches of an ablation-produced zone of α_2 iron. Kamacite grains are 2–3 mm wide, and their length is generally only a few times their width. Areas of recrystallized kamacite are unevenly distributed. Taenite-plessite areas with comb texture, and grain-boundary taenite are present. Schreibersite occurs at grain boundaries and as occasional large crystals. There are a few large troilite-carbon inclusions surrounded by schreibersite, and, in some instances, also cohenite.

The appearance, structure, and chemical data given in Table 3 establish these five specimens as typical coarse octahedrites of Group 1A. The close similarity in the chemical values makes it highly likely that they are all pieces of the same shower.

TABLE 3.—Summary of data on iron meteorites (NMNH = National Museum of Natural History, Smithsonian Institution, Washington, D.C.; NIPR = National Institute of Polar Research, Tokyo; data in 4th to 9th columns from Clarke, Jarosewich, Goldstein, and Baedecker (1980))

Specimen number	*Original wt. (kg)*	*NMNH wt. (kg)*	*NIPR wt. (kg)*	*Chemical group*	*Structural classification*	*%Ni*	*ppm Ga*	*ppm Ge*	*ppm Ir*
ALHA76002*	1.51	0.307	?**	IA	Og	6.84	92.1	404	2.9
77250	10.5	4.69	5.42	IA	Og	6.84	91.5	455	3.1
77263*	1.68	0.839	0.779	IA	Og	6.84	92.8	414	3.0
77289*	2.19	1.08	1.01	IA	Og	6.84	92.6	386	3.0
77290	3.78	1.93	1.73	IA	Og	6.84	93.7	407	3.0
PGPA77006*	18.9	7.75	8.16	IA	Og	7.27	78.2	245	2.5
ALHA77283	10.5	5.68	4.34	IA	Og	7.33	69.0	230	2.2
ALHA78100	0.085	0.040	0.040	IIA	H				
DRPA78001	15.2		15.2						
78002	7.21	7.21							
78003	0.144		0.144						
78004	0.134	0.134							
78005	18.4	18.4							
78006	0.389	0.389							
78007	11.9		11.9						
78008	59.4	30.1	26.1	IIB	Ogg				
78009	138	65.8	67.6	IIB	Ogg				
ALHA78252	2.79	1.41	1.32	IVA	Of	9.33	2.5	<100	0.45
ALHA77255*	0.767	0.387	0.367	Anom	D	12.23	0.6	<200	12.0

* Specimens listed in Marvin and Mason, editors (1980).
** Specimen material at both the National Institute of Polar Research, Tokyo and the Field Museum of Natural History, Chicago.

PGPA77006 (18.9 kg).—This specimen from Purgatory Peak in the Victoria dry valley was described with a photograph by King et al. (1980:42).

A macroetched surface revealed kamacite band-width in the 1.5 to 2 mm range, with length-to-width ratios ranging from 4 to 10. Neumann bands are abundant, and along the rim of the specimen kamacite has been converted to α_2 by atmospheric ablation. Taenite and taenite-plessite areas occupy at least half of the length of kamacite grain boundaries, and a number of areas of comb plessite are present. Schreibersite occurs along grain boundaries, and occasional schreibersites surrounded by cohenite are present. No large inclusions were observed on the small surface available. The structural and chemical data from Table 3 establish that this is a typical coarse octahedrite, a chemical group IA meteorite. It is chemically and structurally distinct from both the ALHA76002 group and from ALHA77283.

ALHA77283 (10.5 kg; 16.5 × 16 × 12.5 cm).—The specimen has a generally rounded anterior surface that is suggestive of aerodynamic shaping during oriented atmospheric flight and a slightly concave posterior surface. The specimen has been severely weathered, particularly on the posterior surface. Wind erosion while on the ice also appears to have been important. Taenite bands stand out in relief over much of the surface, revealing the internal octahedrite structure of the meteorite.

Clarke et al. (1981) have studied this specimen and shown it to contain preterrestrial, impact-produced diamond and lonsdaleite. The meteorite is a carbon-rich, coarse octahedrite of chemical group IA (Table 3). It is similar in composition and structure to carbon-rich Canyon Diablo specimens and its metallography indicates shock load-

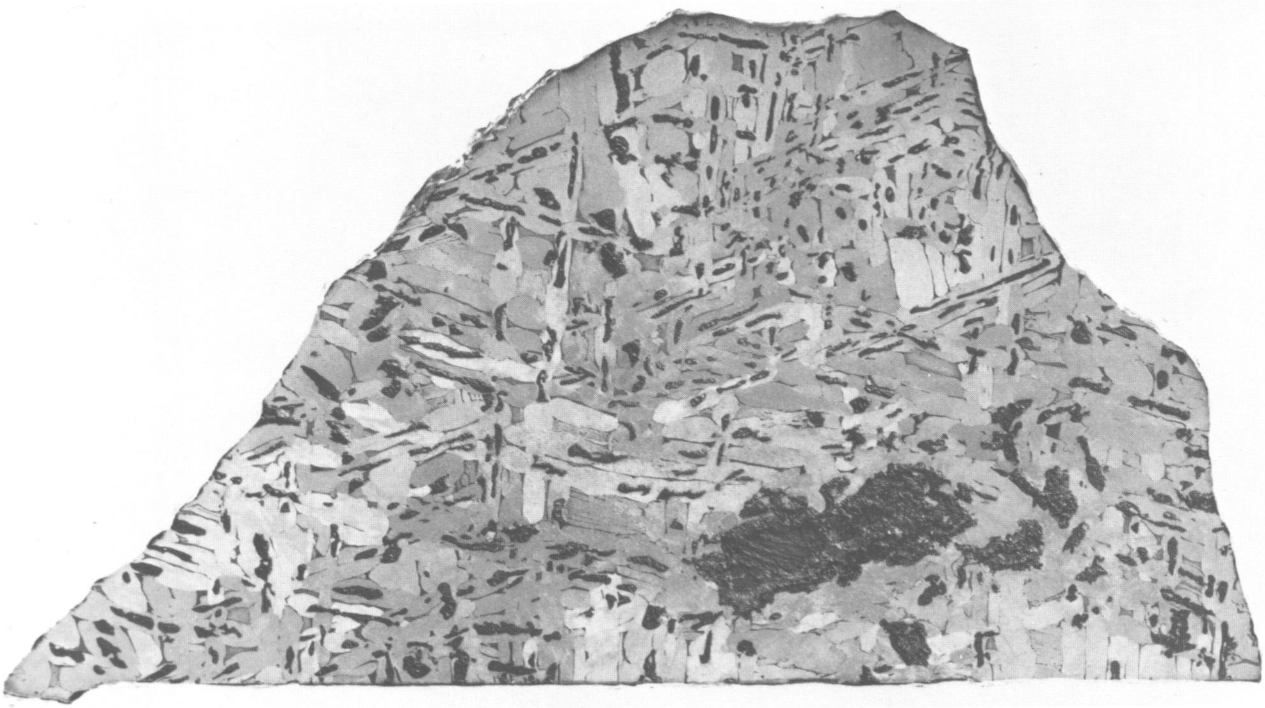

FIGURE 36.—Polished and etched slice of ALHA77283: large inclusion at lower right is troilite-carbon-schreibersite-cohenite; carbonado-like material containing diamond and lonsdaleite found in number of such inclusions, generally at borders between troilite and schreibersite; dark mineral distributed throughout surface and generally at centers of kamacite lamellae is cohenite; kamacite lamellae are arranged in coarse Widmanstätten pattern, with their lengths short compared to their widths; taenite lamellae and taenite-plessite fields present at borders of kamacite lamellae (length of bottom edge of specimen = 9.5 cm).

ing to moderate intensity. It contains a number of troilite-carbon-schreibersite-cohenite inclusions that are rich in carbonado-like material containing diamond and lonsdaleite (Figure 36). The presence of an ablation-produced, heat-altered zone indicates an uninterrupted passage through the atmosphere and a non-explosive impact on the earth. This establishes that the diamond and lonsdaleite were produced preterrestrially.

Hexahedrite

GROUP IIA

ALHA78100 (85.0 g; 5 × 4.5 × 0.9 cm).—This specimen, unlike others, was found frozen within the ice. It is a thin, flat, slightly irregular plate that appears to have been oriented during atmospheric flight. The anterior surface is rounded at the edges and the posterior surface has been affected more severely. It is covered with an essentially featureless, reddish-brown oxide. The anterior surface contains numerous 1 to 2 mm pockmarks.

A microetched median section of the specimen reveals single-crystal kamacite containing Neumann bands and inclusions. Schreibersite is abundant as rhabdites, and is also present as lamellar schreibersite and as hieroglyphic schreibersite surrounding troilite-daubreelite inclusions. Troilite-daubreelite inclusions are present with only small bordering schreibersites. The edge of the anterior surface has an ablation rim averaging about 0.7 mm wide. No α_2 was observed on the posterior surface. Fusion crust was not present, and surfaces are covered with terrestrial oxide up to 0.25 mm thick. The specimen is a Group IIA hexahedrite.

FIGURE 37.—Derrick Peak irons: *left*, DRPA78009, largest of irons found on mountainside; unusual appearance due to both lustrous, deep, reddish brown color and protruding schreibersite crystals; combination of corrosion and erosion appears to have affected an originally regmaglypt-covered surface. *Above*, Photograph of polished and etched surface of DRPA78008; dominant metallographic structures are areas of swathing kamacite surrounding large schreibersite or schreibersite-troilite inclusions; areas of coarsest Widmanstätten pattern are interspersed.

Coarsest Octahedrite

Group IIB

DRPA78002 Group

Nine iron meteorites were recovered from among the boulders covering the slopes of Derrick Peak, in the Darwin Mountains. They are assumed to be from the same fall because of their distribution over the mountainside (Marvin, this issue) and their similar and strikingly unusual appearances. No other iron meteorites are known that have the same atypical, rich, reddish brown color and large protruding blades of schreibersite. This distinctive appearance is probably due to a combination of corrosion and erosion of surfaces of schreibersite-rich specimens in the polar environment (Figure 37).

It was decided by the Meteorite Working Group that for this group of specimens it would be better to distribute the smaller specimens between the United States and Japanese collections rather than to cut each specimen in half. DRPA78001, 78003, and 78007 were selected for the National Institute of Polar Research, Tokyo, in consultation with Professor T. Nagata. Specimens DPRA78002, 78004, 78005, 78006 were selected for the United States Collection. The two largest specimens, DRPA78008 and 78009, have been sawed in half and distributed to the two collections (Table 3). The United States specimens are listed below. Up to this time, only DRPA78008 and 78009 have been prepared for metallographic examination.

DRPA78002 (7.21 kg; 24 × 21 × 9 cm).—This is a roughly fan-shaped specimen with a smooth bottom surface that had been in contact with the ground and a highly irregular and sculptured upper surface. Depressions in the upper surface resemble regmaglypts but may be corrosion pits. Large schreibersites protrude from both surfaces. Part of the bottom is covered with light-colored and fresh-appearing corrosion products.

DRPA78004 (134 g; 4.5 × 4 × 2.5 cm).—All surfaces of this specimen are highly corroded. The top has a lustrous, reddish-brown oxide coating; the bottom is lighter and has soil particles attached.

DRPA78005 (18.4 kg; 26 × 21 × 13 cm).—The bottom surface of this specimen has been rounded by deep weathering. Most of the specimen appears to have been above ground level but is also deeply corroded and eroded. The specimen is comparatively featureless with only a few protruding schreibersites.

DRPA78006 (389 g; 8 × 6 × 3 cm).—This is a roughly rectangular specimen, the bulk of which appears to have been exposed for a prolonged period to atmospheric corrosion and erosion. About one-quarter of the specimen appears to have been below ground. It is deeply corroded with soil attached. Large schreibersites protrude from the top.

DRPA78008 (59.4 kg; 34 × 24 × 20 cm).—This is a large, blocky specimen that has been severely corroded and eroded. Its upper surfaces are generally smooth with some areas of deep pitting. The under surface is more deeply corroded, with some soil attached.

This is the first of the Derrick Peak specimens to be examined structurally. A large area of macroetched surface was prepared. The dominant structural units distributed over more than half of the surface are broad and irregular areas of swathing kamacite enclosing large hieroglyphic schreibersites; some of these schreibersites border centimeter-size troilites. Between these swathing kamacite areas are areas of coarsest octahedrite structure. Grain boundary schreibersite is common throughout the surface, and lamellar schreibersites are present in many areas of kamacite. Neumann bands are abundant in the kamacite, and deformation zones are a common feature. Taenite and plessite are present in areas of coarsest octahedrite structure. Weathering has penetrated the section, particularly along grain boundaries bordering swathing kamacite areas.

What appears to be cleavage cracks are present in some areas of kamacite. This specimen is a coarsest octahedrite, a Group IIB meteorite similar to Santa Luzia.

DRPA78009 (138 kg; 42 × 23 × 34 cm).—This specimen is generally egg-shaped and sculptured over much of its surface by regmaglypts that have been deepened by terrestrial corrosion and erosion. Many schreibersites stand out in relief, particularly within depressions in the surface. A large cut surface reveals that this specimen has the same structure and composition as DRPA78008. Although the other Derrick Peak irons have not yet been analyzed, they clearly derive from the same fall.

FIGURE 38.—Iron meteorite ALHA78252: *left*, as found on slope leading up to the polar plateau; *below*, polished and etched slice of meteorite showing fine octahedrite structure (top curved surface was anterior surface during atmospheric flight; thick rim of fusion crust accumulated on posterior surface and is separated from body of specimen by thin layer of corrosion; width = 10 cm).

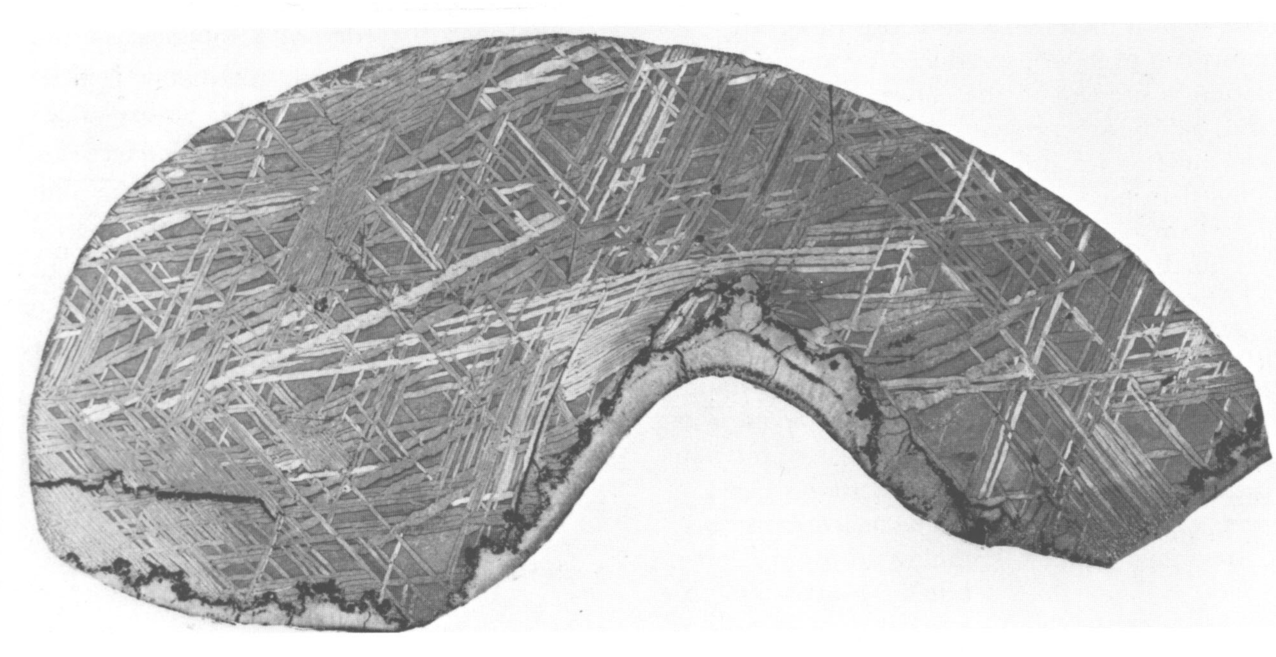

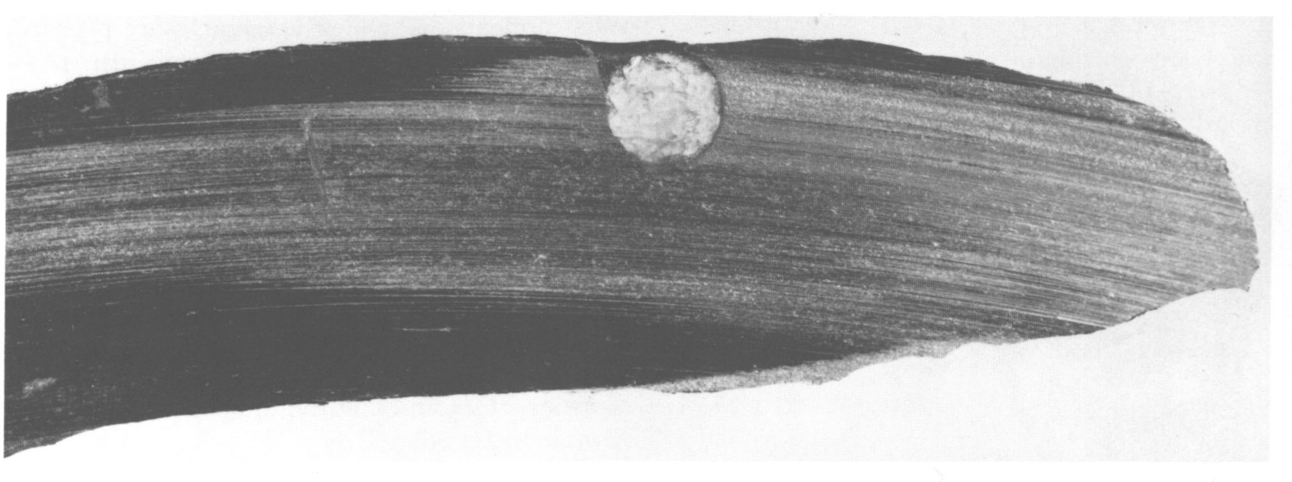

FIGURE 39.—Sawed surface of ALHA77255 revealing large spherical silicate inclusion at anterior edge of aerodynamically shaped meteorite (inclusion approximately 5 mm in diameter).

Fine Octahedrite

GROUP IVA

ALHA78252 (2.79 kg; 17 × 9.5 × 5 cm).—The specimen has an elongated dome shape, a smooth convex surface, and a slightly more irregular concave surface. The shape is highly suggestive of oriented atmospheric flight.

Examination of a macroetched surface revealed kamacite band widths in the less than 0.5 mm range, with a high length-to-width ratio. A continuous rim of α_2 iron produced by atmospheric ablation is present on the convex surface. Neumann bands are present, the kamacite has a matte appearance, and some kamacite bands are mildly deformed. Taenite bands continuously border kamacite bands, and taenite-plessite areas cover much of their surface. Several small troilites are present. The specimen is a fine octahedrite, a group IVA meteorite (Figure 38).

Ataxite

ANOMALOUS

ALHA77255 (767 g; 15 × 8 × 2 cm). This specimen was described with a photograph in Marvin and Mason (1980:42). It is boomerang-shaped with slightly convex anterior and concave posterior surfaces suggestive of oriented atmospheric flight. A saw cut to remove a slice for study passed through the edge of a spherical silicate inclusion approximately 5 mm in diameter (Figure 39).

Metallographic examination revealed an ataxitic structure. Occasional oriented kamacite spindles are present in a dense plessite matrix. Several small troilites are visible. It is an anomalous ataxite, similar in composition and structure to the Nordheim meteorite.

Overview of Antarctic Irons

Roy S. Clarke, Jr.

Antarctica has enriched meteorite collections in recent years by providing specimens from 10 different iron meteorite falls representing six structural classes. A total of 22 individual specimens has been reported. The meteorites are listed with their structural and chemical classifications in Table 4 in the order of their date of recovery. This note briefly summarizes the information available in the literature on these meteorites.

Lazarev, Humboldt Mountains (found 1961).—This specimen was originally described as a coarse octahedrite containing approximately 10% Ni. Buchwald (1975) has reviewed the available data and finds it to be more appropriate for a pallasite than for an iron meteorite. He suggested that the meteorite should be re-examined with this in mind. It is listed herein for completeness but is not counted as one of the 10 separate iron meteorite falls.

Neptune Mountains, Pensacola Mountains (found 1964).—This coarse octahedrite was discovered by a U.S. Geological Survey field party and was first reported by Schmidt (1964). Buchwald (1975) described it in detail, and Scott and Wasson (1976) established it as belonging to chemical group IA.

Yamato 75031, Yamato Mountains, Eastern Queen Maud Land.—The plessitic octahedrite has been described by Fisher, Spangler, and Nagata (1978); Fisher, Goldstein, and Nagata (1978); Nagata (1978); and Kracher, Willis, and Wasson (1980), who list it as anomalous, ungrouped chemically.

Yamato 75105, Yamato Mountains, Eastern Queen Maud Land.—This reheated hexahedrite has been described by Nagata, Fisher, and Suguira (1976); Fisher, Goldstein, and Nagata (1978); and Kracher, Willis, and Wasson (1980) who grouped it as IIA.

Eighteen iron meteorite specimens were collected by the first three expeditions to Victoria Land in 1976–1977, 1977–1978, and 1978–1979. In addition, the Purgatory Peak iron (PGA77006) came into the collection after being recovered from the Victoria Valley by a University of Maine field party.

The current location of all Antarctic irons and a summary of information available on them is given in Table 4. Specimens grouped together in the table are thought to be individual pieces from the same fall. The Allan Hills grouping is based on appearance, metallography, and chemical composition (Clarke et al., 1980). The Derrick Peak grouping is based on their apparent distribution in a strewn field on a mountainside and striking similarlity of highly unusual external appearances. In all, seven separate falls are indicated representing five meteorite classes.

Descriptions of the individual iron meteorite specimens collected in Victoria Land are given elsewhere in this volume (p. 49). For tabulations of data see tables 3 and 4.

Roy S. Clarke, Jr., Department of Mineral Sciences, National Museum of Natural History, Smithsonian Institution, Washington, D.C. 20560.

TABLE 4.—Data on Antarctic iron meteorites (collection numbers: 1 = Mining Institute, Leningrad and Committee of Meteorites, Moscow; 2 = Division of Meteorites, National Museum of Natural History, Smithsonian Institution; 3 = National Institute of Polar Research, Tokyo; 4 = Meteorite Working Group, National Museum of Natural History, Smithsonian Institution; 5 = specimen of ALHA76002 in the Field Museum of Natural History, Chicago)

Name/Specimen number	*Structural class*	*Chemical group*	*Number of specimens*	*Collection(s)*
Lazarev (1961)	Pallasite ?		2	1
Neptune Mountains (1964)	Og	IA	1	2
Yamato 75031	Opl	Anom	1	3
Yamato 75105	H	IIA	1	3
ALHA76002 Group*	Og	IA	5	3, 4, 5
ALHA77255	D	Anom	1	3, 4
ALHA77283	Og	IA	1	3, 4
PGPA77006	Og	IA	1	3, 4
ALHA78100	H	IIA	1	3, 4
ALHA78252	Of	IVA	1	3, 4
DRPA78002 Group**	Ogg		9	3, 4

* ALHA76002, 77250, 77263, 77289, 77290.
** DRPA78001 to 78009.

Overview of Antarctic Achondrites

Arch M. Reid

Introduction

The channeling of research energies into the study of extraterrestrial materials brought about by the lunar exploration program has led to a renewed interest in the achondritic meteorites. Recent studies of achondrites have helped elucidate the nature of igneous processes active very early in solar system history and also have revealed the existence of a number of meteorites that have relatively young crystallization ages. Despite substantial improvement in analytical techniques, which have allowed extensive studies to be made on very small amounts of meteorite material, the restricted availability of achondrites has constrained investigations of these irreplacable samples. It is thus a great pleasure to record that Japanese and United States expeditions to the Antarctic over the 10-year period, 1969–1979, added 62 specimens of achondrites to the available collections, and the 1979–1980 Japanese and United States teams collected over 100 additional achondritic fragments (see Tables 5 and 6).

The museums of the world contain probably less than a hundred achondrites collected outside Antarctica. Table 7 compares the distribution of achondrite classes in the Antarctic and non-Antarctic collections. The numbers in the non-Antarctic column are an unreliable guide to the real distribution of achondrite types in the total terrestrial infall because of the vagaries of observation, recognition, and recovery. The Antarctic meteorites may provide a better guide since they are more easily recognized and are all carefully studied and catalogued. A problem with the Antarctic collection, however, is that it is highly probable that several individual samples are fragments from a single event, i.e., pieces of the same meteorite or fragments from a shower.

Table 7 shows that there are marked differences between the Antarctic and non-Antarctic achondrite collections. Diogenites are more abundant in the Antarctic collection, comprising over half the classified samples. The preponderance of diogenites may well be misleading, as the majority of the samples are very similar to each other, all having an uncommon granoblastic texture. These recrystallised diogenites could all be fragments from a single fall (Takeda, Miyamoto, Yanai, and Haramura, 1978). The second most abundant group of Antarctic achondrites are the eucrites.

TABLE 5.—Number of achondrite specimens in Antarctic meteorite collections

Expeditions	*Number of specimens*	*Number of achondrites*
pre-1969	4	0
Yamato Mountains		
1969 Japanese	9	1
1973 Japanese	12	1
1974 Japanese	663	28
1975 Japanese	307	12
1979 Japanese	>3000	>100
Victoria Land		
1976 United States-Japanese	11	1
1977 United States-Japanese	300	4
1978 United States-Japanese	309	6
1979 United States	73	7

Arch M. Reid, Geology Department, University of Cape Town, Rondebosch, South Africa.

TABLE 6.—Types of achondrites in the Antarctic meteorite collections

Year/Location	*Diogenite*	*Howardite*	*Eucrite*		*Shergottite*	*Ureilite*	*Aubrite*
			poly-mict	*mono-mict*			
1969 Yamato Mts.	1						
1973 Yamato Mts.		1					
1974 Yamato Mts.	22		2	1		3	
1975 Yamato Mts.	7		5				
1976 Allan Hills			1				
1977 Allan Hills	1		1		1	1	
1978 Allan Hills		1	4			2	1
1979* Allan Hills, Reckling Peak, Elephant Moraine	1	1	2	1	1		
Totals	32	3	16	2	2	6	1

* The 1979 Japanese expedition to the Yamato Mountains returned with over 100 achondrites that have not all been classified (Yanai, 1980).

Eucrites and howardites are the most common achondrites in the non-Antarctic compilation. The Antarctic samples are distinctive in that howardites and monomict eucrites are not common and that a particular type of eucrite makes up the bulk of the collection. This type is the polymict eucrite, described below, which is rare in non-Antarctic collections. As with the diogenites, several of the polymict eucrites are very similar and may be from a single fall. It should be noted, however, that this unusual type of eucrite is common at both the Yamato and Allan Hills sites which are almost 3000 km apart.

Aubrites are rather rare in the Antarctic collection and so far none of the very unusual achondrites such as Nakhla, Chassigny, or Angra dos Reis have been found. It is of great interest to note that two shergottite meteorites, related to, but not identical with, the two previously known members of the shergottite class, have been recovered.

The differences between the Antarctic and non-Antarctic collections are intriguing and while any attempt to understand these differences may be yet premature, we can speculate that: (a) the differences are an artifact produced by inadequate sampling; (b) there is some factor that results in the achondrite flux in the Antarctic region of the earth being different from elsewhere; or, (c) the distribution of achondrite meteorites reaching the earth has changed with time and the Antarctic collection represents an average over a much longer time increment.

Descriptions of the individual meteorites are presented by Score et al., in this volume, and in a variety of other publications. Some of the more interesting characteristics of the collection are briefly summarised below, with particular emphasis on the aspects of the collection that appear to be unique.

ACKNOWLEDGMENTS.—I thank Roberta Score for substantial help. The research reported in this paper was done while the author was a National

TABLE 7.—Comparison between Antarctic (excluding those from the 1979–1980 Japanese expedition) and non-Antarctic (Wasson, 1974:292) achondrites

Class	*Antarctic*	*Non-Antarctic*
Diogenites	32	8
Howardites	3	19
Eucrites	18	24
Shergottites	2	2
Ureilites	6	6
Aubrites	1	9
Others	0	13
Totals	62	81

Research Council Associate at the Johnson Space Center in Houston, Texas and a Visiting Scientist at the Lunar and Planetary Institute, which is operated by the Universities Space Research Association under Contract No. NASW-3389 with the National Aeronautics and Space Administration. This paper is LPI Contribution number 435.

Diogenites

TABLE 8

The initial 1969 Japanese collection of 9 meteorites in the Yamato Mountain regions contained one achondrite, originally named Yamato (b), but now renamed Yamato 692. This 138 g diogenite was described by Okada (1975), Okada et al. (1975), and by Takeda et al. (1975). While mineralogically and compositionally similar to the known diogenites, it is texturally unique, having a granoblastic texture rather than the brecciated texture of most diogenites. The recovery of 22 diogenites in the 1974 Yamato expedition demonstrated that this texture, indicative of severe recrystallisation, is characteristic of the diogenites from this region of the Antarctic. As noted above many, if not all, of these diogenites may represent a single fall as they are petrographically alike and occur in the same geographic region. The six diogenites in the 1975 Yamato collection also include samples with granoblastic textures.

TABLE 8.—Data on diogenites in the Antarctic meteorite collections

Locality	*Specimen number*	*Weight (g)*
Yamato Mountains	692	138.0
Yamato Mountains	74005	3.8
Yamato Mountains	74010	298.5
Yamato Mountains	74011	206.0
Yamato Mountains	74013	2059.5
Yamato Mountains	74031	6.1
Yamato Mountains	74037	591.9
Yamato Mountains	74096	16.1
Yamato Mountains	74097	2193.9
Yamato Mountains	74109	43.5
Yamato Mountains	74125	107.0
Yamato Mountains	74126	14.5
Yamato Mountains	74136	725.0
Yamato Mountains	74150	33.4
Yamato Mountains	74151	49.1
Yamato Mountains	74162	3.9
Yamato Mountains	74344	1.4
Yamato Mountains	74347	7.8
Yamato Mountains	74368	4.1
Yamato Mountains	74448	17.7
Yamato Mountains	74546	7.3
Yamato Mountains	74606	2.9
Yamato Mountains	74648	185.5
Yamato Mountains	75001	4.1
Yamato Mountains	75004	37.0
Yamato Mountains	75007	2.6
Yamato Mountains	75014	3.0
Yamato Mountains	75285	3.1
Yamato Mountains	75299	9.1
Allan Hills	ALHA77256	676.2
Elephant Moraine	EETA79002	2843.0

The Yamato diogenites are orthopyroxenites with pyroxenes around En_{74-72}. One sample in the 1975 collection, 75032, is more iron-rich than other diogenites and approaches the more magnesian eucrites in composition. Yamato 75032 is an unrecrystallised monomict diogenite that has as its dominant phase orthopyroxene (approximately En_{65}) with exsolved lamellae and blebs of augite. Takeda et al. (1979) conclude that the major primary phase in Yamato 75032 was a low-Ca pigeonite now inverted to orthopyroxene, but that primary orthopyroxene may also be present. The meteorite is transitional between the diogenites and the more magnesian eucrites and fills in the "apparent" gap in pyroxene crystallisation trends between diogenites and eucrites.

The one diogenite from the Allan Hills region (ALHA77256) weighs 676 g and is described as a normal diogenite. The 2.8 kg diogenite from Elephant Moraine (EETA79002) has the minerals of a normal diogenite but is a very fine breccia with a few dark, fine-grained, lithic clasts. The Antarctic diogenites thus extend the boundaries of the diogenite class in composition, mineral assemblage, and texture.

Eucrites and Howardites

TABLE 9

Both eucrites and howardites have been found in the Antarctic but the most abundant samples of this type are the "polymict eucrites." Their

TABLE 9.—Data on eucrites and howardites in the Antarctic meteorite collections

Locality	*Type/Specimen number*	*Weight (g)*
	EUCRITES	
Yamato Mountains	74365	10.0
Elephant Moraine	EETA79004	390.3
	POLYMICT EUCRITES	
Yamato Mountains	74159	98.2
Yamato Mountains	74450	235.6
Yamato Mountains	75011	121.5
Yamato Mountains	75015	166.6
Yamato Mountains	75295	8.8
Yamato Mountains	75296	8.6
Yamato Mountains	75305	7.9
Allan Hills	ALHA76005	1425.0
Allan Hills	ALHA77302	235.5
Allan Hills	ALHA78040	211.7
Allan Hills	ALHA78132	656.0
Allan Hills	ALHA78158	15.1
Allan Hills	ALHA78165	20.9
Allan Hills	ALHA79017	310.0
	HOWARDITES	
Yamato Mountains	7308	480.0
Allan Hills	ALHA78006	8.0
Elephant Moraine	EETA79006	716.0

discovery has led to a welcome revision in the nomenclature of basaltic achondrites (see Score et al., this volume). Howardites are polymict pyroxene-plagioclase achondrites containing magnesian pyroxene that probably indicates admixture of a diogenitic component. Polymict eucrites are polymict pyroxene-plagioclase achondrites in which magnesian pyroxene, like that in diogenites, is absent or rare. Eucrites can be monomict or polymict and polymict eucrites can contain cumulate and/or non-cumulate eucritic clasts, and fragments of equilibrated or unequilibrated eucrite.

The Antarctic collection of eucrites and howardites is dominated by the polymict eucrites, which are rare or absent in other collections. The meteorite Macibini may be the only other known example. The Antarctic polymict eucrites are all fine breccias with no large clasts and with mineral clasts (mostly pyroxene and plagioclase) predominating over lithic fragments. The lithic clasts are mostly eucritic, and fragments with fine-grained basaltic textures predominate. In a single sample there is generally a wide range of clast types, including clasts with extremely fine quench textures, clasts with more slowly cooled ophitic textures, clasts with cumulate textures, and eucrites with partly recrystallized and granoblastic textures. Equilibrated and unequilibrated eucrite fragments may be present in the same sample: pyroxene compositions cover a wide range and individual grains may be homogeneous, zoned, or rimmed, and may or may not be exsolved. Textures indicative of rapid, near-surface cooling are most common; more plutonic fragments are rarer, especially in the Allan Hills and Elephant Moraine samples. Glass and devitrified glass fragments occur in some samples. The meteorites are truly polymict but many of the fragments appear to be derived from a closely related sequence of rocks. The oxygen isotope data, however, suggest that clasts from different oxygen isotope reservoirs may be present in the same sample (Clayton et al., 1979). In addition, preliminary chemical and isotopic studies (Wooden et al., 1981) indicate significant differences between the larger clasts and the bulk meteorites.

To date only one of the Antarctic polymict eucrites, ALHA76005, has been described in detail (Olsen et al., 1978; Miyamoto et al., 1979; Grossman et al., 1981). The similarities among the 16 known samples are great, however, and it seems certain that they do not all represent individual falls. Consortia studies of several of the Allan Hills samples, and particularly of separated clasts, are currently underway.

Two eucrites in the collections, Yamato 74365 and Elephant Moraine 79004, appear to be normal monomict eucrites. There also are two howardites, Yamato 7308 and Elephant Moraine 79006, that contain a variety of mineral and rock fragments. The presence of magnesian pyroxenes indicates a diogenetic component in these breccias. These are howardites but they are very similar in most respects to the polymict eucrites and may only represent a slightly different sampling of a diverse source region that runs the gamut from magnesian diogenite to iron-rich eucrite.

Eucrites and howardites from the Antarctic are breccias of igneous and metamorphic fragments in which eucritic material predominates. Most breccias are polymict but the fragments comprise a series of materials that may be closely related, i.e., that reflect the effects of a range of different thermal histories on compositionally similar materials or that comprise a limited range of rock types related by simple igneous processes. Truly exotic particles appear to be rare but we must await more detailed studies, including isotopic analyses, to test the preliminary petrographic observations.

The samples may be representative of regolith material on the basaltic achondrite parent body. The distribution of clast sizes and the relative absence of severe shock effects and melting is consistent with a regolith generated by a very large number of low momentum impacts. Most igneous fragments appear to derive from rapidly cooled surface or near-surface environments. Textures indicative of slow cooling are not common (though they may be more abundant in the Yamato polymict eucrites; Takeda, pers. comm.). The apparent scarcity of plutonic materials will also need to be tested in future work as the degree of comminution in these breccias is not conducive to the preservation of coarse-grained polymineralic fragments.

The regolith sampled by these achondrites is dominantly composed of fragments of eucritic lavas or hypabyssal intrusives and their derivatives. Coarser-grained diogenites may have existed at greater depth, as suggested in the layered crust model of Takeda (1979). The differences among the various achondrites may reflect different sampling of a partly stratified surface region. The nature of the regolith sampled by the Antarctic eucrites and howardites is different from the type of material sampled by most non-Antarctic basaltic achondrites. If all the eucrites derive from a single parent body then the surface of that parent varied with respect to place and/or time.

Shergottites

The Antarctic program has doubled the number of available samples of the rare meteorite group, the shergottites. This group has been the focus of much recent attention since it represents the third example of extraterrestrial basaltic volcanism (in addition to the moon and the eucrites). This interest was augmented by the discovery that the shergottites have relatively young crystallisation ages (<1.3 b.y., Nyquist et al., 1979), raising the problem of the location of heat sources for basaltic volcanism late in solar system history. Difficulties in interpreting the evolutionary history of the shergottites and in speculating on their possible parent bodies will be eased by the results of studies of two new shergottites, ALHA77005 and EETA79001, which are apparently related to, but certainly not identical with, Shergotty and Zagami.

Allan Hills 77005 is a 482.5 g achondrite that is heterogeneous, with regions containing cumulate olivine and chromite poikilitically enclosed by low-Ca and high-Ca magnesian pyroxenes (McSween et al., 1979). Other regions consist of olivine with interstitial maskelynite, chromite, ilmenite, troilite, whitlockite, and pyroxene. The meteorite is apparently a heterogeneous cumulate that may have formed from a magma similar to that which gave rise to the shergottites or alternately may be representative of the type of source material from which the shergottite parent magma was derived.

While credible petrogenetic models can be made linking ALHA77005 to the other shergottites, the isotopic data (Nyquist et al., 1979) indicate that they cannot be comagmatic. Like the shergottites, ALHA77005 appears to have a young crystallisation age and also has undergone shock metamorphism that converted the plagioclase to maskelynite. The fourth meteorite in this group is a recent discovery from the 1979 U.S. Antarctic collection, EETA79001. The feldspar in this meteorite also has converted to maskelynite, indicative of a shock history. The mineral assemblage is similar to, but not identical with, the shergottites, and as yet no information on its age is available.

EETA79001 contains two distinct lithologies. The main mass is a pyroxenite with large, complexly zoned pyroxenes set in a mostly pigeonite-maskelynite groundmass. In comparison with the other shergottites, the pyroxenes in EETA79001 are more magnesian and less Ca-rich. The other lithology in EETA79001 is texturally and mineralogically similar to Shergotty but finer-grained and seems on first inspection to lack high-Ca pyroxenes. These two lithologies are in conjunction along what appears to be an undisturbed igneous contact. Obviously the detailed study of EETA79001 will add considerably to our knowledge of the shergottites. If the young ages of Shergotty and Zagami and ALHA77005 are crystallisation ages and indicate melting late in solar system history, then melting could be the result of magmatic or impact events. An increase in the number of related but distinct igneous rocks with young ages argues for magmatic processes rather than impact melting.

Ureilites

TABLE 10

There are six ureilites recovered from Antarctica but only one, ALHA77257, is sizeable, weighing almost 2 kg. These samples extend the range of known variability within the group, as could be expected since there were only eight known ureilites prior to the Antarctic discoveries. Of particular interest is Yamato 74659, which is a low-Fe ureilite carrying the most magnesian pigeonite recorded from the group. The meteorite also has a higher pyroxene to olivine ratio than the other ureilites. At the other end of the spectrum Yamato 74130 carries augite rather than pigeonite and has an unusually Fe-rich olivine (Fo_{76}).

TABLE 10.—Data on ureilites in the Antarctic meteorite collections

Locality	*Specimen number*	*Weight (g)*
Yamato Mountains	74123	69.9
Yamato Mountains	74130	17.9
Yamato Mountains	74695	18.9
Allan Hills	ALHA77257	1995.7
Allan Hills	ALHA78019	30.3
Allan Hills	ALHA78262	26.2

Aubrites

The 1978 collection from the Allan Hills area contains a single sample of an aubrite, ALHA78113 (298.6 g). The sample is a breccia with enstatite grains, described as being up to 2.5 × 2.0 cm, which are essentially iron-free, along with minor nickel-iron and troilite.

Conclusions

The Antarctic meteorite collections have already yielded a substantial number of unique achondrites. Future collections will undoubtedly add to their number and there may be many surprises still to come. With further extension of the search areas we may be able to obtain reasonable statistics on the relative abundances of the various achondrite types. The overall differences between Antarctic and non-Antarctic achondrite abundances may simply be an indication that both data sets are still too small to be representative. The reason for the abundance of polymict eucrites in the Antarctic is not, however, readily apparent.

Overview of Antarctic Carbonaceous Chondrites

Carleton B. Moore

Seven carbonaceous chondrite specimens have been collected from the Yamato Mountains and three from the Allan Hills region of Antarctica. At the Sixth Symposium on Antarctic Meteorites held on 19 February 1981, at the National Institute of Polar Research, Tokyo, it was reported that, of the approximately 3000 meteorites collected during the 1979–1980 field season, an additional 20 uncharacterized, small, carbonaceous, chondrite pieces were recovered. This relatively low yield compared to the large number of ordinary chondrites recovered leads to speculation that in Antarctica there are processes that act against the recovery of this interesting meteorite type. The possibility that the recovered carbonaceous chondrites fell near their recovery sites and have not been transported long distances by moving ice may ultimately be tested by measurements of their terrestrial residence times.

The Antarctic carbonaceous chondrites are mostly C2 chondrites. In addition there are three C3 and one C4 chondrite. The precise classification of several small specimens from the Yamato area has not been reported. The carbonaceous chondrite yield from the Antarctic meteorite expeditions is shown in Table 11.

The Antarctic carbonaceous chondrites appear to be relatively fresh, unweathered, and uncontaminated with terrestrial organic molecules. The white precipitates of carbonates and sulfates (reported by Marvin and Motylewski, 1980) on one C3 (ALHA77307) are only minor surface features.

Carleton B. Moore, Center for Meteorite Studies, Arizona State University, Tempe, Arizona 85281.

Interior and exterior samples of ALHA77306 do not show significant differences in bulk chemical composition (Table 12).

The concentrations of amino acids in two large C2 Antarctic meteorites, Yamato 74662 and ALHA77306, have been well established. Analyses of interior and exterior splits support the assertion that these meteorite finds are clean, pristine specimens (see also Lipschutz, this issue). Analyses done in different laboratories using different techniques give results that do not differ significantly in the abundances of individual amino acids. The C2 chondrite, Yamato 74662, is similar to the Murchison C2 chondrite, while ALHA77306 shows greater similarities to the Nogoya C2 chondrite. Petrographic study of ALHA77306 by McSween (1979) establishes its similarity with Nogoya and other matrix-rich C2 chondrites. ALHA77306 and Nogoya have significantly lower total amino acid concentrations than Yamato 74662 and Murchison (Cronin et al., 1979; Shimoyama, Ponnamperuma, and Yanai, 1979a,b; Kotra et al., 1979). Holzer and Oro (1979) reported that pyrolysis products detected in ALHA77306 are also lower than those in Murchison. Unpublished work by Cronin (Arizona State University laboratory) on ALHA 77307, a C3 chondrite, showed no significant indigeneous or terrestrial amino acids.

Magnetic studies of Yamato 74662 and Yamato 693 by Nagata (1980) confirm their classification as C2 and C3 chondrites, respectively. Brecher (1980) has studied Yamato 74662 and confirms Nagata's magnetic results.

Hyman and Rowe (1979) suggest that the mag-

TABLE 11.—Data on carbonaceous chondrites in the Antarctic meteorite collections

Locality	*Specimen number*	*Type*	*Weight (g)*
Yamato Mountains	693	C3	150
Yamato Mountains	74641	C?	4.5
Yamato Mountains	74642	C2	10.6
Yamato Mountains	74662	C2	151
Yamato Mountains	75003	C?	1.5
Yamato Mountains	75260	C2	4.0
Yamato Mountains	75293	C?	8.1
Allan Hills	ALHA77003	C3	779
Allan Hills	ALHA77306	C2	19.9
Allan Hills	ALHA77307	C3V	181
Allan Hills	ALHA78261	C2	5.1

TABLE 12.—Partial chemical analyses of Antarctic carbonaceous chondrites (Allan Hills analyses by M.-S. Ma and R.H. Schmitt, in litt., June 1980; Yamato analyses by Jochum et al., 1980; carbon and sulfur analyses by Gibson and Andrawes, 1980)

Constituent	*ALHA77036*		*ALHA77307*	*Yamato 74662*	*Yamato 693*
	Exterior	*Interior*			
Al_2O_3	2.1%	2.1%	2.7%	2.1%	2.5%
FeO	25.4	25.6	30.7	30.1	33.2
MgO	18.3	18.5	21.0	19.8	24.8
CaO	1.9	1.8	2.2	1.7	2.4
Na_2O	0.52	0.56	0.15	0.22	0.43
K_2O	0.045	0.038	0.029	0.037	0.039
Co	0.052	0.052	0.051	0.061	0.062
Ni	1.1	1.1	1.0	1.4	1.3
C	—	1.32	0.83	1.5	0.06
S	—	3.86	1.52	3.49	1.60

netic properties of ALHA77306 indicate that it contains less than 0.8% magnetite.

Clayton, Mayeda, and Onuma (1979) state that Yamato 693 has oxygen isotopic compositions virtually identical with Karoonda, classified as a C4 or C5.

Matrix phyllosilicates of ALHA77306 have been studied by McKee and Moore (1980) using high-resolution, transmission electron microscopy. They have been identified as various components of the serpentine group. ALHA77306 appears to have the most complete assemblage of the various phyllosilicate groups thus far identified in a single meteorite.

Available data on the Antarctic carbonaceous chondrites through 1980 are still rather sparse; however, numerous current investigations will make more complete characterization possible in the near future.

Weathering Effects in Antarctic Meteorites

Michael E. Lipschutz

The large number of Antarctic meteorites already recovered includes samples of previously rare and unknown types, and future recoveries will enlarge the sample base even further. Potentially, this should permit more complete characterization of extraterrestrial parent objects and the genetic and evolutionary processes that formed them; compositional data are essential in this regard. Chemical studies are useful, however, only to the extent that the preterrestrial composition is unaltered by weathering during the meteorites' terrestrial residence (see accompanying summary by Evans, Reeves, and Rancitelli). I review herein those chemical data bearing upon effects of chemical alteration by weathering of Antarctic stony and stony-iron meteorites.

In more temperate regions, weathering effects in meteoritic finds generally involve contamination—usually to such an extent that trace element data of finds are viewed very suspiciously. Conditions in Antarctica are sufficiently different that the principal weathering effect in meteoritic finds there is element-loss by leaching; contamination, however, is observed for some elements. Different elements in the same meteorite can respond differently to weathering; thus, absence of a weathering effect for one element need not mean that another will be unaffected. Conceivably, element lability could be affected by host-siting; thus, an element could be unaffected in one type of meteorite while being very labile in another weathered under the same conditions for an identical period.

Michael E. Lipschutz, Department of Chemistry, Purdue University, West Lafayette, Indiana 47907.

Even in meteoritic falls, indigenous compositions vary widely, particularly for elements present at the ppb-ppt levels. Thus, weathering effects in Antarctic meteorites, all of which are finds, must be established by comparing their compositions with those of similar falls and/or by uncovering systematic compositional variations in exterior versus interior portions.

Macroscopically, stony meteorites are classified by degree of weathering and fracturing, increasing in severity from class A to C. Minor weathering (A) is characterized by traces of rust halos around metal grains and oxide staining along cracks. Moderate weathering (B) produces large rust halos around metal grains and extensive oxide staining along internal cracks. Severely weathered (C) specimens are uniformly stained brown and retain little or no metal. Slightly fractured (A) specimens exhibit few or no cracks and none penetrate the entire specimen. In moderate fracturing (B) several cracks may extend across the specimen, which can be readily broken along the fractures. Severely fractured (C) specimens exhibit many extensive cracks and readily crumble.

Some samples (e.g., seven of ~ 300 collected in 1977–1978) exhibit white surficial deposits that, Marvin and Motylewski (1980) identify as hydrated magnesium carbonates and sulfates. These authors attribute these deposits to early stages of weathering after the samples' exposure on the ice surface. (The seven specimens include five of weathering type A and one each of types B and C.) Marvin and Motylewski (1980) suggest that the deposits were formed from salts leached from the meteorites by liquid water produced from snow on sun-warmed meteoritic surfaces.

Inorganic carbon-containing compounds (and some organic ones) should be especially sensitive to weathering. Cronin et al. (1979) report that amino acid composition and contents in interior and exterior samples of the weathering type A C2 chondrite ALHA77306 are similar to those of C2 chondrite falls. Total C contents in this chondrite (and Yamato 74662) are lower than those in other C2 chondrite falls; S contents are not atypical, however (Gibson and Yanai, 1979a,b). Total C and S contents of a ureilite and C4 and E4 chondrites recovered from the Yamato Mountains region resemble those of similar meteorites (Gibson and Yanai, 1979a,b) from other regions. Gibson and Andrawes (1980) report that most of the 25 ALH meteorites they studied have C and S contents within ranges reported for similar falls. (This sampling includes ordinary chondrites of petrologic types 3-6, C2 and C3 chondrites, and a ureilite.) Evidence for weathering effects sometimes appears. The weathering type B L6 chondrite ALHA77281 contains 250μg C/g compared with 160–200μg C/g in the possibly related chondrites 77280 and 77282. Surface samples of the type B chondrites ALHA77002(L5) and 77269(L6) contain nearly twice as much C as interior samples of the same stones. Exterior samples are depleted in S by about 10% compared with interior ones. Stepwise pyrolysis of exterior and interior samples of 77002 and an interior sample of another weathering type B L6 chondrite, ALHA77273, demonstrates CO_2 evolution, presumably from secondary cabonates. The C contents of several weathering type C meteorites seem high but S contents seem normal.

Trace elements should, in principle, be most informative about weathering processes because even a small absolute change in concentration should be reflected in a large relative change. For example, Patchett and Tatsumoto (1980) studied Lu/Hf isotopic systematics in eucrites and report that data for ALHA77302 (a weathering type A meteorite) lie slightly off the ^{176}Hf/^{177}Hf vs. ^{176}Lu/^{177}Hf isochron defined by 9 other eucrites. They attribute this to loss of Lu by leaching during weathering, although it is not clear why Lu should be leached preferentially. Unfortunately, meteoritic contents of trace elements (particularly the more volatile/mobile ones) are intrinsically variable since they can be affected by primary nebular condensation, secondary thermal processes in parent bodies, or tertiary shock-heating. While weathering effects can be established at times by comparing data for interior and exterior portions of a sample and by examining data for meteorites of a similar type, it is not always possible to eliminate the possibility that trace element variations pre-date terrestrial residence.

Thus far, trace elements studies of Antarctic meteorites have involved mainly those of weathering type A. Biswas, Ngo, and Lipschutz (1980) determined Ag, As, Au, Bi, Cd, Co, Cs, Cu, Ga, In, Rb, Sb, Se, Te, Tl, and Zn in exterior and interior portions of ALHA77257 ureilite and 77278 L3 chondrite. They found significant Cs and Rb enrichments in the exterior samples of both meteorites and attributed this to deposition of wind-borne oceanic aerosol. Six elements (As, Au, Co, Cu, Ga, and Zn) seem unaffected by weathering even in surface samples. The eight other elements exhibit contrasting trends in exterior/interior parts of the two meteorites.

Trace element data for the 16 elements in interior samples of Antarctic meteorites (i.e., those obtained at depths $\geq$ 1 cm below exterior surfaces) generally accord well with results for similar meteoritic falls. Thus far, comparisons are available involving the following ALH meteorites: 77005 with shergottites (McSween et al., 1979; Biswas, Ngo, and Lipschutz 1980); 77081 with Acapulco and 77307 with C3V chondrites (Biswas et al., unpublished data); 77257 with ureilites, 77278 with L3 chondrites and 77299 with H3 chondrites (Biswas, Ngo, and Lipschutz 1980); 78113 with enstatite achondrites (Biswas, Walsh et al. 1980). The comparison for 77005 also includes K, Th, and U. In each case, concordance between data for Antarctic and non-Antarctic meteorites is typically as good as that between samples of any two similar meteorite falls.

In summary, Antarctic meteorite compositions can be affected by weathering but are unaltered for interior portions of type A meteorites, at least. Where weathering effects can be detected, they generally involve elemental loss by leaching. Contents of a few elements—C and alkali metals—reflect contamination. With proper precautions, data obtained from Antarctic meteorites are as reliable as those determined for meteoritic falls.

ACKNOWLEDGMENT.—This research was supported in part by NASA grant NGL 15-005-140.

Aluminum-26: Survey of Victoria Land Meteorites

J.C. Evans, J.H. Reeves, and L.A. Rancitelli

Over the past two years an extensive survey of the ^{26}Al ($t_{1/2}$ = 720,000 y) content of Victoria Land meteorites has been carried out by nondestructive gamma-ray analysis. To date a total of 104 samples from the Victoria Land region has been studied. Most of the samples have been ordinary chondrites from the Allan Hills region. Future studies will, however, increasingly emphasize specimens from other regions, as well as including larger numbers of achondrites. The ultimate goal of this work is to establish terrestrial ages for meteorites recovered from the Antarctic ice sheet. This information can then be used to infer information on long-term movement of the ice sheet, as well as helping to provide an understanding of the accumulation mechanism for meteorites at specific sites. Terrestrial residence times can, in principle, be derived from a measurement of the decay of a cosmic ray-produced isotope from its saturation level in space. Shielding and complex exposure history can influence the production rate in space, making calculation of a terrestrial residence time from a single ^{26}Al measurement rather uncertain for individual meteorites. The ^{26}Al measurements are thus most useful as a survey to identify interesting cases requiring more detailed analysis by other more time-consuming techniques. Such additional measurements may include ^{10}Be, ^{14}C, ^{36}Cl, ^{53}Mn, noble rare gases, cosmic ray tracks, and thermoluminescence.

J.C. Evans, J.H. Reeves, and L.A. Rancitelli, Battelle Pacific Northwest Laboratories, P. O. Box 999, Richland, Washington, 99352.

Measurements of ^{14}C are useful for estimating terrestrial ages of less than ~35 × 10^3 years for setting lower bounds on terrestrial ages. Exposure history is less significant for ^{14}C age estimates than ^{26}Al age estimates. Ten Allan Hills meteorites have been investigated for ^{14}C (Fireman 1979, 1980; Fireman et al., 1981). These are listed in Table 13. One L chondrite, ALHA77003, has a positive ^{14}C content, 3.6±1.0 dpm/kg, giving a ^{14}C terrestrial age of (21 ± 4) × 10^3 years. Cosmogenic ^{14}C was observed in the achondrite ALHA77256 and in the H chondrite ALHA77294, giving them ^{14}C terrestrial ages of (11±1) × 10^3 years and (30±2) × 10^3 years, respectively. Only limit values for ^{14}C were obtained for the other seven meteorites; their lower limit ages range from 25 × 10^3 years for ALHA77214 to 32 × 10^3 years for the others.

When combined with ^{26}Al measurements, the most useful isotopes for determining terrestrial ages in the 0.1 to 1 m.y. range have been ^{36}Cl ($t_{1/2}$ = 300,000 y) and ^{53}Mn ($t_{1/2}$ = 3.7 m.y.). Chlorine-36 has been measured in several Antarctic meteorites by a La Jolla-Rochester collaboration using the newly developed Van de Graaff accelerator technique. Manganese-53 was measured on the same samples in La Jolla (Nishiizumi et al., 1978; Nishiizumi et al., 1980) by the now-routine neutron activation procedure. These published data have been included in Table 13, along with the much larger volume of ^{26}Al data. For the meteorite studies, by all three methods, it is possible to derive terrestrial ages with some degree of confidence.

TABLE 13.—Cosmogenic isotope content of Victoria Land meteorites (expected saturation values: ^{26}Al L = 59 ± 9 dpm/kg, H = 55 ± 8 dpm/kg; ^{36}Cl = 25 ± 4 dpm/kg (Fe + Co + Ni + 6 Ca); ^{53}Mn = 450 ± 90 dpm/kg (Fe + 1/3 Ni); ^{14}C = 60 ± 6 dpm/kg

Specimen number	*Class*	*Weathering category*	^{26}Al *dpm/kg*	^{26}Al *Terrestrial age* (10^5 y)	^{14}C *dpm/kg*	^{14}C *Terrestrial age* (10^5 y)	^{36}Cl *(dpm/kg Fe+ Co+Ni+6Ca)*	^{53}Mn *(dpm/kg Fe+1/3 Ni)*
ALHA76004	LL3	A	58 ± 6	≤3[a]				
ALHA76005	Eucrite		89 ± 9		<1.0[b]	≥0.3[b]		
ALHA76006	H6	B	51 ± 5	≤3[a]	<1.7[b]	≥0.3[b]		
ALHA76007	L6	C	45 ± 4	≤5[a]	<1.2[b]	≥0.3[b]		
ALHA76008	H6	C	11 ± 1	≤1[c]	<1.7[b]	≥0.3[b]	9.4 ± 1.0[d]	22 ± 2[d]
ALHA77001	L6	A	52 ± 5	≤1.2[d]			20.1 ± 1.2[d]	422 ± 13[d]
ALHA77002	L5	B	30 ± 3	7 ± 2[e]			4.6 ± 1.1[e]	255 ± 8[e]
ALHA77003	C3	A	45 ± 5	≤1.8[e]	4.6 ± 1.0[f]		18.4 ± 1.2[e]	317 ± 13[e]
ALHA77004	H4	C	52 ± 5		<1.4[g]	≥0.3[g]		
ALHA77009	H4	C	32 ± 2					
ALHA77010	H4	C	49 ± 3	≤3[a]				
ALHA77011	L3	C	39 ± 4	≤7[a]				
ALHA77025	H5	C	54 ± 5	≤3[a]				
ALHA77062	H5	B	47 ± 5	≤4[a]				
ALHA77071	H5	B	55 ± 6	≤3[a]				
ALHA77081	H	B	42 ± 4	≤5[a]				
ALHA77086	H5	C	58 ± 6	≤2[a]				
ALHA77118	H5	C	53 ± 5	≤3[a]				
ALHA77124	H5	C	70 ± 7	≤1[a]				
ALHA77144	H6	B	56 ± 6	≤2[a]				
ALHA77150	L6	C	43 ± 4	≤6[a]				
ALHA77164	L3	C	44 ± 5	≤6[a]				
ALHA77177	H5	C	54 ± 3	≤6[a]				
ALHA77182	H5	B	41 ± 4	≤3[a]				
ALHA77190	H4	C	51 ± 3	≤3[a]				
ALHA77191	H4	C	56 ± 4	≤3[a]				
ALHA77192	H4	C	55 ± 6	≤3[a]				
ALHA77208	H4	C	52 ± 3	≤3[a]				
ALHA77214	L3	C	56 ± 6	1.3 ± 0.8[f]	<3.0[f]		17.0 ± 0.8[e]	151 ± 6[e]
ALHA77215	L3	B	36 ± 4	≤8[a]				
ALHA77216	L3	B	40 ± 3	≤6[a]				
ALHA77217	L3	B	38 ± 3	≤7[a]				
ALHA77224	H4	C	51 ± 3	≤3[a]				
ALHA77225	H4	C	51 ± 3	≤4[a]				
ALHA77230	L4	B	51 ± 3	≤2[a]				
ALHA77232	H4	C	54 ± 3	≤2[a]				
ALHA77233	H4	C	47 ± 3	≤4[a]				
ALHA77249	L3	C	37 ± 2	≤7[a]				
ALHA77256	Diog.	A		0.11 ± .01[f]	16.0 ± 1.5[f]			
ALHA77258	H6	B	29 ± 2	≤9				
ALHA77260	L3	B	37 ± 2					
ALHA77261	L6	B	36 ± 4					
ALHA77262	H4	B	47 ± 5					
ALHA77270	L6	B	40 ± 3					
ALHA77272	L6	B	35 ± 4	5.4 ± 8[e]	<0.5[f]		6.6 ± 3.3[e]	213 ± 11[e]
ALHA77278	LL3	A	28 ± 3	3.2 ± 9[e]			10.9 ± 0.7[e]	264 ± 11[e]

TABLE 13.—Continued

Specimen number	Class	Weathering category	^{26}Al dpm/kg	^{26}Al Terrestrial age (10^5 y)	^{14}C dpm/kg	^{14}C Terrestrial age (10^5 y)	^{36}Cl (dpm/kg Fe+Co+Ni+6 Ca)	^{53}Mn (dpm/kg Fe+1/3 Ni)
ALHA77282	L6	B	49 ± 3					
ALHA77284	L6	B	45 ± 5					
ALHA77285	H6	C	38 ± 4					
ALHA77294	H5	A		0.30 ± .02[g]	1.6 ± 0.3[g]			
ALHA77297	L6	B	70 ± 7	≤1[a]				
ALHA77299	H3	A	43 ± 4	≤1.6[e]			18.9 ± 8[e]	317 ± 19[e]
ALHA77300	H5	C	54 ± 4	≤5[a]				
ALHA77304	LL3	B	50 ± 3	≤2[a]				
ALHA78001			50 ± 4					
ALHA78003			59 ± 4					
ALHA78038	L3	C	36 ± 3	≤8[a]				
ALHA78039	L6	B	42 ± 3	≤6[a]				
ALHA78041			38 ± 3					
ALHA78043	L6	B	38 ± 3	≤7[a]				
ALHA78044	L4	B	51 ± 4					
ALHA78045	L6	B/C	34 ± 3	≤8[a]				
ALHA78046			46 ± 5					
ALHA78048	L6	B	59 ± 5	≤2[a]				
ALHA78049			52 ± 3					
ALHA78050	L6	B	44 ± 3	≤5[a]				
ALHA78051			38 ± 3					
ALHA78052			56 ± 4	≤3[a]				
ALHA78076	H6	B	52 ± 4	≤5[a]				
ALHA78077	H4	C	42 ± 3					
ALHA78102	H5	C	35 ± 3	≤7[a]				
ALHA78103	L6	B	58 ± 3	≤2[a]				
ALHA78104	L6	B	53 ± 3	≤3[a]				
ALHA78105	L6	B	61 ± 7	≤2[a]				
ALHA78106	L6	B	44 ± 4	≤6[a]				
ALHA78109	LL5	B	46 ± 3	≤5[a]				
ALHA78112	L6	B	42 ± 3	≤6[a]				
ALHA78114	L6	C	38 ± 2	≤7[a]				
ALHA78115	H6	B	43 ± 3	≤5[a]				
ALHA78126	L6	B	45 ± 3	≤5[a]				
ALHA78128	H5	C	34 ± 2	≤7[a]				
ALHA78130	L6	C	51 ± 4	≤4[a]				
ALHA78131	L6	C	40 ± 3	≤6[a]				
ALHA78132	Eucrite	A	68 ± 4					
ALHA78134	H4	C	61 ± 3	≤1[a]				
ALHA78251	L6	B	56 ± 6	≤3[a]				
RKPA78001	L6	C	49 ± 3	≤4[a]				
RKPA78003	L6	C	50 ± 3	≤4[a]				
RKPA78004	H4	A	39 ± 2	≤6[a]				
META78001	H4	C	53 ± 3	≤2[a]				
META78002	L6	B	47 ± 3	≤5[a]				
META78003	L6	B	50 ± 3	≤4[a]				
META78004			49 ± 4					
META78005	L6	B	44 ± 3	≤5[a]				
META78006	H6	C	60 ± 4	≤1[a]				

TABLE 13.—Continued

Specimen number	Class	Weathering category	^{26}Al dpm/kg	^{26}Al Terrestrial age (10^5 y)	^{14}C dpm/kg	^{14}C Terrestrial age (10^5 y)	^{36}Cl (dpm/kg Fe+Co+Ni+6Ca)	^{53}Mn (dpm/kg Fe+1/3Ni)
META78009			68 ± 4					
META78010	H5	B	56 ± 3	≤2[a]				
META78018			58 ± 4					
META78019			108 ± 6					
META78021			52 ± 12					
META78023			54 ± 12					
META78025			33 ± 2					
META78028	L6	B	56 ± 3	≤3[a]				
BTNA78001	L6	B	65 ± 4					
BTNA78004	LL6	B	49 ± 3	≤1[a]				
BTNA78005			40 ± 2	≤4[a]				

[a] This work. Ages given are one sigma upper limits based on the uncertainties in both the expected and measured ^{26}Al. Ages have not been calculated for samples lacking type classification.
[b] Fireman, 1979.
[c] Evans et al., 1979.
[d] Nishiizumi et al., 1979.
[e] Nishiizumi et al., 1980.
[f] Fireman, 1980.
[g] Fireman and Norris, 1981.

Of particular interest are ALHA77002 and ALHA77272, for which Nishiizumi et al. (1980) have derived terrestrial ages of 0.69±0.17 and 0.54±0.08 × 10^6 years, respectively. Terrestrial ages in excess of 500,000 years may thus be fairly common. ALHA76008 has been discussed in detail elsewhere (Evans et al., 1979; Nishiizumi et al., 1979). The low ^{26}Al found in this meteorite led Fireman et al. (1979) to conclude that it had a long terrestrial age — $1.54 \pm^{0.14 \text{ m.y.}}_{0.28 \text{ m.y.}}$. Chlorine-36 and ^{53}Mn measurements made subsequently by Nishiizumi et al. (1979) convincingly demonstrated that this meteorite had experienced a complete bombardment history followed by a relatively short terrestrial residence. A similar situation was also in evidence for one of the Yamato meteorites, Yamato 7301. This clearly demonstrates the hazards of using a single isotopic measurement for an age determination.

An alternative approach involves a statistical analysis of the whole body of data. Figure 40 is a histogram of the frequency distribution of ^{26}Al contents of 87 Antarctic meteorites for which type information was available. A target element correction factor has been included to normalize the data to an L chondrite composition. The dashed line on the figure is the shape of the distribution for contemporary falls and finds obtained by making similar corrections on falls and finds. It is quite clear that the Antarctic meteorites are distributed toward lower ^{26}Al contents.

Figure 41 shows the same type of distribution for H and L chondrites. It appears that most of the low ^{26}Al values are found amongst the L chondrite population, suggesting a possible shower contribution. There is, nevertheless, a strong suggestion that terrestrial ages somewhat in excess of 500,000 years may be fairly common, while at the same time there is no evidence as yet of any samples having ages in excess of one million years. At present only a fraction of the collection has been surveyed. Future work may yet turn up older cases as the data base continues to expand.

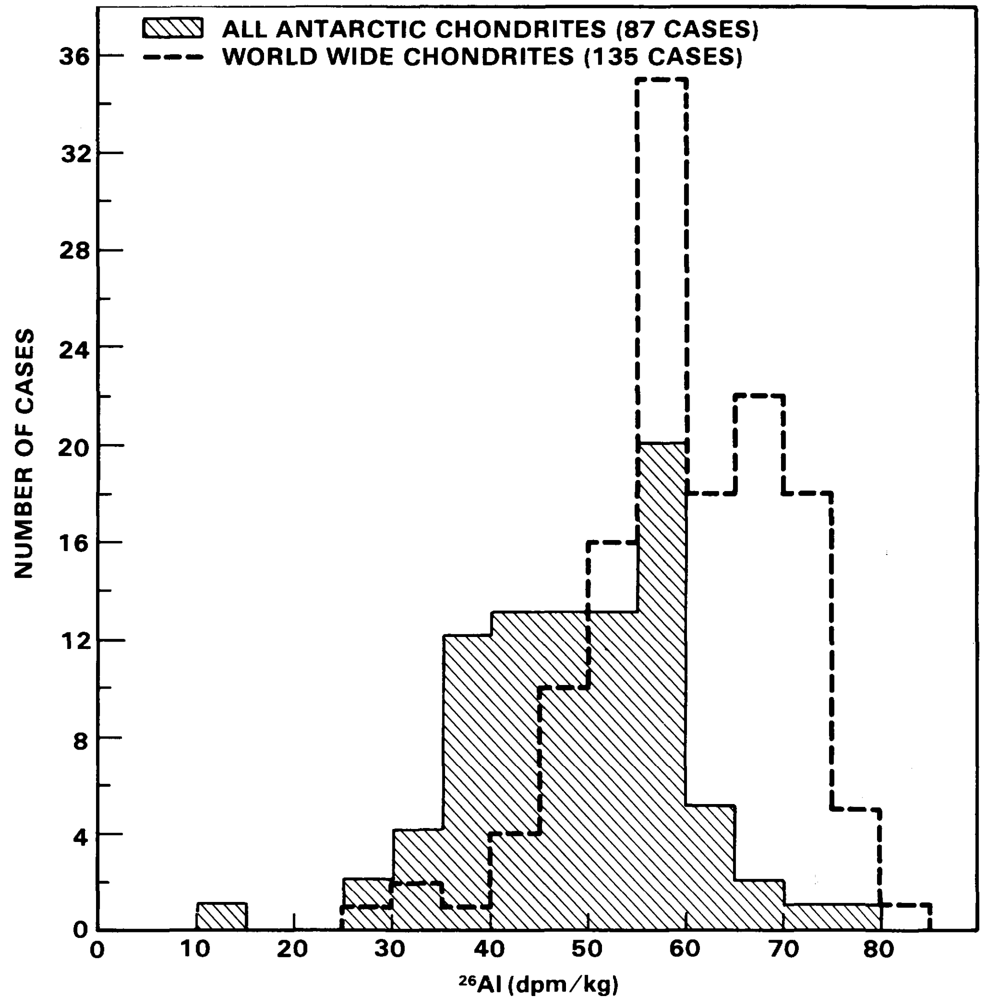

FIGURE 40.—^{26}Al content of Antarctic chondrites normalized to L-type composition. Dashed line shows expected distribution taken from literature survey of ^{26}Al measurements made on meteorites recovered from other parts of earth.

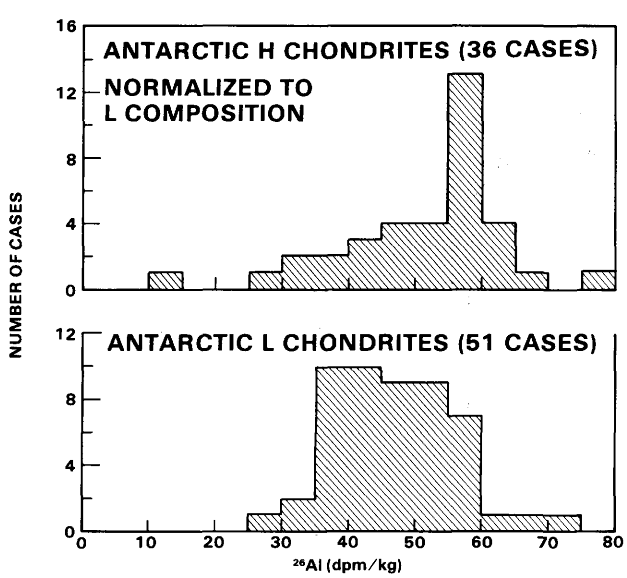

FIGURE 41.—^{26}Al content of Antarctic chondrites by class normalized to L-type composition.

Bibliography of Antarctic Meteorites

Karen Motylewski

Agosto, W.N., R.H. Hewins, and R.S. Clarke, Jr.
1980. Allan Hills A77219, the First Antarctic Mesosiderite. In *Proceedings of the Eleventh Lunar and Planetary Science Conference,* pages 1027–1045. New York: Pergamon Press.

Allen, J.S., S. Nozette, and L.L. Wilkening
1980. A Study of Chondrule Rims and Chondrule Irradiation Records in Unequilibrated Ordinary Chondrites. *Geochimica et Cosmochimica Acta,* 44:1161–1175.

Annexstad, J.O.
1978. Processing and Distributing Antarctic Meteorites Collected during 1977–78. *Antarctic Journal of the United States,* 13(4):219–220.

Balacescu, A., and H. Wänke
1977. Ar^{39}–Ar^{40} Ages of Achondrites. *Meteoritics,* 12: 171–172.

Bart, G., S. Biswas, H. Ngo-The, and M.E. Lipschutz
1979. Volatile Trace Elements in Gas-Rich and Antarctic Meteorites. In *Lunar and Planetary Science X,* pages 66–67. Houston: Lunar and Planetary Institute.

Bayly, P.G.W., and F.L. Stillwell
1923. The Adelie Land Meteorite: Australasian Antarctic Expedition, 1911–1914. *Science Reports,* series A, 4:1–11.

Berkley, J.L., G.J. Taylor, K. Keil, G.E. Harlow, and M. Prinz
1980. The Nature and Origin of Ureilites. *Geochimica et Cosmochimica Acta,* 44:1579–1597.

Biswas, S., H.T. Ngo, and M.E. Lipschutz
1979. Antarctic Meteorites: Volatile Trace Element Trends. *Meteoritics,* 14:350.
1980. Trace Element Contents of Selected Antarctic Meteorites, I: Weathering Effects and ALHA-77005, A77257, A77278 and A77299. *Zeitschrift für Naturforschung,* 35a:191–196.

Karen Motylewski, Smithsonian Astrophysical Observatory, 60 Garden Street, Cambridge, Massachusetts 02138.

Bogard, D.D., and J.O. Annexstad
1980. Curation and Allocation Procedures. *In* U.B. Marvin and B. Mason, editors, Catalog of Antarctic Meteorites, 1977–1978. *Smithsonian Contributions to the Earth Sciences,* 23:8–11.

Brecher, A.
1980. Meteorites As Magnetic Probes: Recent Results. In *Lunar and Planetary Science XI,* pages 106–108. Houston: Lunar and Planetary Institute.

Bull, R.K., and S.A. Durrani
1979. Particle-Track Record of Some Antarctic Achondrites. In *Lunar and Planetary Science X,* pages 162–163. Houston: Lunar and Planetary Institute.
1981. ALHA77005: Uranium Content of Phosphates and Thermoluminescence Studies. In *Lunar and Planetary Science XII,* pages 118–119. Houston: Lunar and Planetary Institute.

Cassidy, W.A.
1977. Antarctic Search for Meteorites. *Antarctic Journal of the United States,* 12(4):96–98.
1978. Antarctic Search for Meteorites during the 1977–78 Field Season. *Antarctic Journal of the United States,* 13(4):39–40.
1979. Antarctic Search for Meteorites (ANSMET 1978–79). *Antarctic Journal of the United States,* 15(5):41–42.
1979. Antarctic Meteorites. *Transactions of the American Geophysical Union (EOS),* 60:175–177.
1980. Field Occurrences and Collecting Procedures. *In* U.B. Marvin and B. Mason, editors, Catalog of Antarctic Meteorites, 1977–1978. *Smithsonian Contributions to the Earth Sciences,* 23:3–7.
1980. Antarctic Meteorites. *Geotimes,* 25(6):22–23.

Cassidy, W.A., J.O. Annexstad, L.A. Rancitelli, and L. Benda
1980. Results of the 1979–80 U.S. Antarctic Meteorite Expedition. In *Lunar and Planetary Science XI,* page 128. Houston: Lunar and Planetary Institute.

Cassidy, W.A., E. Olsen, and K. Yanai
1977. Antarctica: A Deep-Freeze Storehouse for Meteorites. *Science,* 198:727–731.

Christophe Michel-Levy, M., J.C. Lorin, H. Palme, L. Schultz, B. Spettel, H. Wänke, and H.W. Weber
1979. Comparison of Two Unusual Chondritic Meteorites: ALHA77081 and Acapulco. *Meteoritics,* 14:364–366.

Clarke, R.S. Jr., E. Jarosewich, J.I. Goldstein, and P.A. Baedecker
1980. Antarctic Iron Meteorites from Allan Hills and Purgatory Peak. *Meteoritics,* 15:273–274.

Clayton, R.N., T.K. Mayeda, J.L. Gooding, K. Keil, and E.J. Olsen
1981. Redox Processes in Chondrules and Chondrites. In *Lunar and Planetary Science XII,* pages 154–156. Houston: Lunar and Planetary Institute.

Clayton, R.N., T.K. Mayeda, and N. Onuma
1979. Oxygen Isotopic Compositions of Some Antarctic Meteorites. In *Lunar and Planetary Science X,* pages 221–223. Houston: Lunar and Planetary Institute.

Cronin, J.R., S. Pizzarello, and C.B. Moore
1979. Amino Acids in the Allan Hills, Antarctica C-2 Carbonaceous Chondrite ALHA77306. In *Lunar and Planetary Science X,* pages 251–253. Houston: Lunar and Planetary Institute.
1979. Amino Acids in an Antarctic Carbonaceous Chondrite. *Science,* 206:335–337.

Delaney, J.S., R. Bedell, S. Fishman, R. Klimentidis, G.E. Harlow, and M. Prinz
1980. Highly Differentiated Eucritic Clasts in Polymict Breccias in Allan Hills A78040 and A77302. *Meteoritics,* 15:280–281.

Delaney, J.S., C.E. Nehru, and M. Prinz
1980. Olivine Clasts from Mesosiderites and Howardites: Clue to the Nature of Achondritic Parent Bodies. In *Proceedings of the Eleventh Lunar and Planetary Science Conference,* pages 1073–1087. New York: Pergamon Press.

Englert, P., and W. Herr
1979. Exposure and Terrestrial Ages of Chondrites Based on ^{26}Al- and ^{53}Mn-measurements. *Meteoritics,* 14:391–393.

Evans, J.C., and L.A. Rancitelli
1979. Non-Destructive ^{26}Al Measurements on Antarctic Meteorites. In *Lunar and Planetary Science X,* pages 373–375. Houston: Lunar and Planetary Institute.
1980. Terrestrial Ages. *In* U.B. Marvin and B. Mason, editors, Catalog of Antarctic Meteorites, 1977–1978, *Smithsonian Contributions to the Earth Sciences,* 23:45–46.

Evans, J.C., L.A. Rancitelli, and J.H. Reeves
1979. ^{26}Al Content of Antarctic Meteorites: Implications for Terrestrial Ages and Bombardment History. In *Proceedings of the Tenth Lunar and Planetary Science Conference,* pages 1061–1072. New York: Pergamon Press.

Feierberg, M.A., and M.J. Drake
1980. The Meteorite-Asteroid Connection: The Infrared Spectra of Eucrites, Shergottites, and Vesta. *Science,* 209:805–807.

Fireman, E.L.
1978. Carbon-14 in Lunar Soil and Meteorites. In *Proceedings of the Ninth Lunar and Planetary Science Conference,* pages 1647–1654. New York: Pergamon Press.
1979. ^{14}C and ^{39}Ar Abundances in Allan Hills Meteorites. In *Proceedings of the Tenth Lunar and Planetary Science Conference,* pages 1053–1060. New York: Pergamon Press.
1980. Carbon-14 and Argon-39 in ALHA Meteorites. In *Proceedings of the Eleventh Lunar and Planetary Science Conference,* pages 1215–1221. New York: Pergamon Press.
1980. Carbon-14 Dating of Antarctic Meteorites and Antarctic Ice. In *Lunar and Planetary Science XI,* pages 288–290. Houston: Lunar and Planetary Institute.

Fireman, E.L., and T. Norris
1981. ^{14}C Ages of Antarctic Meteorites and Ice and the Composition of the Air Trapped in the Ice. In *Lunar and Planetary Science XII,* pages 282–284. Houston: Lunar and Planetary Institute.

Fireman, E.L., L.A. Rancitelli, and T. Kirsten
1979. Terrestrial Ages of Four Allan Hills Meteorites: Consequences for Antarctic Ice. *Science,* 203:453–455.

Fisher, R.M., J.M. Goldstein, and T. Nagata
1978. A Note on New Antarctic Iron Meteorites. *Memoirs of the National Institute of Polar Research* (Japan), special issue, 8:260–267.

Fisher, R.M., C.E. Spangler, Jr., and T. Nagata
1978. Metallographic Properties of Yamato Iron Meteorite, Yamato-75031, and Stony-iron Meteorite, Yamato-74044. *Memoirs of the National Institute of Polar Research* (Japan), special issue, 12:270–282.

Fisher, R.M., C.E. Spangler, Jr., T. Nagata, and M. Funaki
1979. Metallographic and Magnetic Properties of Allan Hills 762 Iron Meteorite. *Memoirs of the National Institute of Polar Research* (Japan), special issue, 12:270–282.

Ford, A.B., and R.W. Tabor
1971. The Thiel Mountains Pallasite of Antarctica. *United States Geological Survey Professional Paper,* 750-D:D56–D60.

Fujii, N., K. Ito, and M. Miyamoto
1981. Vibrational Fracturing Rate: A New Strength Measure for Chondrites. In *Lunar and Planetary Science XII,* pages 312–314. Houston: Lunar and Planetary Institute.

Gibson, E.K., Jr.
1980. Carbon Abundances in Antarctic Meteorites. In *Lunar and Planetary Science XI,* pages 323–325. Houston: Lunar and Planetary Institute.

Gibson, E.K., Jr., and F.F. Andrawes
1980. The Antarctic Environment and its Effect upon the Total Carbon and Sulfur Abundances in Recovered Meteorites. In *Proceedings of the Eleventh Lunar and Planetary Science Conference,* pages 1223–1234. New York: Pergamon Press.

Gibson, E.K., Jr., J. Karsten, and K. Yanai
1979. A Survey of Carbon and Sulfur Abundances in Antarctic Meteorites. In *Lunar and Planetary Science X,* pages 428–429. Houston: Lunar and Planetary Institute.

Gibson, E.K., Jr., and K. Yanai
1979. Total Carbon and Sulfur Abundances in Antarctic Meteorites. *Memoirs of the National Institute of Polar Research* (Japan), special issue, 15:189–195.
1979. Total Carbon and Sulfur Abundances in Antarctic Meteorites. In *Proceedings of the Tenth Lunar and Planetary Science Conference,* pages 1045–1051. New York: Pergamon Press.

Gooding, J.L.
1981. Mineralogical Changes during Terrestrial Weathering of Antarctic Chondrites. In *Lunar and Planetary Science XII,* pages 350–352. Houston: Lunar and Planetary Institute.

Goswami, J.H.
1980. Pre-compaction Solar Flare Irradiation Records in Antarctic Meteorites. In *Lunar and Planetary Science XII,* pages 282–284. Houston: Lunar and Planetary Institute.

Haggerty, S.E., S.B. Simon, and J.M. Rhodes
1979. Antarctic Meteorites: Petrology and Chemistry of 77001 (L6), 77002 (L5) and 77299 (H3). In *Lunar and Planetary Science X,* pages 485–487. Houston: Lunar and Planetary Institute.

Harlow, G.E., and R. Klimentidis
1980. Clouding of Pyroxenes and Plagioclase in Eucrites: Implications for Post-Crystallization Processing. In *Lunar and Planetary Science Conference XI,* pages 398–400. Houston: Lunar and Planetary Institute.
1980. Clouding of Pyroxene and Plagioclase in Eucrites: Implications for Post-Crystallization Processing. In *Proceedings of the Eleventh Lunar and Planetary Science Conference,* pages 1131–1143. New York: Pergamon Press.

Hintenberger, H., K.P. Jochum, O. Braun, P. Christ, and W. Martin
1978. The Antarctic Meteorite Yamato 74123 — A New Ureilite. *Earth and Planetary Science Letters,* 40:187–193.

Holzer, G., and J. Oro
1979. The Organic Composition of the Allan Hills Carbonaceous Chondrite (77306) as Determined by Pyrolysis-Gas Chromatography-Mass Spectrometry and Other Methods. *Journal of Molecular Evolution,* 13:265–270.

Huss, G.I.
1977. Significance of the Yamato Meteorites. *Meteoritics,* 12:141–144.

Hyman, M., and M.W. Rowe
1979. Magnetic Contents of Carbonaceous Meteorites. *Transactions of the American Geophysical Union (EOS),* 60:308.

Ikeda, Y., and H. Takeda
1979. Petrology of the Yamato-74191 Chondrite. *Memoirs of the National Institute of Polar Research* (Japan), special issue, 12:38–58.
1979. Petrology of the Yamato-74442 Chondrite. *Memoirs of the National Institute of Polar Research* (Japan), special issue, 15:123–139.

Imamura, M., K. Nishiizumi, and M. Honda
1979. Cosmogenic ^{53}Mn in Antarctic Meteorites and Their Exposure History. *Memoirs of the National Institute of Polar Research* (Japan), special issue, 15:227–242.

Ishii, T., M. Miyamoto, and H. Takeda
1976. Pyroxene Geothermometry and Crystallization—Subsolidus Equilibration Temperatures of Lunar and Achondritic Pyroxene. In *Lunar Science VII,* pages 408–410. Houston: Lunar and Planetary Institute.

Ishii, T., H. Takeda, and K. Yanai
1979. A Three-Pyroxene Achondrite from Allan Hills, Antarctica, and Its Pyroxene Geothermometry. In *Lunar and Planetary Science X,* pages 601–603. Houston: Lunar and Planetary Institute.

Ishii, T., H. Takeda, K. Yanai, and M. Miyamoto
1978. The Significance of Low-Ca Inverted Pigeonites in Crystallization Trends of Diogenites and Eucrites. In *Lunar and Planetary Science IX,* pages 573–575. Houston: Lunar and Planetary Institute.

Jochum, K.P., K.I. Grais, and H. Hintenberger
1980. Chemical Composition and Classification of 19 Yamato Meteorites. *Meteoritics,* 15:31–39.

Kallemeyn, G.W., and J.T. Wasson
1981. Multielement Analytical Study of New and Unusual Carbonaceous Chondrites. In *Lunar and Planetary Science XII,* pages 528–530. Houston : Lunar and Planetary Institute.

Kamaguchi, A., and J. Okano
1978. K-Ar Age of Yamato Meteorite, Yamato-74190-01 (L). *Memoirs of the National Institute of Polar Research* (Japan), special issue, 8:225–232.
1979. K-Ar Ages of Yamato-74 Meteorites. *Memoirs of the National Institute of Polar Research* (Japan), special issue, 12:178–185.

Kaneoka, I., M. Ozima, and M. Yanagisawa
1979. ^{40}Ar-^{39}Ar Age Studies of Four Yamato-74 Meteorites. *Memoirs of the National Institute of Polar Research* (Japan), special issue, 12:186–206.

Kimura, M., and K. Yagi
1980. Crystallization of Chondrules in Ordinary Chon-

drites. *Geochimica et Cosmochimica Acta,* 44:589–602.

Kimura, M., K. Yagi, and Y. Oba
1978. Petrological Studies of Yamato-74 Meteorites, 2. *Memoirs of the National Institute of Polar Research* (Japan), special issue, 8:156–159.

Kimura, M., K. Yagi, and K. Onuma
1979. Classification and Petrography of Some Yamato Chondritic Meteorites. *Memoirs of the National Institute of Polar Research* (Japan), special issue, 15: 41–53.
1979. Petrological Studies on Chondrules in Yamato-74 Meteorites. *Memoirs of the National Institute of Polar Research* (Japan), special issue, 12:114–133.

King, T.V.V., R. Score, E.M. Gabel, and B. Mason
1979. Meteorite Descriptions. *In* U.B. Marvin and B. Mason, editors, Catalog of Antarctic Meteorites, 1977–1978. *Smithsonian Contributions to the Earth Sciences,* 23:12–44.

Kirsten, T., D. Ries, and E.L. Fireman
1978. Exposure and Terrestrial Ages of Four Allan Hills Antarctic Meteorites. *Meteoritics,* 13:519–522.

Knab, H.-J., and H. Hintenberger
1978. Isotope Dilution Analyses of 20 Trace Elements in 9 Carbonaceous Chondrites by Spark Source Mass Spectrography. *Meteoritics,* 13:522–527.

Kobayashi, S.
1979. Some Features of the Turbulent Transfer on the Bare Ice Field near the Yamato Mountains, East Antarctica. *Memoirs of the National Institute of Polar Research* (Japan), special issue, 8:9–18.

Kotra, R.K., A. Shimoyama, C. Ponnamperuma, and P.E. Hare
1979. Amino Acids in a Carbonaceous Chondrite from Antarctica. *Journal of Molecular Evolution,* 13: 179–184.

Kracher, A., J. Willis, and J.T. Wasson
1980. Chemical Classification of Iron Meteorites, IX: A New Group (IIF), Revision of IAB and IIICD, and Data on 57 Additional Irons. *Geochimica et Cosmochimica Acta,* 44:773–787.

Krinov, E.L., editor
1961. Discovery of the Lazarev Iron Meteorite. *The Meteoritical Bulletin,* 20:1.
1962. Discovery of the Horlick Mountains [Thiel Mountains] Stony-iron Meteorite, Antarctica. *The Meteoritical Bulletin,* 24:1; 25:4.
1965. Discovery of Neptune Mountains Iron Meteorite, Antarctica. The *Meteoritical Bulletin,* 34:2–3.

Kushiro, I., and Mysen, B.O.
1979. Melting Experiments on a Yamato Chondrite. *Memoirs of the National Institute of Polar Research* (Japan), special issue, 15:165–170.

Kusunoki, K.
1975. A Note on the Yamato Meteorites Collected in December 1969. *National Institute of Polar Research* (Japan), special issue, 5:1–8.

Labotka, T.C., and J.J. Papike
1980. Howardites: Samples of the Regolith of the Eucrite Parent-Body: Petrology of Frankfort, Pavlovka, Yurtuk, Malvern, and ALHA77302. In *Proceedings of the Eleventh Lunar and Planetary Science Conference,* pages 1103–1130. New York: Pergamon Press.
1980. Petrology of a Quickly Cooled Pigeonite-Basalt Clast in the Antarctic Meteorite ALHA77302. In *Lunar and Planetary Science XI,* pages 590–592. Houston: Lunar and Planetary Institute.

Maran, S.P.
1980. Meteorites—How Science Reads Them for New Clues to the Birth of the Solar System. *Popular Science,* 216(4):78–82, 172.

Marvin, U.B., and K. Motylewski
1980. Mg-Carbonates and -Sulfates on Antarctic Meteorites. In *Lunar and Planetary Science XI,* pages 669–670. Houston: Lunar and Planetary Institute.

Masuda, A., and T. Tanaka
1978. REE, Ba, Sr, and Rb in the Yamato Meteorites, with Special Reference to Yamato-691(a), -692(b) and -693(c). *Memoirs of the National Institute of Polar Research* (Japan), special issue, 8:229–232.

Masuda, A., T. Tanaka, H. Shimizu, T. Wakisaka, and N. Nakamura
1979. Rare-earth Geochemistry of Antarctic Diogenites. *Memoirs of the National Institute of Polar Research* (Japan), special issue, 15:177–188.

Matsueda, H., H. Kano, and K. Yanai
1979. A Preliminary Classification of Yamato Chondrites with Reference to Metal-Sulfide Equilibrium. *Memoirs of the National Institute of Polar Research* (Japan), special issue, 15:24–40.

Matsui, T., and M. Osako
1979. Thermal Property Measurement of Yamato Meteorites. *Memoirs of the National Institute of Polar Research* (Japan), special issue, 15:243–252.

Matsui, T., K. Shun-ichiro, and T. Yokokura
1980. Stress Histories Retained in Olivines from Pallasite Meteorites. In *Proceedings of the Eleventh Lunar and Planetary Science Conference,* pages 1047–1054. New York: Pergamon Press.

Matsumoto, Y.
1978. Collection of Yamato Meteorites, East Antarctica, in November and December 1975, and January 1976. *Memoirs of the National Institute of Polar Research* (Japan), special issue, 8:38–50.

Matsumoto, Y., M. Hayashi, M. Miyamoto, H. Takeda, and K. Yanai
1979. A Classification of the Yamato-75 Chondrites Based on Chemical Compositions of Olivines and Pyroxenes. *Memoirs of the National Institute of Polar Research* (Japan), special issue, 12:72–81.

McKee, T.R., and C.B. Moore
1980. Matrix Phyllosilicates of the Antarctic C2 Chon-

drite ALHA77306. In *Lunar and Planetary Science XI,* pages 703–704. Houston: Lunar and Planetary Institute.

McKeever, S.W.S., and S.A. Durrani
1980. Upper Limits for the Terrestrial Ages of Some Antarctic Meteorites Using Thermoluminescence. In *Lunar and Planetary Science XI,* pages 705–707. Houston: Lunar and Planetary Institute.

McSween, H.Y., Jr.
1979. Matrix Variations in CM Chondrites. In *Lunar and Planetary Science X,* pages 810–812. Houston: Lunar and Planetary Institute.

McSween, H.Y., Jr., and D. Stoffler
1980. Shock Metamorphic Features in Allan Hills 77005 Meteorite. In *Lunar and Planetary Science XI,* pages 717–719. Houston: Lunar and Planetary Institute.

McSween, H.Y., Jr., and L.L. Wilkening
1980. A Note on the Allan Hills A77278 Unequilibrated Ordinary Chondrite. *Meteoritics,* 15:193–199.

McSween, H.Y., Jr., E.M. Stolper, L.A. Taylor, R.A. Muntean, G.D. O'Kelley, J.S. Eldridge, S. Biswas, H.T. Ngo, and M.E. Lipschultz
1979. Petrogenetic Relationship between Allan Hills 77005 and Other Achondrites. *Earth and Planetary Science Letters,* 45:275–284.

McSween, H.Y., Jr., L.A. Taylor, and E.M. Stolper
1979. Allan Hills 77005: A New Meteorite Type Found in Antarctica. *Science,* 204:1201–1203.

McSween, H.Y., Jr., L.A. Taylor, E.M. Stolper, R.A. Muntean, G.D. O'Kelley, and J.S. Eldridge
1979. Petrogenesis of the Allan Hills 77005 Achondrite. In *Lunar and Planetary Science X,* pages 813–815. Houston: Lunar and Planetary Institute.

Melcher, C.L.
1979. Thermoluminescence Measurements of Antarctic Meteorites. In *Lunar and Planetary Science X,* pages 825–827. Houston: Lunar and Planetary Institute.

Miyamoto, M., A. Mito, and H. Takeda
1981. Spectral Reflectance (250–2500nm) of Powdered Samples of Olivines and Some Meteorites. In *Lunar and Planetary Science XII,* pages 708–710. Houston: Lunar and Planetary Institute.

Miyamoto, M., H. Takeda, and T. Ishii
1976. The Origin of Howardite as Inferred from Pyroxene Mineralogy of Frankfort and Yamato (1) and a Primordial Lunar Crust Model. *Lunar Science VII,* pages 568–570. Houston: Lunar and Planetary Institute.

Miyamoto, M., H. Takeda, and K. Yanai
1978. Pasamonte-like Clasts in Eucrite Polymict Breccias. In *Lunar and Planetary Science IX,* pages 744–746. Houston: Lunar and Planetary Institute.
1978. Yamato Achondrite Polymict Breccias. *Memoirs of the National Institute of Polar Research* (Japan), special issue, 8:185–197.
1979. Eucritic Polymict Breccias from Allan Hills and Yamato Mountains, Antarctica. In *Lunar and Planetary Science X,* pages 847–849. Houston: Lunar and Planetary Institute.

Miyamoto, M., H. Takeda, K. Yanai, and H. Haramura
1979. Mineralogical Examination of the Allan Hills No. 5 Meteorite. *Memoirs of the National Institute of Polar Research* (Japan), special issue, 12:59–71.

Miyamoto, M., H. Takeda, K. Yanai, and Y. Matsumoto
1979. A Classification for Some Small Chondrites in the Yamato-74 and -75 Meteorites. *Memoirs of the National Institute of Polar Research* (Japan), special issue, 15:140–147.

Miyamoto, M., K. Yanai, and H. Takeda
1977. Movements of Materials on the Surface of an Achondrite Parent Body as Inferred from Its Crust Model and the Yamato Achondrites. In *Lunar Science VIII,* pages 670–672. Houston: Lunar and Planetary Institute.

Nagahara, H.
1979. Petrological Studies on Yamato-74354, -74190, -74362, -74646, and -74115 Chondrites. *Memoirs of the National Institute of Polar Research* (Japan), special issue, 15:77–110.
1979. Petrological Study of Ni-Fe metal in Some Ordinary Chondrites. *Memoirs of the National Institute of Polar Research* (Japan), special issue 15:111–122.

Nagao, K., and N. Takaoka
1979. Rare Gas Studies of Antarctic Meteorites. *Memoirs of the National Institute of Polar Research* (Japan), special issue 12:207–222.

Nagata, T.
1976. Yamato Meteorites Collected in Antarctica in 1969. *Meteoritics,* 11:181–184.
1977. Japanese Scientific Activities in the McMurdo Region, 1976–1977. *Antarctic Journal of the United States,* 12(4):95–96.
1977. Yamato Meteorites Collected in Antarctica. *Meteoritics,* 12:323.
1978. A Possible Mechanism of Concentration of Meteorites within the Meteorite Ice Field in Antarctica. *Memoirs of the National Institute of Polar Research* (Japan), special issue, 8:70–92.
1978. Japanese Scientific Activities in the McMurdo Region, 1977–1978. *Antarctic Journal of the United States,* 13(4):14–15.
1978. Magnetic Properties of an Iron Meteorite (Yamato-75031) and a Pallasite (Yamato 74044). *Memoirs of the National Institute of Polar Research* (Japan), special issue, 8:240–247.
1979. Japanese Scientific Activities in Victoria Land, 1978–79. *Antarctic Journal of the United States,* 14(5):44–45.
1979. Magnetic Classification of Antarctic Stony Meteorites (III). *Memoirs of the National Institute of Polar Research* (Japan), special issue, 12:223–237.
1979. Magnetic Properties and Paleointensity of Achon-

drites in Comparison with Those of Lunar Rocks. In *Proceedings of the Tenth Lunar and Planetary Science Conference*, pages 2199–2210. New York: Pergamon Press.

1979. Magnetic Properties of Yamato-7301(j), -7305(k), and -7304(m) Chondrites in Comparison with Their Mineralogical and Chemical Compositions. *Memoirs of the National Institute of Polar Research* (Japan), special issue, 12:250–269.

1979. Meteorite Magnetism and the Early Solar System Magnetic Field. *Physics of the Earth and Planetary Interiors*, 20:324–341.

1979. Natural Remanent Magnetism of Antarctic Meteorites. *Memoirs of the National Institute of Polar Research* (Japan), special issue, 12:238–249.

1979. Natural Remanent Magnetization of the Fusion Crust of Meteorites. *Memoirs of the National Institute of Polar Research* (Japan), special issue, 15:253–272.

1980. Magnetic Classification of Antarctic Meteorites. In *Lunar and Planetary Science XI*, pages 783–785. Houston: Lunar and Planetary Institute.

1980. Magnetic Classification of Antarctic Meteorites. In *Proceedings of the Eleventh Lunar and Planetary Science Conference*, pages 1789–1799. New York: Pergamon Press.

Nagata, T., R.M. Fisher, and N. Sugiura

1976. Metallographic and Magnetic Properties of a Yamato Iron Meteorite-Yamato-75-105. *Memoirs of the National Institute of Polar Research* (Japan), series C, 10:1–11.

Nagata, T., and M. Funaki

1981. The Composition of Natural Remanent Magnetization of an Antarctic Chondrite, ALHA 76008 (L6). In *Lunar and Planetary Science XII*, pages 747–749. Houston: Lunar and Planetary Institute.

Nagata, T., and N. Sugiura

1976. Magnetic Classification of Some Yamato Meteorites—Magnetic Classification of Stone Meteorites. *Memoirs of the National Institute of Polar Research* (Japan), series C, 10:30–58.

1977. Paleomagnetic Field Intensity Derived from Meteorite Magnetization. *Physics of the Earth and Planetary Interiors*, 13:373–379.

Nagata, T., N. Sugiura, and F.C. Schwerer

1975. Notes on Magnetic Properties of the Yamato Meteorites. *Memoirs of the National Institute of Polar Research* (Japan), special issue, 5:91–110.

1976. Magnetic Properties of Yamato-7304 and Yamato-7307 Meteorites. *Memoirs of the National Institute of Polar Research* (Japan), series C, 10:12–29.

Nakamura, N.

1979. A Preliminary Isotopic Study on Four Yamato Diogenites — Sm-Nd and Rb-Sr Systematics. *Memoirs of the National Institute of Polar Research* (Japan), special issue, 15:219–226.

Nakamura, N., A. Masuda, D. Coffrant, and M. Tatsumoto

1979. REE Abundances and Sm/Nd Systematics of Antarctic Eucrite, Allan Hills No. 5 Meteorite. *Meteoritics*, 14:492–493.

Naruse, R.

1979. Dynamical Features of the Meteorite Ice Field, Antarctica. *Memoirs of the National Institute of Polar Research* (Japan), special issue, 12:19–24.

Nishida, N., N. Onuma, and Y. Ohtsuka

1979. A Classification of Several Yamato-74 Chondrites. *Memoirs of the National Institute of Polar Research* (Japan), special issue, 12:144–160.

Nishida, N., Y. Suzuki, Y. Ohtsuka, and N. Onuma

1979. A Classification of Several Yamato-74 Chondrites. *Memoirs of the National Institute of Polar Research* (Japan), special issue, 15:215–218.

Nishiizumi, K.

1978. Cosmic Ray Produced ^{53}Mn in Thirty-one Meteorites. *Earth and Planetary Science Letters*, 41:91–100.

Nishiizumi, K., and J.R. Arnold

1980. Ages of Antarctic Meteorites. In *Lunar and Planetary Science XI*, pages 815–817. Houston: Lunar and Planetary Institute.

1981. Cosmogenic Nuclides in Antarctic Meteorites. In *Lunar and Planetary Science XII*, pages 771–773. Houston: Lunar and Planetary Institute.

Nishiizumi, K., J.R. Arnold, D. Elmore, R.D. Ferraro, H.E. Gove, R.C. Finkel, R.P. Beukens, K.H. Chang, and L.R. Kilius

1979. Measurements of ^{36}Cl in Antarctic Meteorites and Antarctic Ice Using a Van de Graaff Accelerator. *Earth and Planetary Science Letters*, 45:285–292.

Nishiizumi, K., M. Imamura, and M. Honda

1978. Cosmic Ray Induced ^{53}Mn in Yamato-7301(j), -7305(k) and -7304(m) Meteorites. *Memoirs of the National Institute of Polar Research* (Japan), special issue, 8:209–219.

1979. Cosmic Ray Produced Radionuclides in Antarctic Meteorites. *Memoirs of the National Institute of Polar Research* (Japan), special issue, 12:161–177.

Nishiizumi, K., M.T. Murrell, J.R. Arnold, D. Elmore, R.D. Ferraro, H.E. Gove, and R.C. Finkel

1981. Cosmic Ray Produced ^{36}Cl and ^{53}Mn in Allan Hills-77 Meteorites. *Earth and Planetary Science Letters*, 52:31–38.

Nishio, F., and J.O. Annexstad

1979. Glaciological Survey in the Bare Ice Area near the Allan Hills in Victoria Land, Antarctica. *Memoirs of the National Institute of Polar Research* (Japan), special issue, 15:13–23.

Nishio, F., and S. Mae

1979. Temperature Profile in the Bare Ice Area Near the Yamato Mountains, Antarctica. *Memoirs of the National Institute of Polar Research* (Japan), special issue, 12:25–37.

Nyquist, L.E., D.D. Bogard, J.L. Wooden, C.-Y. Shih, B.M. Bansal, and G. McKay
1979. Early Differentiation, Late Magmatism, and Recent Bombardment on the Shergottite Parent Planet. *Meteoritics*, 14:502.

Okada, A.
1975. Petrological Studies of the Yamato Meteorites, Part 1: Mineralogy of the Yamato Meteorites. *Memoirs of the National Institute of Polar Research* (Japan), special issue, 5:14-66.

Okada, A., and M. Shima
1979. Yamato-694 Meteorite: Chemical Composition of Silicate Minerals and Petrographic Nature. *Memoirs of the National Institute of Polar Research* (Japan), special issue, 12:109-113.

Okada, A., K. Yagi, and M. Shima
1975. Petrological Studies of the Yamato Meteorites, Part 2: Petrology of the Yamato Meteorites. *Memoirs of the National Institute of Polar Research* (Japan), special issue, 5:67-82.

Olsen, E.J., A. Noonan, K. Fredriksson, E. Jarosewich, and G. Moreland
1978. Eleven New Meteorites from Antarctica, 1976-1977. *Meteoritics*, 13:209-225.

Onuma, N., R.N. Clayton, T.K. Mayeda, and K. Yanai
1978. Oxygen Isotopes in Several Yamato Meteorites. *Memoirs of the National Institute of Polar Research* (Japan), special issue, 18:220-224.

Onuma, N., N. Nishida, Y. Ohtsuka, M. Kimura, and K. Yanai
1979. Origin and Evolution of Chondrules Based on Na/Al-dispersion and -Convergence in Yamato-74 Ordinary Chondrites. *Memoirs of the National Institute of Polar Research* (Japan), special issue, 15:206-214.

Palme, H., H. Baddenhausen, K. Blum, M. Cendales, G. Dreibus, H. Hofmeister, H. Kruse, C. Palme, B. Spettel, E. Vilcsek, and H. Wänke
1978. New Data on Lunar Samples and Achondrites and a Comparison of Least Fractionated Samples from the Earth, the Moon, and the Eucrite Parent Body. In *Proceedings of the Ninth Lunar and Planetary Science Conference*, pages 25-57. New York: Pergamon Press.

Ponnamperuma, C.
1979. Uncontaminated Carbonaceous Chondrites from the Antarctic. *Antarctic Journal of the United States*, 14(5):42-44.

Prinz, M., C.E. Nehru, J.S. Delaney, G.C. Harlow, and R.L. Bedell
1980. ALHA77219: A New Antarctic Mesosiderite and a Comparison with Other Mesosiderites and Related Achondrites. In *Lunar and Planetary Science XI*, pages 899-901. Houston: Lunar and Planetary Institute.
1980. Modal Studies of Mesosiderites and Related Achondrites, Including the New Mesosiderite ALHA77219. *Proceedings of the Eleventh Lunar and Planetary Science Conference*, pages 1055-1071. New York: Pergamon Press.

Prinz, M., D.G. Waggoner, and P.G. Hamilton
1980. Winonaites: A Primitive Achondritic Group Related to Silicate Inclusions in IAB Irons. In *Lunar and Planetary Science XI*, pages 902-904. Houston: Lunar and Planetary Institute.

Reid, A.M., and C.M. Schwarz
1980. Antarctic Polymict Eucrites. *Meteoritics*, 15: 353-354.

Rhodes, J.M., and C.R. Fulton
1981. Chemistry of Some Antarctic Meteorites. In *Lunar and Planetary Science XII*, pages 880-882. Houston: Lunar and Planetary Institute.

Rubin, A.E., S. McKinley, E.R.D. Scott, G.J. Taylor, and K. Keil
1981. A New Kind of Unequilibrated Ordinary Chondrite with a Graphite-Magnetite Matrix. In *Lunar and Planetary Science XII*, pages 908-910. Houston: Lunar and Planetary Institute.

Schaeffer, O.A.
1980. Meteorite Chronology: ^{39}Ar-^{40}Ar Ages of Antarctic Meteorites. In *Lunar and Planetary Science XI*, pages 982-983. Houston: Lunar and Planetary Institute.

Schaeffer, O.A., and R. Warasila
1981. ^{39}Ar-^{40}Ar Study of Allan Hills Meteorite 77005, a Unique Achondrite. In *Lunar and Planetary Science XII*, pages 932-933. Houston: Lunar and Planetary Institute.

Schultz, L., H. Palme, B. Spettel, H. Wänke, and H.W. Weber
1980. Chemistry and Noble Gases of the Unusual Stony Meteorite Allan Hills A77081. In *Lunar and Planetary Science XI*, pages 1003-1005. Houston: Lunar and Planetary Institute.

Score, R., C.M. Schwarz, T.V.V. King, B. Mason, D.D. Bogard, and E.M. Gabel
1981. Antarctic Meteorite Descriptions — 1976, 1977, 1978, 1979. *Antarctic Meteorite Newsletter*, 4(1): 1-144.

Scott, E.R.D., G.J. Taylor, A.E. Rubin, A. Okada, K. Keil, B. Hudson, and C.M. Hohenberg
1981. Graphite-Magnetite Inclusions in Ordinary Chondrites: An Important Constituent in the Early Solar System. In *Lunar and Planetary Science XII*, pages 955-957. Houston: Lunar and Planetary Institute.

Sears, D.
1979. Rocks on the Ice. *New Scientist*, 22:959-961.

Sears, D.W., and S.A. Durrani
1980. Thermoluminescence and the Terrestrial Age of Meteorites: Some Recent Results. *Earth and Planetary Science Letters*, 46:159-166.

Shih, C.-Y., L.E. Nyquist, B.M. Bansal, H. Weismann, J.L. Wooden, and G. McKay

1981. REE, Sr, and Nd Isotopic Studies on Shocked Achondrites — Shergotty, Zagami, and ALHA 77005. In *Lunar and Planetary Science XII*, pages 973–975. Houston: Lunar and Planetary Institute.

Shima, Makoto, and Masako Shima

1973. Mineralogical and Chemical Composition of New Antarctic Meteorites. *Meteoritics*, 8:439–440.

1975. Cosmochemical Studies on the Yamato Meteorites — A Summary of Chemical Studies on Yamato (a), (b), (c), and (d) Meteorites. *Memoirs of the National Institute of Polar Research* (Japan), special issue, 5:9–13.

Shima, Makoto, Masako Shima, and H. Hintenberger

1973. Chemical Composition and Rare Gas Content of Four Newly Detected Antarctic Meteorites. *Earth and Planetary Science Letters*, 19:246–249.

Shima, Makoto, H. Yabuki, and K. Yoshikawa

1978. Study on the Extraterrestrial Materials in Antarctica, VIII: On the Distribution of the Yamato Meteorites. *Memoirs of the National Institute of Polar Research* (Japan), special issue, 8:101–109.

Shima, Masako

1974. The Chemical Composition of the Stone Meteorites, Yamato (a), (b), (c), and (d) and Numakai. *Meteoritics*, 9:123–135.

1979. The Abundances of Titanium, Zirconium, and Hafnium in Stony Meteorites. *Geochimica et Cosmochimica Acta*, 43:353–362.

Shimizu, H., A. Masuda, and T. Tanaka

1979. Two Major Groups of Chondritic REE Abundance Suites: Variable Octad Effect on Heavy REE. *Memoirs of the National Institute of Polar Research* (Japan), special issue, 15:171–176.

Shimoyama, A., C. Ponnamperuma, and K. Yanai

1979. Amino Acids in the Yamato Carbonaceous Chondrites from Antarctica. *Nature*, 282:394–396.

1979. Amino Acids in the Yamato-74662 Meteorite, an Antarctic Carbonaceous Chondrite. *Memoirs of the National Institute of Polar Research* (Japan), special issue, 15:196–205.

Shiraishi, K.

1979. Antarctic Search for Meteorites by U.S.-Japan Joint Party, 1978–1979. *Memoirs of the National Institute of Polar Research* (Japan), special issue, 15:1–12.

Shiraishi, K., R. Naruse, and K. Kusunoki

1976. Collection of Yamato Meteorites, Antarctica, in December 1973. *Nankyoku Shiryô* [Antarctic Record, Japan], 55:49–60.

Simon, S.B., and S.E. Haggerty

1980. Antarctic Meteorites: A Petrographic Study of ALHA77302. In *Lunar and Planetary Science XI*, pages 1033–1035. Houston: Lunar and Planetary Institute.

Suwa, K., and K. Yagi

1979. Plagioclase in Yamato-7308 Meteorite from Antarctica. *Memoirs of the National Institute of Polar Research* (Japan), special issue, 15:148–164.

Takaoka, N., and K. Nagao

1978. Rare Gas Studies of Yamato-7301(j), -7304(m) and -7305(k). *Memoirs of the National Institute of Polar Research* (Japan), special issue, 8:198–208.

Takeda, H.

1979. A Layered Crust Model of the Howardite Parent body. *Icarus*, 40:455–470.

Takeda, H., M.B. Duke, T. Ishii, H. Haramura, and K. Yanai

1979. Some Unique Meteorites Found in Antarctica and Their Relation to Asteroids. *Memoirs of the National Institute of Polar Research* (Japan), special issue, 15:54–76.

Takeda, H., T. Ishii, and M. Miyamoto

1979. Pyroxenes in Early Crustal Cumulates Found in Achondrites and Lunar Highland Rocks. In *Lunar and Planetary Science X*, pages 1200–1202. Houston: Lunar and Planetary Institute.

Takeda, H., and M. Miyamoto

1977. Inverted Pigeonites from Lunar Breccia 76255 and Pyroxene-Crystallization Trends in Lunar and Achondritic Crusts. In *Lunar Science VIII*, pages 922–924. Houston: Lunar and Planetary Institute.

1977. Inverted Pigeonites from Lunar Breccia 76255 and Pyroxene-Crystallization Trends in Lunar and Achondritic Crusts. In *Proceedings of the Eighth Lunar and Planetary Science Conference*, pages 2617–2626. New York: Pergamon Press.

Takeda, H., M. Miyamoto, M.B. Duke, and T. Ishii

1978. Crystallization of Pyroxenes in Lunar KREEP Basalt 15386 and Meteoritic Basalts. In *Proceedings of the Ninth Lunar and Planetary Science Conference*, pages 1157–1171. New York: Pergamon Press.

Takeda, H., M. Miyamoto, M.B. Duke, and K. Yanai

1978. The Yamato-74659 Ureilite and Some New Findings on the Yamato Achondritic Pyroxenes. *Meteoritics*, 13:641–645.

Takeda, H., M. Miyamoto, and T. Ishii

1978. Comparison of the Chemical Trends and Crystallography of Pyroxenes for KREEP Basalts with Those for Eucrites. In *Lunar and Planetary Science IX*, pages 1134–1136. Houston: Lunar and Planetary Institute.

1979. Pyroxenes in Early Crustal Cumulates Found in Achondrites and Lunar Highland Rocks. In *Proceedings of the Tenth Lunar and Planetary Science Conference*, pages 1095–1107. New York: Pergamon Press.

1980. Comparisons of KREEPy Clasts in Lunar Basalts with Basaltic Clasts in Eucritic Polymict Breccias. In *Lunar and Planetary Science XI*, pages 1116–1118.

Houston: Lunar and Planetary Institute.
1980. Comparison of Basaltic Clasts in Lunar and Eucritic Polymict Breccias. In *Proceedings of the Eleventh Lunar and Planetary Science Conference*, pages 135–147. New York: Pergamon Press.

Takeda, H., M. Miyamoto, T. Ishii, and A.M. Reid.
1976. Characterization of Crust Formation on a Parent Body of Achondrites and the Moon by Pyroxene Crystallography and Chemistry. In *Proceedings of the Seventh Lunar and Planetary Science Conference*, pages 3535–3548. New York: Pergamon Press.

Takeda, H., M. Miyamoto, T. Ishii, K. Yanai, and Y. Matsumoto
1979. Mineralogical Examination of the Yamato-75 Achondrites and Their Layered Crust Model. *Memoirs of the National Institute of Polar Research* (Japan), special issue, 12:82–108.

Takeda, H., M. Miyamoto, K. Yanai, and H. Haramura
1978. A Preliminary Mineralogical Examination of the Yamato-74 Achondrites. *Memoirs of the National Institute of Polar Research* (Japan), special issue, 8:170–184.

Takeda, H., A.M. Reid, and T. Yamanaka
1975. Crystallographic and Chemical Studies of a Bronzite and Chromite in the Yamato (b) Achondrite. *Memoirs of the National Institute of Polar Research* (Japan), special issue, 5:83–90.

Takeda, H., and K. Yanai
1979. A New Olivine-Augite Achondrite Found in Antarctica. *Meteoritics*, 14:542–543.
1981. Yamato Polymict Eucrites: Regolith Breccias Excavated from a Layered Crust. In *Lunar and Planetary Science XII*, pages 1071–1073. Houston: Lunar and Planetary Institute.

Takeda, H., K. Yanai, and K. Shiraishi
1980. Yamato and Allan Hills Meteorites and Their Bearing on the Parent Bodies. In *Lunar and Planetary Science XI*, pages 1119–1121. Houston: Lunar and Planetary Institute.

Taylor, G.J., A. Okada, E.R.D. Scott, A.E. Rubin, G.R. Huss, and K. Keil
1981. The Occurrence and Implications of Carbide-Magnetite Assemblages in Unequilibrated Ordinary Chondrites. In *Lunar and Planetary Science XII*, pages 1076–1078. Houston: Lunar and Planetary Institute.

Tsuchiyama, A., H. Nagahara, and I. Kushiro
1980. Experimental Reproduction of Textures of Chondrules. *Earth and Planetary Science Letters*, 48: 155–165.

Watters, T.R., M. Prinz, E.R. Rambaldi, and J.T. Wasson
1980. ALHA78113, Mt. Egerton and the Aubrite Parent Body. *Meteoritics*, 15:386.

Weber, H.W., and L. Schultz
1978. Noble Gases in 10 Stony Meteorites from Antarctica and Their Exposure Ages. *Meteoritics*, 13:658–660.
1980. Noble Gases in Ten Stone Meteorites from Antarctica. *Zeitschrift für Naturforschung*, 35a:44–49.

Wooden, J.L., L.E. Nyquist, D.D. Bogard, B.M. Bansal, H. Wiesmann, C.-Y. Shih, and G.A. McKay
1979. Radiometric Ages for the Achondrites Chervony Kut, Governador Valadares, and Allan Hills 77005. In *Lunar and Planetary Science X*, pages 1379–1381. Houston: Lunar and Planetary Institute.

Wooden, J.L., A.M. Reid, R. Brown, B.M. Bansal, H. Wiesmann, and L.E. Nyquist
1981. Chemical and Isotopic Studies of the Allan Hills Polymict Eucrites. In *Lunar and Planetary Science XII*, pages 1203–1205. Houston: Lunar and Planetary Institute.

Yabuki, H., K. Yagi, and K. Onuma
1978. Petrological Studies of Yamato-74 Meteorites (1). *Memoirs of the National Institute of Polar Research* (Japan), special issue, 8:142–155.

Yagi, K., J.F. Lovering, Makoto Shima, and A. Okada
1978. Mineralogical and Petrological Studies of the Yamato Meteorites, Yamato-7301(j), -7305(k), -7308(l) and -7303(m) from Antarctica. *Memoirs of the National Institute of Polar Research* (Japan), special issue, 8:121–141.
1978. Petrology of the Yamato Meteorites (j), (k), (l), and (m) from Antarctica. *Meteoritics*, 13:23–45.

Yanai, K.
1976. Search and Collection of Yamato meteorites, Antarctica, in October and November, 1974. *Nankyoku Shiryô* [Antarctic Record, Japan], 56:70–81.
1978. First Meteorites Found in Victoria Land, Antarctica, December 1976 and January 1977. *Memoirs of the National Institute of Polar Research* (Japan), special issue, 8:51–69.
1978. Meteorites from Antarctica. *Meteoritics*, 13: 673–677.
1978. Yamato-74 Meteorites Collection, Antarctica, from November to December 1974. *Memoirs of the National Institute of Polar Research* (Japan), special issue, 8:1–37.
1979. Meteorite Search in Victoria Land, Antarctica, in 1977–1978 Austral Summer. *Memoirs of the National Institute of Polar Research* (Japan), special issue, 12:1–8.
1979. *Catalog of Yamato Meteorites in the Collection of National Institute of Polar Research*. 188 pages. Tokyo: National Institute of Polar Research (Japan).

Yanai, K., W.A. Cassidy, M. Funaki, and B.P. Glass
1978. Meteorite Recoveries in Antarctica during Field Season 1977–78. In *Proceedings of the Ninth Lunar and Planetary Science Conference*, pages 977–987. New York: Pergamon Press.

Yanai, K., and H. Haramura
1978. Yamato-74662 Meteorite: A Carbonaceous Chondrite Type II. *Memoirs of the National Institute of Polar Research* (Japan), special issue, 8:264–267.

Yanai, K., M. Miyamoto, and H. Takeda
1978. Classification for the Yamato-74 Chondrites Based on the Chemical Compositions of Their Olivines and Pyroxenes. *Memoirs of the National Institute of Polar Research* (Japan), special issue, 8:110–120.

Yomogida, K., and T. Matsui
1981. Porosity of Ordinary Chondrites—Is It a Good Measure of a Consolidation State of Composite Materials in Chondrites? In *Lunar and Planetary Science XII*, pages 1227–1229. Houston: Lunar and Planetary Institute.

Yoshida, M., H. Ando, K. Omoto, R. Naruse, and Y. Ageta
1971. Discovery of Meteorites near Yamato Mountains, East Antarctica. *Nankyoku Shiryô* [Antarctic Record, Japan], 39:62–65.

Yoshida, Y., and S. Mae
1978. Some Information on Topographic Features and the Characteristics of the Sheet Ice around the Yamato Mountains. *Memoirs of the National Institute of Polar Research* (Japan), special issue 8:93–100.

Appendix

Tables of Victoria Land Meteorites

Terminology

Class and type: Au = aubrite; C = carbonaceous chondrite; Di = diogenite; Eu = eucrite; Ho = howardite; H = high-iron chondrite; L = low-iron chondrite; LL = low-iron low-metal chondrite; M = mesosiderite; Sh = shergottite; Ur = ureilite. Chondrite type is indicated by the digit following the letter.

Olivine composition in mole percent Fe_2SiO_4 (Fa).

Pyroxene (orthopyroxene or low-Ca clinopyroxene) composition in mole percent $FeSiO_3$ (Fs).

Degree of weathering: A = minor; metal flecks have inconspicuous rust halos, oxide stain along cracks is minor. B = moderate; metal flecks show large rust halos, internal cracks show extensive oxide stain. C = severe; specimen is uniformly stained brown, no metal survives.

Degree of fracturing: A = slight; specimen has few or no cracks and none penetrate the entire specimen. B = moderate; several cracks extend across the specimen, which can be readily broken along the fractures. C = severe; specimen has many extensive cracks and readily crumbles.

Locations: ALH = Allan Hills; BTN = Bates Nunatak; DRP = Derrick Peak; EET = Elephant Moraine; MET = Meteorite Hills; MBR = Mount Baldr; PGP = Purgatory Peak; RKP = Reckling Peak.

Table A.—Characteristics of meteorites listed by source area, in numerical sequence

Specimen number	*Weight (g)*	*Class and type*	*%Fa in olivine*	*%Fs in pyroxene*	*Degree of weathering*
ALHA					
76001	20151	L6	25	21	A
76002	1510	Iron			
76003	10495	L6	25	21	A
76004	305	LL3	0–34	0–53	A
76005	1425	Eu		37–57	A
76006	1137	H6	18	16	B
76007	410	L6	24	21	A
76008	1150	H6	19	17	B
76009	407000	L6	24	21	B
77001	252	L6	25	21	B
77002	235	L5	25	22	B
77003	779	C3	4–48	2–25	A
77004	2230	H4	17–20	15–27	C
77005	483	Sh	28	23	A
77009	235	H4	18	16	C
77010	295	H4	18	15–18	C
77011	291	L3	4–36	1–33	C
77012	180	H5	18	16	C
77014	309	H5	18	17	C
77015	411	L3	1–21	4–24	C
77021	16.7	H5	18	17	C
77025	19.4	H5	18	17	C
77033	9.3	L3	8–38	8–9	C
77061	12.6	H5	18	17	B
77062	16.7	H5	18	17	B
77064	6.5	H5	18	17	B
77071	10.9	H5	18	17	B
77074	12.1	H5	18	17	B
77081	8.6	H?	11	11	B
77086	19.4	H5	19	17	C
77088	51.2	H5	19	17	C
77102	12.3	H5	19	15	B
77118	7.8	H5	19	17	C
77119	6.4	H5	18	17	C
77124	4.4	H5	19	16	C

TABLE A.—Continued

Specimen number	Weight (g)	Class and type	%Fa in olivine	%Fs in pyroxene	Degree of weathering
77140	78.6	L3	8–44	2–17	C
77144	7.9	H6	19	17	B
77148	13.1	H6	18	16	C
77150	58.3	L6	25	22	C
77155	305	L6	24	20	A/B
77160	70.4	L3	3–46	6–40	C
77164	38.1	L3	6–39	3–41	C
77165	30.5	L3	8–33	6–35	C
77167	611	L3	2–41	3–17	C
77177	368	H5	18	16	C
77180	190	L6	24	20	C
77182	1134	H5	19	17	B
77183	288	H6	19	16	C
77190	387	H4	17–19	15–22	C
77191	642	H4	16–18	14–16	C
77192	845	H4	16–18	15–21	C
77208	1733	H4	17	14	C
77214	2111	L3	1–49	4–23	C
77215	820	L3	22–26	9–21	B
77216	1470	L3	15–35	14–23	A/B
77217	413	L3	17–25	9–26	B
77219	637	M	26	24–28	B
77221	229	H4	15	13–15	C
77223	207	H4	17	15–23	C
77224	787	H4	19	17	C
77225	5878	H4	17	16	C
77226	15323	H4	18	16	C
77230	2473	L4	22–25	18–29	B
77231	9270	L6	24	21	A/B
77232	6494	H4	17	15	C
77233	4087	H4	14–21	15–17	C
77249	504	L3	7–35	2–25	C
77250	10555	Iron			
77252	343	L3	22–28	2–22	B
77254	246	L5	23	20	A/B
77255	765	Iron			
77256	676	Di		23	A/B
77257	1996	Ur	13	12	A
77258	597	H6	18	16	B/C
77259	294	H5	18	15	C
77260	744	L3	7–23	1–28	C
77261	412	L6	24	21	B
77262	862	H4	15–19	13–16	B
77263	1669	Iron			
77264	11.0	H5	19	16	A/B
77268	272	H5	18	16	C
77269	1045	L6	24	22	B
77270	589	L6	24	21	A/B
77271	610	H6	18	16	C
77272	674	L6	24	20	B/C
77273	492	L6	24	20	B
77274	288	H5	18	16	C
77277	143	L6	24	20	A/B
77278	313	LL3	11–29	9–21	A
77280	3226	L6	24	21	B
77281	1231	L6	24	20	B
77282	4127	L6	24	20	B
77283	10510	Iron			
77284	376	L6	25	21	A/B
77285	271	H6	18	16	C
77286	245	H4	17	12–16	C
77287	230	H5	18	16	C
77288	1880	H6	19	17	B
77289	2186	Iron			
77290	3784	Iron			
77292	199	L6	24	20	B
77294	1351	H5	17	15	A
77296	963	L6	24	21	A/B
77297	952	L6	24	20	A
77299	261	H3	11–21	15–20	A
77300	235	H5	18	16	C
77302	236	Eu		37–64	A
77304	650	LL3	18–27	13–19	B
77305	6444	L6	24	21	B/C
77306	19.9	C2			A
77307	181	C3	1–30	1–12	A
78006	8.0	Ho		25–61	A
78019	30.3	Ur	22	18	B/C
78038	363	L3	4–42	2–19	C
78039	299	L6	24	21	B
78040	211	Eu		33–52	A
78042	214	L6	24	20	B
78043	680	L6	25	21	B
78044	164	L4	23–25	19–24	B/C
78045	396	L6	25	21	B/C
78048	190	L6	24	21	A/B
78050	1045	L6	23	20	B
78053	179	H4	17	16	C
78074	200	L6	24	21	B
78075	280	H5	18	16	B/C
78076	275	H6	18	16	B
78077	330	H4	19	15–18	C
78078	290	L6	24	20	A/B
78084	14280	H3	18	8–24	B/C
78085	219	H5	18	16	B
78100	84.9	Iron			
78102	336	H5	18	17	B/C

TABLE A.—Continued

Specimen number	Weight (g)	Class and type	%Fa in olivine	%Fs in pyroxene	Degree of weathering
78103	589	L6	24	20	B
78104	672	L6	24	20	B
78105	941	L6	23	20	B
78106	464	L6	24	20	A/B
78107	198	H5	18	17	C
78108	172	H5	18	16	B
78109	233	LL5	28	23	A/B
78110	160	H5	18	16	B/C
78111	126	H5	18	16	A
78112	2485	L6	25	20	B
78113	298	Au	0	0	A/B
78114	808	L6	25	20	B/C
78115	847	H6	18	16	B
78126	606	L6	25	21	B
78127	194	L6	24	20	B/C
78128	154	H5	19	17	C
78130	2733	L6	25	21	B/C
78131	268	L6	25	21	B/C
78132	656	Eu		40–68	A
78134	458	H4	18	15–20	B/C
78153	151	LL6	29	24	B/C
78158	15.1	Eu		40–68	A
78165	20.9	Eu		37–61	A
78188	0.8	L3	1–34	5–29	C
78193	13.3	H4	18	16	B/C
78196	11.1	H4	18	16	B/C
78209	12.1	H5	18	15	B/C
78211	11.4	H6	18	16	B/C
78213	9.5	H6	18	15	B/C
78215	6.3	H6	18	16	B/C
78221	5.4	H5	18	16	B
78223	6.4	H4	18	16	B
78225	4.5	H5	18	16	B
78227	2.4	H5	18	16	B/C
78229	1.9	H6	18	15	B
78231	1.8	H6	18	16	B/C
78233	1.3	H5	18	16	B/C
78251	1312	L6	23	20	B
78252	2789	Iron			
78261	5.1	C2	0–50	1–8	A
78262	26.1	Ur	22	19	A
79001	32.3	L3	6–39	2–31	C
79002	222	H6	16	18	C
79003	5.1	L3	10–38	5–26	B
79004	34.9	H5	16	14	B/C
79005	60.0	H6	18	16	B
79006	40.9	H5	18	15	B/C
79007	142	L6	23	19	A/B
79008	12.0	H5	17	15	B
79009	75.7	H5	18	15	C
79010	25.1	H5	17	15	B/C
79011	14.0	H5	18	16	B/C
79012	192	H5	17	15	C
79013	28.3	H5	18	16	C
79014	10.8	H5	18	16	B
79015	64.0	H5	17	15	B
79016	1146	H6	17	15	B/C
79017	310	Eu		28–53	A
79018	120	L6	23	20	B/C
79019	12.1	H6	17	15	B
79020	4.2	H6	17	15	B/C
79021	29.4	H5	18	17	B
79022	31.4	L3	1–28	9–22	A/B
79023	68.1	H4	17	14–17	B/C
79024	21.6	H6	17	15	C
79025	1208	H5	17	15	C
79026	572	H5	18	16	B
79027	133	L6	24	20	B
79028	16.2	H6	18	16	B
79029	505	H5	18	16	C
79031	2.7	H5	16	14	C
79032	2.6	H5	16	14	C
79033	208	L6	24	20	B
79034	12.6	H6	18	16	B
79035	37.6	H4	17	14–18	B
79036	20.2	H5	18	16	B
79037	14.8	H6	18	16	B
79038	49.6	H5	17	15	C
79039	108	H4	16	15	B
79040	13.2	H5	18	15	B
79041	20.1	H5	18	16	B
79042	11.4	H5	18	16	B
79043	62.2	L6	23	20	C
79045	115	L3	2–38	2–29	C
79046	89.7	H5	18	15	B
79047	19.3	H5	18	15	B
79048	36.7	H5	18	16	B
79049	54.0	H6	18	16	C
79050	27.0	H5	18	15	C
79051	24.0	H5	18	15	C
79052	22.6	L6	23	20	B/C
79053	86.0	H5	17	15	B/C
79054	36.0	H5	18	16	B
79055	15.2	H6	18	16	B/C
BTNA					
78001	160	L6	24	21	B
78002	4301	L6	24	20	B

TABLE A.—Continued

Specimen number	Weight (g)	Class and type	%Fa in olivine	%Fs in pyroxene	Degree of weathering
78004	1079	LL6	30	24	B
DRPA					
78001	15200	Iron			
78002	7188	Iron			
78003	144	Iron			
78004	133	Iron			
78005	18600	Iron			
78006	389	Iron			
78007	11800	Iron			
78008	59400	Iron			
78009	138100	Iron			
EETA					
79001	7942	Sh	23–27	16–67	A
79002	2843	Di	24–25	22	B
79003	435	L6	24	20	B
79004	390	Eu		30–61	B
79005	450	Eu		30–61	A
79006	716	Ho		19–57	B
79007	199	H5	18	16	B
79009	140	L5	24	20	B
79010	287	L6	24	20	B
79011	86.4	Eu		30–61	B
META					
78001	624	H4	17	14–21	B/C
78002	542	L6	23	20	B
78003	1726	L6	24	21	B
78005	172	L6	24	20	B
78006	409	H6	18	15	C
78007	174	H6	19	17	B/C
78010	233	H5	19	17	B
78028	20657	L6	25	21	B
MBRA					
76001	4108	H6	18	16	A
76002	13773	H6	18	16	A
PGPA					
77006	19068	Iron			
RKPA					
78001	234	L6	23	20	C
78002	8483	H4	18	15	B
78003	1276	L6	23	20	C
78004	166	H4	17	14–21	A
79001	3006	L6	24	20	B
79002	203	L6	24	20	B
79003	182	H6	18	16	B
79004	370	H5	18	16	B/C
79008	73.0	L3	1–29	2–28	B
79009	55.0	H6	18	16	C
79012	12.8	H6	18	16	B
79013	11.0	L5	23	20	B/C
79014	77.7	H5	18	16	B/C
79015	10022	M		24	

TABLE B.—Meteorites listed by class and source area in numerical sequence

Specimen number	Weight (g)	Class and type	Degree of weathering	Degree of fracturing
	ORDINARY CHONDRITES			
ALHA77299	260	H3	A	A
ALHA78084	14280	H3	B/C	B
ALHA77004	2230	H4	C	C
ALHA77009	235	H4	C	A
ALHA77010	295	H4	C	A
ALHA77190	387	H4	C	C
ALHA77191	642	H4	C	B
ALHA77192	845	H4	C	C
ALHA77208	1733	H4	C	C
ALHA77221	229	H4	C	A
ALHA77223	207	H4	C	C
ALHA77224	786	H4	C	C
ALHA77225	5878	H4	C	C
ALHA77226	15323	H4	C	C
ALHA77232	6494	H4	C	C
ALHA77233	4087	H4	C	B
ALHA77262	861	H4	B	B
ALHA78286	245	H4	C	B

TABLE B.—Continued

Specimen number	Weight (g)	Class and type	Degree of weathering	Degree of fracturing
ALHA78053	179	H4	C	B
ALHA78077	330	H4	C	B
ALHA78134	458	H4	B/C	B
META78001	624	H4	B/C	B
RKPA78002	8483	H4	B	A
RKPA78004	166	H4	A	A
ALHA79023	68.1	H4	B/C	C
ALHA79039	108	H4	B	B
ALHA79035	37.6	H4	B	B
ALHA78193	13.3	H4	B/C	A
ALHA78196	11.1	H4	B/C	B
ALHA78223	6.4	H4	B	B
ALHA77012	180	H5	C	A
ALHA77014	308	H5	C	B
ALHA77021	16.6	H5	C	A
ALHA77025	19.4	H5	C	B
ALHA77061	12.4	H5	B	A
ALHA77062	16.7	H5	B	B
ALHA77064	6.4	H5	B	B
ALHA77071	10.8	H5	B	B
ALHA77074	12.0	H5	B	B
ALHA77086	19.4	H5	C	B
ALHA77088	51.1	H5	C	B
ALHA77102	12.2	H5	B	B
ALHA77118	7.8	H5	C	B
ALHA77119	6.3	H5	C	B
ALHA77124	4.4	H5	C	A
ALHA77177	368	H5	C	A
ALHA77182	1134	H5	B	B
ALHA77259	294	H5	C	B
ALHA77264	10.9	H5	A/B	A
ALHA77268	272	H5	C	C
ALHA77274	288	H5	C	A
ALHA77287	230	H5	C	A
ALHA77294	1351	H5	A	A
ALHA77300	234	H5	C	B
ALHA78075	280	H5	B/C	B
ALHA78085	219	H5	B	B
ALHA78102	336	H5	B/C	B
ALHA78107	198	H5	C	A
ALHA78108	172	H5	B	B
ALHA78110	160	H5	B/C	B
ALHA78128	154	H5	C	B
META78010	233	H5	B	A
ALHA79004	34.9	H5	B/C	B
ALHA79006	40.9	H5	B/C	B
ALHA79008	12.0	H5	B	B
ALHA79009	75.7	H5	C	A
ALHA79010	25.1	H5	B/C	B
ALHA79011	14.0	H5	B/C	A
ALHA79012	191	H5	C	B
ALHA79013	28.3	H5	C	B
ALHA79014	10.8	H5	B	A
ALHA79015	64.0	H5	B	B
ALHA79021	29.4	H5	B	A
ALHA79025	1208	H5	C	A
ALHA79026	572	H5	B	B
ALHA79029	505	H5	C	B
ALHA79031	2.7	H5	C	B
ALHA79036	20.2	H5	B	B
ALHA79038	49.6	H5	C	B

TABLE B.—Continued

Specimen number	Weight (g)	Class and type	Degree of weathering	Degree of fracturing
ALHA79040	13.2	H5	B	A
ALHA79041	20.1	H5	B	B
ALHA79042	11.4	H5	B	A
ALHA79046	89.7	H5	B	B
ALHA79047	19.3	H5	B	B
ALHA79048	36.7	H5	B	B
ALHA79050	27.0	H5	C	B
ALHA79051	24.0	H5	C	A
ALHA79053	86.0	H5	B/C	B
ALHA79054	36.0	H5	B	A
EETA79007	199	H5	B	B
RKPA79004	370	H5	B/C	B
RKPA79014	77.7	H5	B/C	B
ALHA79032	2.6	H5	C	B
ALHA78209	12.1	H5	B/C	B
ALHA78221	5.3	H5	B	A
ALHA78225	4.5	H5	B	A
ALHA78227	2.4	H5	B/C	B
ALHA78233	1.3	H5	B/C	B
ALHA76006	271	H6	C	B
ALHA76008	281	H6	B/C	B
MBRA76001	1096	H6	B/C	B
ALHA77144	7.8	H6	B	A
ALHA77148	13.1	H6	C	B
ALHA77183	288	H6	C	A
ALHA77258	597	H6	B/C	A
ALHA77271	609	H6	C	A
ALHA77285	271	H6	C	B
ALHA77288	1880	H6	B	B
ALHA78076	275	H6	B	B
ALHA78115	847	H6	B	A
META78006	409	H6	C	B
META78007	174	H6	B/C	B
ALHA79002	222	H6	C	B
ALHA79005	60.0	H6	B	B
ALHA79016	1146	H6	B/C	B
ALHA79019	12.1	H6	B	A
ALHA79020	4.2	H6	B/C	B
ALHA79024	21.6	H6	C	B
ALHA79028	16.2	H6	B	B
ALHA79037	14.8	H6	B	B
ALHA79049	54.0	H6	C	B
ALHA79055	15.2	H6	B/C	B
RKPA79003	182	H6	B	A
RKPA79009	55.0	H6	C	B
RKPA79012	12.8	H6	B	B
ALHA79034	12.6	H6	B	A
ALHA78211	11.4	H6	B	B
ALHA78213	9.5	H6	B	B
ALHA78215	6.3	H6	B/C	B
ALHA78229	1.9	H6	B	B
ALHA78231	1.8	H6	B/C	B
ALHA77081	8.5	H?	B	A
ALHA77011	291	L3	C	A
ALHA77015	411	L3	C	B
ALHA77033	9.3	L3	C	B
ALHA77140	78.6	L3	C	B
ALHA77160	70.4	L3	C	B
ALHA77164	38.1	L3	C	C
ALHA77165	30.5	L3	C	C

TABLE B.—Continued

Specimen number	Weight (g)	Class and type	Degree of weathering	Degree of fracturing
ALHA77167	611	L3	C	B
ALHA77214	2111	L3	C	C
ALHA77215	819	L3	B	B
ALHA77216	1470	L3	A/B	B
ALHA77217	413	L3	B	B
ALHA77249	503	L3	C	C
ALHA77252	343	L3	B	C
ALHA77260	744	L3	C	C
ALHA78038	363	L3	C	C
ALHA79001	32.3	L3	C	A
ALHA79003	5.1	L3	B	B
ALHA79022	31.4	L3	A/B	B
ALHA79045	115	L3	C	B
RKPA79008	73.0	L3	B	B
ALHA78188	0.8	L3	C	B
ALHA77230	2473	L4	B	B
ALHA77002	235	L5	B	A
ALHA77254	245	L5	A/B	A
EETA79009	140	L5	B	B
RKPA79013	11.0	L5	B/C	B
ALHA76007	78.5	L6	B	A
ALHA76009	3950	L6	B	B
ALHA77001	252	L6	B	B
ALHA77150	58.3	L6	C	B
ALHA77155	305	L6	A/B	A
ALHA77180	190	L6	C	A
ALHA77231	9270	L6	A/B	A
ALHA77261	411	L6	B	B
ALHA77269	1045	L6	B	A
ALHA77270	588	L6	A/B	B
ALHA77272	674	L6	B/C	B
ALHA77273	492	L6	B	B
ALHA77277	142	L6	A/B	A
ALHA77280	3226	L6	B	B
ALHA77281	1231	L6	B	B
ALHA77282	4127	L6	B	B
ALHA77284	376	L6	A/B	B
ALHA77292	199	L6	B	A
ALHA77296	963	L6	A/B	A
ALHA77297	951	L6	A	B
ALHA77305	6444	L6	B/C	B
ALHA78039	299	L6	B	B
ALHA78042	214	L6	B	A
ALHA78043	680	L6	B	B
ALHA78045	396	L6	B/C	B
ALHA78048	190	L6	A/B	B
ALHA78050	1045	L6	B	B
ALHA78074	200	L6	B	B
ALHA78078	290	L6	A/B	A
ALHA78103	589	L6	B	B
ALHA78104	672	L6	B	A
ALHA78105	941	L6	B	A
ALHA78106	464	L6	A/B	A
ALHA78112	2485	L6	B	B
ALHA78114	808	L6	B/C	B
ALHA78126	606	L6	B	B
ALHA78127	194	L6	B/C	B
ALHA78130	2733	L6	B/C	B
ALHA78131	268	L6	B/C	A
ALHA78251	1312	L6	B	A

TABLE B.—Continued

Specimen number	*Weight (g)*	*Class and type*	*Degree of weathering*	*Degree of fracturing*
BTNA78001	160	L6	B	B
BTNA78002	4301	L6	B	A
META78002	542	L6	B	A
META78003	1726	L6	B	B
META78005	172	L6	B	B
META78028	20657	L6	B	B
RKPA78001	234	L6	C	B
RKPA78003	1276	L6	C	B
ALHA79007	142	L6	A/B	B
ALHA79018	120	L6	B/C	A
ALHA79027	133	L6	B	A
ALHA79033	208	L6	B	A
ALHA79043	62.2	L6	C	B
ALHA79052	22.6	L6	B/C	B
EETA79003	435	L6	B	B
EETA79010	287	L6	B	C
RKPA79001	3006	L6	B	C
RKPA79002	203	L6	B	B
ALHA76004	52.5	LL3	A	A
ALHA77278	312	LL3	A	A
ALHA77304	650	LL3	B	B
ALHA78109	233	LL5	A/B	A
ALHA78153	151	LL6	B/C	B
BTNA78004	1079	LL6	B	A
Subtotals				
H3	14,571			
H4	50,969			
H5	10,550			
H6	8,883			
H?	8.5			
L3	8,536			
L4	2,473			
L5	632			
L6	83,062			
LL3	1,014			
LL5	233			
LL6	1,230			
Total	182,161			
		CARBONACEOUS CHONDRITES		
ALHA77003	779	Carbonaceous C3	A	A
ALHA77306	19.9	Carbonaceous C2	A	A
ALHA77307	181.3	Carbonaceous C3	A	A
ALHA78261	5.1	Carbonaceous C2	A	A
Total	985.3			
		ACHONDRITES		
ALHA78113	298	Aubrite	A/B	A
ALHA77256	676	Diogenite	A/B	A
EETA79002	2843	Diogenite	B	B
ALHA78006	8.0	Howardite	A	A
EETA79006	716	Howardite	B	B

TABLE B.—Continued

Specimen number	*Weight (g)*	*Class and type*	*Degree of weathering*	*Degree of fracturing*
EETA79004	390	Monomict Eucrite	B	B
ALHA76005	317	Polymict Eucrite	A	A
ALHA77302	235	Polymict Eucrite	A	A
ALHA78040	211	Polymict Eucrite	A	A
ALHA78132	656	Polymict Eucrite	A	A
ALHA78158	15.1	Polymict Eucrite	A	A
ALHA78165	20.9	Polymict Eucrite	A	A
ALHA79017	310	Polymict Eucrite	A	A
EETA79005	450	Polymict Eucrite	A	B
EETA79011	86.4	Polymict Eucrite	B	B
ALHA77005	482	Shergottite	A	A
EETA79001	7942	Shergottite	A	A
ALHA77257	1995	Ureilite	A	B
ALHA78019	30.3	Ureilite	B/C	C
ALHA78262	26.1	Ureilite	A	A
Subtotals				
Aubrites	298			
Diogenites	3,519			
Howardites	724			
Monomict Eucrites	390			
Polymict Eucrites	2,303			
Shergottites	8,424			
Ureilites	2,052			
Total	17,710			
		IRONS		
ALHA76002	307	Iron-Group IA or Og		
ALHA77250	10555	Iron-Group I or Og		
ALHA77255	765	Iron-Group Anom (D)		
ALHA77263	1669	Iron-Group I or Og		
ALHA77283	10510	Iron-Group I or Og		
ALHA77289	2186	Iron-Group I or Og		
ALHA77290	3784	Iron-Group I or Og		
PGPA77006	19068	Iron-Group I or Og		
ALHA78252	2789	Iron-Group IVA		
DRPA78001	15200	Iron-Group IIB		
DRPA78002	7188	Iron-Group IIB		
DRPA78003	144	Iron-Group IIB		
DRPA78004	133	Iron-Group IIB		
DRPA78005	18600	Iron-Group IIB		
DRPA78006	389	Iron-Group IIB		
DRPA78007	11800	Iron-Group IIB		
DRPA78008	59400	Iron-Group IIB		
DRPA78009	138100	Iron-Group IIB		
ALHA78100	85.0	Iron-Group IIA		
Total	302,672			

TABLE B.—Continued

Specimen number	*Weight (g)*	*Class and type*	*Degree of weathering*	*Degree of fracturing*
		STONY-IRON		
ALHA77219	637	Mesosiderite	B	B
RKPA79015	10022	Mesosiderite		
Total	10659			
		UNCLASSIFIED		
ALHA78044	164		B/C	B
ALHA78111	126		B/C	A
Total	290			

TABLE C.—Meteorites tentatively identified as paired specimens

Class	*Paired specimens*	*Reference*
Eucrite	ALHA 76005, 77302, 78040, 78132, 78158, 78165, 79017	Score et al. (this volume)
L3	ALHA 77015, 77033, 77034, 77036, 77043, 77047, 77049, 77050, 77052, 77140, 77162, 77167, 77170, 77178, 77214	McKinley et al. (1981)
	ALHA 77160, 77164, 77165, 77249, 77260	Paired with ALHA 77015 group on evidence in King et al. (1980:18, 42)
	ALHA 77033, 77214	Separately paired by King et al. (1980:42)
	ALHA 79001, 79003	Score et al. (this volume)
L4	ALHA 77215, 77216, 77217	King et al. (1980)
L6	ALHA 77270, 77277, 77284	King et al. (1980)
	ALHA 77001, 77296, 77297	King et al. (1980)
	ALHA 77001, 77296, 77297	King et al. (1980)
	ALHA 77150, 77305	King et al. (1980)
	ALHA 77231, 77272, 77273, 77280	King et al. (1980)
	BTNA 78002 (2 stones)	Score et al. (this volume)
	RKPA 78001, 78003, 79001, 79002	Score et al. (this volume)
H4	ALHA 77004, 77191, 77192, 77208, 77224, 77233	King et al. (1980)
H5	ALHA 77014, 77264	King et al. (1980)
	ALHA 77021, 77061, 77062, 77064, 77071, 77086, 77088, 77102	King et al. (1980)
	ALHA 77118, 77119, 77124	King et al. (1980)
	RKPA 79004 (6 stones)	Score et al. (this volume)
H6	ALHA 77144, 77148	King et al. (1980)
	ALHA 77271, 77288	King et al. (1980)
Diogenite	Yamato 6902 (b), Yamato 74010, 74011, 74037, 74097, 74136, 74648	Takeda, Miyamoto, Yanai, Haramura (1978)
Iron, IA/Og	ALHA 76002, 77250, 77263, 77289, 77290	Clarke (this volume)
	DRPA 78001, 78002, 78003, 78004, 78005, 78006, 78007, 78008, 78009	Clarke (this volume)

Literature Cited

Annexstad, J.O., and F. Nishio
1980. Glaciological Studies in the Allan Hills, 1979–1980. *Antarctic Journal of the United States*, 15(5):65–66.

Berkley, J.L., H.G. Brown IV, K. Keil, N.L. Carter, J.-C. C. Mercier, and G. Huss
1976. The Kenna Ureilite: An Ultramafic Rock with Evidence for Igneous, Metamorphic, and Shock Origin. *Geochimica et Cosmochimica Acta*, 40:1429–1439.

Biswas, S., H.T. Ngo, and M.E. Lipschutz
1980. Trace Element Contents of Selected Antarctic Meteorites, I: Weathering Effects and ALH A77005, A77257, A77278, and A77299. *Zeitschrift für Naturforschung*, 35a:191–196.

Biswas, S., T. Walsh, G. Bart, and M.E. Lipschutz
1980. Thermal Metamorphism of Primitive Meteorites, XI: The Enstatite Meteorites: Origin and Evolution of a Parent Body. *Geochimica et Cosmochimica Acta*, 44:2097–2110.

Brecher, A.
1980. Meteorites as Magnetic Probes: Recent Results. In *Lunar and Planetary Science XI*, pages 106–108. Houston: Lunar and Planetary Institute.

Buchwald, V.F.
1975. *Handbook of Iron Meteorites*. 1418 pages. Berkeley: University of California Press.

Cassidy, W.A.
1978. Antarctic Search for Meteorites. *Antarctic Journal of the United States*, 12(4):96–98.
1979. Antarctic Search for Meteorites (ANSMET 1978–79). *Antarctic Journal of the United States*, 14(5):41–42.

Clarke, R.S., Jr., D.E. Appleman, and D.R. Ross
1981. Allan Hills A77283: An Antarctic Iron Meteorite Containing Preterrestrial Impact-Produced Diamond and Lonsdaleite. *Nature*, 291:396–398.

Clarke, R.S., Jr., E. Jarosewich, J.I. Goldstein, and P.A. Baedecker
1980. Antarctic Iron Meteorites from Allan Hills and Purgatory Peak. *Meteoritics*, 15:273–274.

Clayton, R.N., T.K. Mayeda, and N. Onuma
1979. Oxygen Isotopic Compositions of Some Antarctic Meteorites. In *Lunar and Planetary Science X*, pages 221–223. Houston: Lunar and Planetary Institute.

Cronin, J.R., S. Pizzarello, and C.B. Moore
1979. Amino Acids in an Antarctic Carbonaceous Chondrite. *Science*, 206:335–337.

Delaney, J.S., R. Bedell, S. Fishman, R. Klimentidis, G.E. Harlow, and M. Prinz
1980. Highly Differentiated Eucritic Clasts in Polymict Breccias Allan Hills A78040 and A77302. *Meteoritics*, 15:280–281.

Drewry, D.J.
1980. Pleistocene Bimodal Response of Antarctic Ice. *Nature*, 287(5779):214–216.

Duke, M.B. and L.T. Silver
1967. Petrology of Eucrites, Howardites and Mesosiderites. *Geochimica et Cosmochimica Acta*, 31:1637–1665.

Evans, J.C., L.A. Rancitelli, and J.H. Reeves
1979. ^{26}Al Content of Antarctic Meteorites: Implications for Terrestrial Ages and Bombardment History. In *Proceedings of the Tenth Lunar and Planetary Science Conference*, pages 1061–1072. New York: Pergamon Press.

Fireman, E.L.
1979. ^{14}C and ^{39}Ar Abundances in Allan Hills Meteorites. In *Proceedings of the Tenth Lunar and Planetary Science Conference*, pages 1053–1060. New York: Pergamon Press.
1980. Carbon-14 and Argon-39 in ALHA Meteorites. In *Proceedings of the Eleventh Lunar and Planetary Science Conference*, pages 1215–1221. New York: Pergamon Press.

Fireman, E.L., and T. Norris
1981. ^{14}C Ages of Antarctic Meteorites and Ice and the Composition of the Air Trapped in the Ice. In *Lunar Science XII*, pages 282–284. Houston: Lunar and Planetary Institute.

Fireman, E.L., L.A. Rancitelli, and T. Kirsten
1979. Terrestrial Ages of Four Allan Hills Meteorites: Consequences for Antarctic Ice. *Science*, 203:453–455.

Fisher, R.M., J.I. Goldstein, and T. Nagata
1978. A Note on New Antarctic Iron Meteorites. *Memoirs of the National Institute of Polar Research* (Japan), special issue, 8:260–263.

Fisher, R.M., C.E. Spangler, Jr., and T. Nagata
1978. Metallographic Properties of Yamato Iron Meteorite, Yamato 75031, and a Stony-iron Meteorite, Yamato 74044. *Memoirs of the National Institute of Polar Research* (Japan), special issue, 8:248–259.

Gibson, E.K., Jr., and F.F. Andrawes
1980. The Antarctic Environment and Its Effect upon the Total Carbon and Sulfur Abundances in Recovered Meteorites. In *Proceedings of the Eleventh*

Lunar and Planetary Science Conference, pages 1223–1234. New York: Pergamon Press.

Gibson, E.K., Jr., and K. Yanai
1979a. Total Carbon and Sulfur Abundances in Antarctic Meteorites. In *Proceedings of the Fourth Symposium on Antarctic Meteorites*, pages 189–195. Tokyo: National Institute of Polar Research.
1979b. Total Carbon and Sulfur Abundances in Antarctic Meteorites. In *Proceedings of the Tenth Lunar and Planetary Science Conference*, pages 1045–1051. New York: Pergamon Press.

Grossman, L., E. Olsen, A.M. Davis, T. Tanaka, and G.J. MacPherson
1981. The Antarctic Achondrite ALHA76005: A Polymict Eucrite. *Geochimica et Cosmochimica Acta*, 45:1267–1279.

Holzer, G., and J. Oro
1979. The Organic Composition of the Allan Hills Carbonaceous Chondrite (77306) as Determined by Pyrolysis-Gas Chromatography-Mass Spectrometry and Other Methods. *Journal of Molecular Evolution*, 13:265–270.

Hyman, M., and M.W. Rowe
1979. Magnetic Contents of Carbonaceous Meteorites. *Transactions of the American Geophysical Union (EOS)*, 60:308.

Jochum, K.P., K.I. Grais, and H. Hintenberger
1980. Chemical Composition and Classification of 19 Yamato Meteorites. *Meteoritics*, 15:31–40.

King, T.V.V., R. Score, E.M. Gabel, and B. Mason
1980. Meteorite Descriptions. *In* U.B. Marvin and B. Mason, editors, Catalog of Antarctic Meteorites, 1977–1978. *Smithsonian Contributions to the Earth Sciences*, 23:12–44.

Kotra, R.K., A. Shimoyama, C. Ponnamperuma, and P.E. Hare.
1979. Amino Acids in a Carbonaceous Chondrite from Antarctica. *Journal of Molecular Evolution*, 13:179–184.

Kracher, A., J. Willis, and J.T. Wasson
1980. Chemical Classification of Iron Meteorites, IX: A New Group (IIF), Revision of IAB and IIICD, and Data on 57 Additional Irons. *Geochimica et Cosmochimica Acta*, 44:773–787.

Marvin, U.B. and Mason, B., editors
1980. Catalog of Antarctic Meteorites, 1977–1978. *Smithsonian Contributions to the Earth Sciences*, 23: 50 pages.

Marvin, U.B., and K. Motylewski
1980. Mg-carbonates and -Sulfates on Antarctic Meteorites. In *Lunar and Planetary Science XI*, pages 669–670. Houston: Lunar and Planetary Institute.

McKee, T.R., and C.B. Moore
1980. Matrix Phyllosilicates of the Antarctic C2 Chondrite ALHA77306. In *Lunar and Planetary Science XI*, pages 703–704. Houston: Lunar and Planetary Institute.

McKinley, S.G., E.R.D. Scott, G.J. Taylor, and K. Keil
1981. A Unique Type 3 Ordinary Chondrite Containing Graphite-Magnetite Aggretates — Allan Hills A77011. *Meteoritics*, 16:357–358.

McSween, H.Y., Jr.
1979. Matrix Variations in CM Chondrites. In *Lunar and Planetary Science X*, pages 810–812. Houston: Lunar and Planetary Institute.

McSween, H.Y., Jr., E.M. Stoper, L.A. Taylor, R.A. Muntean, G.C. O'Kelley, J.S. Eldridge, S. Biswas, H.T. Ngo, and M.E. Lipschutz
1979. Petrogenetic Relationship between Allan Hills 77005 and Other Achondrites. *Earth and Planetary Science Letters*, 45:275–284.

Miyamoto, M., H. Takeda, K. Yanai, and H. Haramura
1979. Mineralogical Examination of the Allan Hills No. 5 Meteorite. *Memoirs of the National Institute of Polar Research* (Japan), special issue, 12:59–71.

Nagata, T.
1978. Magnetic Properties of an Iron Meteorite (Yamato 75031) and a Pallasite (Yamato 74044). *Memoirs of the National Institute of Polar Research* (Japan), special issue, 8:240–247.
1980. Magnetic Classification of Antarctic Meteorites. In *Proceedings of the Eleventh Lunar and Planetary Science Conference*, pages 1789–1799. New York: Pergamon Press.

Nagata, T., R.M. Fisher, and N. Suguira
1976. Metallographic and Magnetic Properties of a Yamato Iron Meteorite Yamato-75-105. *Memoirs of the National Institute of Polar Research* (Japan), series C, 10:1–11.

Naruse, R.
1978. Surface Flow and Strain of the Ice Sheet Measured by a Triangulation Chain. *Memoirs of the National Institute of Polar Research* (Japan), special issue, 7:198–226.

Nishiizumi, K., J.R. Arnold, D. Elmore, R.D. Ferraro, H.E. Gove, and R.C. Finkel
1981. Cosmic Ray-produced ^{36}Cl and ^{53}Mn in Allan Hills-77 Meteorites. *Earth and Planetary Science Letters*, 52:31–38.

Nishiizumi, K., M. Imamura, and M. Honda
1978. Cosmic Ray Induced ^{53}Mn in Yamato-7301(j), -7305(k) and -7304(m) Meteorites. *Memoirs of the National Institute of Polar Research* (Japan), special issue, 8:209–219.
1979. Cosmic Ray Produced Radionuclides in Antarctic Meteorites. *Memoirs of the National Institute of Polar Research* (Japan), special issue, 12:161–177.

Nishiizumi, K., M.T. Murrell, J.R. Arnold, M. Imamura, and M. Honda
1980. Cosmogenic ^{53}Mn Survey of Yamato Meteorites. *Memoirs of the National Institute of Polar Research* (Japan), special issue, 17:202–209.

Nishio, F., and J.O. Annexstad
1979. Glaciological Survey in the Bare Ice Area near the Allan Hills in Victoria Land, Antarctica. *Memoirs of the National Institute of Polar Research* (Japan), special issue, 15:13–23.
1980. Glaciological Survey in the Bare Ice Area near the Allan Hills in Victoria Land, Antarctica. *Memoirs of the National Institute of Polar Research* (Japan), special issue, 17:14–20.

Nyquist, L.E., D.D. Bogard, J.L. Wooden, C.-Y. Shih, B.M. Bansal, and G. McKay
1979. Early Differentiation, Late Magmatism, and Recent Bombardment on the Shergottite Parent Planet. *Meteoritics*, 14:502.

Okada, A.
1975. Mineralogy of the Yamato Meteorites. *Memoirs of the National Institute of Polar Research* (Japan), special issue, 5:14–66.

Okada, A., K. Yagi, and Makoto Shima
1975. Petrology of the Yamato Meteorites. *Memoirs of the National Institute of Polar Research* (Japan), special issue, 5:67–82.

Olsen, E.J., A. Noonan, K. Fredriksson, E. Jarosewich, and G. Moreland
1978. Eleven New Meteorites from Antarctica, 1976–1977. *Meteoritics*, 13:209–225.

Patchett, P.J., and M. Tatsumoto
1980. Lu-Hf Total-Rock Isochron for the Eucrite Meteorites. *Nature*, 288:571–574.

Reid, A.M., and C.M. Schwarz
1980. Antarctic Polymict Eucrites. *Meteoritics*, 15:353–354.

Schmidt, D.L.
1964. Geology of the Pensacola Mountains. *Bulletin of the Antarctic Projects Officer*, 5:98–101.

Scott, E.R.D., and J.T. Wasson
1976. Chemical Classification of Iron Meteorites, VIII: Groups IC, IIE, IIIF, and 97 Other Irons. *Geochimica et Cosmochimica Acta*, 40:103–115.

Shimoyama, A., C. Ponnamperuma, and K. Yanai
1979a. Amino Acids in the Yamato Carbonaceous Chondrites from Antarctica. *Nature*, 282:394–396.
1979b. Amino Acids in the Yamato 74662 Meteorite, an Antarctic Carbonaceous Chondrite. *Memoirs of the National Institute of Polar Research* (Japan), special issue, 15:196–205.

Takeda, H.
1979. A Layered Crust Model of the Howardite Parent Body. *Icarus*, 40:455–470.

Takeda, H., M. Miyamoto, M.B. Duke, and T. Ishii
1978. Crystallization of Pyroxenes in Lunar KREEP Basalt 15386 and Meteoritic Basalts. In *Proceedings of the Ninth Lunar Science Conference*, pages 1157–1171. New York: Pergamon Press.

Takeda, H., M. Miyamoto, T. Ishii, K. Yanai, and Y. Matsumoto
1979. Mineralogical Examination of the Yamato-75 Achondrites and Their Layered Crust Model. *Memoirs of the National Institute of Polar Research* (Japan), special issue, 12:82–108.

Takeda, H., M. Miyamoto, K. Yanai, and H. Haramura
1978. A Preliminary Mineralogical Examination of the Yamato-74 Achondrites. *Memoirs of the National Institute of Polar Research* (Japan), special issue, 8:170–184.

Takeda, H., H. Mori, K. Yanai, and K. Shiraishi
1980. Mineralogical Examination of the Allan Hills Achondrites and Their Bearing on the Parent Bodies. *Memoirs of the National Institute of Polar Research* (Japan), 17:119–144.

Takeda, H., A.M. Reid, and T. Yamanaka
1975. Crystallographic and Chemical Studies of a Bronzite and Chromite in the Yamato(b) Achondrite. *Memoirs of the National Institute of Polar Research* (Japan), special issue, 5:83–90.

Takeda, H., and K. Yanai
1979. A New Olivine-Augite Achondrite Found in Antarctica. *Meteoritics*, 14:542–543.

Takeda, H., K. Yanai, and K. Shiraishi
1980. Yamato and Allan Hills Meteorites and Their Bearing on the Parent Bodies. In *Lunar and Planetary Science XI*, pages 1119–1121. Houston: Lunar and Planetary Institute.

Taylor, G.J., A. Okada, E.R.D. Scott, A.E. Rubin, G.R. Huss, and K. Keil
1981. The Occurrence and Implications of Carbide-Magnetite Assemblages in Unequilibrated Ordinary Chondrites. In *Lunar and Planetary Science XII*, pages 1076–1078. Houston: Lunar and Planetary Institute.

Van Schmus, W.R., and J.A. Wood
1967. A Chemical-Petrographic Classification for the Chondritic Meteorites. *Geochimica et Cosmochimica Acta*, 31:747–765.

Wasson, J.T.
1974. *Meteorites*. Heidelberg: Springer-Verlag. 316 pages.

Watters, T.R., M. Prinz, E.R. Rambaldi, and J.T. Wasson
1980. ALHA 78113, Mt. Egerton, and the Aubrite Parent Body. *Meteoritics*, 15:386.

Wooden, J., A.M. Reid, R. Brown, B. Bansal, H. Weismann, and L. Nyquist
1981. Chemical and Isotopic Studies of the Allan Hills Polymict Eucrites. In *Lunar and Planetary Science XII*, pages 1203–1205. Houston: Lunar and Planetary Institute.

Yanai, K.
1980. Over 4,000 New Antarctic Meteorites Collected in the 1979–1980 Season. *Meteoritics*, 15:389.